Analytical Investigation of Reinforced Concrete Beam Strengthened by Carbon Fiber Reinforced Polymer

Omar M M MURTAJA

T.C.
BURSA ULUDAĞ UNIVERSITY
GRADUATE SCHOOL OF NATURAL AND APPLIED SCIENCES

**Analytical Investigation of Reinforced Concrete Beams Strengthened by Carbon
Fiber Reinforced Polymer**

Omar M. M. Murtaja
0000-0002-7824-6452

Ass. Dr. Serkan SAĞIROĞLU
(Supervisor)

MSc
DEPARTMENT OF CİVİL ENGİNEERİNG

BURSA – 2021

THESIS APPROVAL

This thesis titled "ANALYTICAL INVESTIGATION OF REINFORCED CONCRETE BEAMS STRENGTHENED BY CARBON FIBER REINFORCED POYLMER" and prepared by OMAR M M MURTAJA has been accepted as a MSc THESIS in Bursa Uludag University Graduate School of Natural and Applied Sciences, Department of Civil Engineering following a unanimous vote of the jury below.

Supervisor : Ass. Prof. Dr. Serkan SAĞIROĞLU

Head:	Ass. Prof. Dr. Serkan SAĞIROĞLU 0000-0001-7248-3409 Bursa Uludag University, Faculty of Engineering, Department of Civil Engineering	Signature
Member:	Assoc. Prof. Dr. Hakan Tacettin TÜRKER 0000-0001-5820-0257 Bursa Uludag University, Faculty of Engineering, Department of Civil Engineering	Signature
Member:	Dr. Emrah TAŞDEMİR 0000-0002-2482-1642 Bilecik Şeyh Edebali University, Faculty of Engineering, Department of Civil Engineering	Signature

I approve the above result

Prof. Dr. Hüseyin Aksel EREN
Institute Director
../../….

I declare that this thesis has been written in accordance with the following thesis writing rules of the U.U Graduate School of Natural and Applied Sciences;

– All the information and documents in the thesis are based on academic rules,

– audio, visual and written information and results are in accordance with scientific code of ethics,

– in the case that the works of others are used, I have provided attribution in accordance with the scientific norms,

– I have included all attributed sources as references,

– I have not tampered with the data used,

– and that I do not present any part of this thesis as another thesis work at this university or any other university.

20/09/2021

Omar M M Murtaja

ÖZET

Yüksek Lisans

Karbon Elyaf Takviyeli Polimer ile Güçlendililmiş Betonarme Kirişlerin Analitik İncelemesi

Omar M M Murtaja

Bursa Uludag Üniversitesi
Fen Bilimleri Enstitüsü
İnşaat Mühendisliği Anabilim Dalı

Danışman: Dr. Öğr. Üyesi Serkan SAĞIROĞLU

Betonarme kirişlerin karbon fiber takviyeli polimer CFRP ile güçlendirilmesi, nispeten hızlı ve pratik bir çözüm olarak görülmektedir. Bu araştırmanın amacı, ABAQUS adı verilen doğrusal olmayan bir sonlu elemanlar programı kullanarak güçlendirilmiş betonarme kirişlerin performansını ve farklı parametrelerin güçlendirilmiş kirişlerin performansına etkisini araştırmaktır. İncelenen parametreler arasında ceketlenecek kiriş tarafı sayısı, katman sayısı ve CFRP Uzunluğu yer almaktadır. Sonlu eleman analizlerinden elde edilen sonuçlar, kirişlerin merkezindeki yük-sehim eğrisi ile sunulmakta ve oluşturulan modelleri doğrulamak için literatürden elde edilen deneysel verilere çok yakın göstermektedir.

Sadece çekme tarafında güçlendirilen kritik eğilme kirişleri için, üç kat fiber kullanıldığında nihai yük kapasitesindeki maksimum artış elde edilir. Bu durumda, kirişin eğilme mukavemeti, güçlendirilmemiş kontrol kirişine kıyasla, %52,72 artar ve kırılmadaki orta açıklık sehimi %18,90 azalır. U-şekli kullanılarak kritik eğilme kirişleri güçlendirilirken, dört kat fiber kullanıldığında nihai yük kapasitesindeki maksimum artış. Bu durumda kirişin eğilme mukavemeti kontrol kirişine göre %113,5 artar ve sehim değeri %20,09 azalır. Öte yandan, %75 ve %100 CFRP uzunluklu çekme tarafındaki güçlendirilmiş betonarme kirişlerin nihai dayanım ve sehim değerleri çok yakındır.

U-şekli yöntemi ile güçlendirilen kesme kritik kirişler için, nihai kapasitedeki maksimum artışın, dört kat fiber kullanıldığında elde edildiğini göstermiştir. Bu durumda kirişin kesme mukavemeti %16,10 artar ve sehim %37,58 azalır. Kayma kirişler sarılı yöntemle güçlendirilirken, dört kat lif kullanıldığında nihai yük kapasitesindeki maksimum artış elde edilir.

Anahtar Kelimeler: Batonarme, Kirişler, Onarım, Güçlendirme, Karbon Fiber Takviye Polimeri, Rehabilitasyon.

2021, ix + 99 sayfa.

ABSTRACT

MSc Thesis

Analytical Investigation of Reinforced Concrete Beams Strengthened by Carbon Fiber Reinforced Polymer

Omar M M Murtaja

Bursa Uludag University
Graduate School of Natural and Applied Sciences
Department of Civil Engineering

Supervisor: Ass. Dr. Serkan SAĞIROĞLU

Strengthening reinforced concrete beams with carbon fiber reinforced polymer CFRP is considered as comparatively fast and practical solution. The objective of this research is to investigate the performance of strengthened reinforced concrete beams by using a non-linear finite element program which is called ABAQUS and the influence of different parameters on strengthened beams' performance. The studied parameters included the number of beam side to be jacketed, the number of layers and Length of CFRP. The obtained results from finite element analyses are presented by the load-deflection curve at the center of beams and show very close to the experimental data obtained from literature to verify the generated models.

For flexural critical beams strengthened only at the tensile side, the maximum increase in the ultimate load capacity is obtained when three layers of fibers are used. In this case the flexural strength of the beam increases 52.72% and the mid-span deflection at failure reduces 18.90% compared to un-strengthened control beam. While strengthening flexural critical beams by using U-shape, the maximum increase in the ultimate load capacity when four layers of fibers are used. In this case the flexural strength of the beam increases 113.5% and the deflection value decrease by 20.09% compared to control beam. On the other hand, the ultimate strength and deflection values of strengthened RC beams at tension side with CFRP length 75% and 100% are very close.

For shear critical beams strengthened by U-shape method showed that the maximum increase in the ultimate capacity is obtained when four layers of fibers are used. In this case the shear strength of the beam increases by 16.10% and the deflection decreases by 37.58%. While, shear beams strengthened by wrapped method, the maximum increasing in the ultimate load capacity is obtained when four layers of fibers are used.

Key words: Reinforced Concrete Beam, Carbon Fiber Reinforcement Polymer, Ultimate Strength, Deflection, Repair and Rehabilitation.

2021, ix + 99 pages.

ACKNOWLEGDEMENT

I would like to give my thanks to my beloved parents, brothers and sister who have supported me the entire way.

I would like to thanks my sincere gratitude to my thesis supervisor, Dr. Serkan Sağıroğlu, Department of Civil engineering, Uludag University, for their efforts and keen which has remained a valuable asset for the successful completion of this work.

<div align="right">

Omar M M MURTAJA
20/09/2021

</div>

CONTENTS

SYMBOLS and ABBREVIATIONS

Symbols   **Definition**

fc'	Concrete compressive strength.
Ec	Modulus elasticity of concrete.
F	Function of the principal stress state (σ_{xp}, σ_{yp}, σ_{zp}).
S	Failure surface of concrete expressed in terms of principal stresses and five input parameters f_t, f_c, f_{cb}, f_1 and f_2.
σ_{xp}	Principal stresses in x direction.
σ_{yp}	Principal stresses in y direction.
σ_{zp}	Principal stresses in z direction.
f_t	Ultimate uniaxial tensile strength of concrete.
f_y	Yield strength of steel.
ε_y	The stain at which steel yields.
f_u	Peak strength of steel.
ε_u	The stain at which peak strength of steel is achieved.
f_s	The stain at which steel fracture.
ε_{max}	The stain at which fracture of steel occurs.
v	Poisson's ratio.

Abbreviation   **Definition**

RC	Reinforced concrete
$CFRP$	Carbon fiber reinforced polymer
FE	Finite element
FEA	Finite element analysis
FEM	Finite element method
CDP	Concrete Damaged Plasticity

FIGURES

TABLES

1. INTRODUCTION

Concrete is one of the essential materials in construction engineering. Reinforced concrete (RC) is the primary material in buildings, bridges, underground structures, and even military construction. The reasons for the success of reinforced concrete material are durability, rigidity, low cost, minimum deflection, and the expected life span is extended. (Abd et al. 2009)

Beams are structural members carrying transverse loads that cause bending, shear, and perhaps also may happen torsion. Every reinforced concrete member should be designed to afford a particular of loading in their life span. However, some of the construction members exposed to unexpected cases such as fire, earthquake, chemical attacks, overloading, change in use, and errors in designing or construction cases (Jumaat et al. 2006).

Fiber reinforced polymer (FRP) is considered one of the most attractive solutions to strengthen reinforced concrete elements because it has several advantages, such as high tensile capacity, high durability, excellent strength to self-weight ratio, and large fatigue resistance capacity. (Pravin ve Waghmare 2011)

This research investigates the performance of strengthened reinforced concrete beams by using a non-linear finite element program called ABAQUS. Recommendations are given based on a theoretical and experimental study supported by published studies.

1.1. The Need for Rehabilitation

Rehabilitation of structures can be divided into two types are repair and strengthening. Repair is the rehabilitation of over-loaded or damaged elements in a structure by using suitable materials. On the other hand, strengthening by definition is the rehabilitation of unloaded or undamaged elements in structure (Raval and Dave 2013).

In the last few decades, structural rehabilitation has become essential and attracted

increasing international attention. Therefore, it has begun to play a role in construction engineering, and the strengthening materials have good quality and achieve the desired purpose. For example, the China Academy of Engineering has published about the influences of steel corrosion in reinforced concrete structures and which suffers heavy losses to the government about 140 billion dollars per year. In the USA, in 2010, the rehabilitation of deficient or deteriorated brides was 50 billion dollars(Li et al. 2009).

Structural degradation can be divided into the following categories (Emmons 1994) and(Li et al. 2009):

1. Design phase errors: Faulty designer, poor detailing.
2. Construction period phase: Faulty workmanship as shown in Figure 1.1., constructor, materials inelegances.
3. Physical: climatic changes, abrasion, fire Figure 1.2., thermal effects, moisture effects, freezing, fatigue, cracking.
4. Mechanical: Earthquakes, vibration, explosion, impact, settlement etc.
5. Chemical: embedded metal corrosion Fıgure 1.3.,
6. Service life span: changes in use, overloading Fıgure 1.4. and accidents.

Figure 1.1. Faulty workmanship (Rogerson, 2018).

Figure 1.2. The effect of fire on RC elements (Emmons 1994).

Figure 1.3. Example of steel corrosion (Chong 2004).

Figure 1.4. The effect of overloading (Muneeb, 2015)
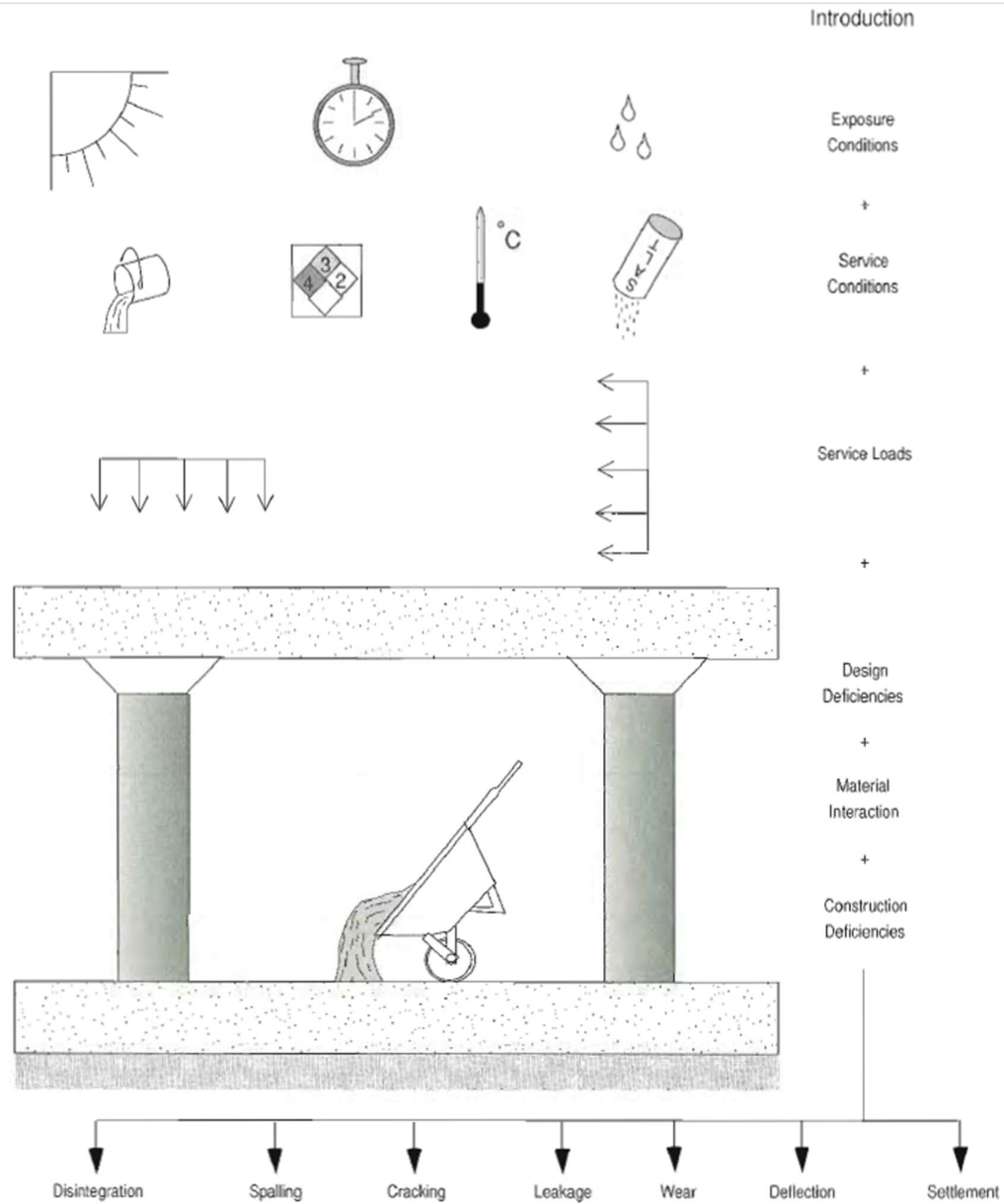
Figure 1.5. The summary about the life span of structures(Emmons 1994).

1.2. Statement of the problems

This research studies how to range the effect of different types of strengthening methods on RC beams using CFRP and studying the behaviour of strengthened RC beams in shear and flexure failure. This research hypothesis include:

1. What are the changes on (performance, ultimate carrying capacity, and deflection value) RC beams when using a different method of strengthening like a U-shape, at the tensile side and wrapped method?

2. What are the changes on (performance, ultimate carrying capacity, and deflection value) RC beams when using a different number of strengthening layers?

3. What are the changes on (performance, ultimate carrying capacity, and deflection value) RC beams when using a different length of CFRP at the tensile side?

In this research, the influence of some important parameters on the overall response of the strengthened RC beams have been investigated, to achieve the optimum utilization of such strengthening techniques in term of load carrying capacity and deflection values.

1.3. Strengthening Techniques

Basically, the strengthening techniques can be divided into two main approaches:

1. Addition of new structural elements.

2. Strengthening of the existing structural elements.

The strengthening techniques have been developed in the last decades particularly. Several types of strengthening techniques include enlarging the sectional area, adding reinforcements, pre-stressed retrofit, changing load path, sticking steel plates or Fiber Reinforced Polymers, and encasing members with steel (Abdel Baky et al. 2014). Figure 1.6. shows the retrofitting techniques for structures.
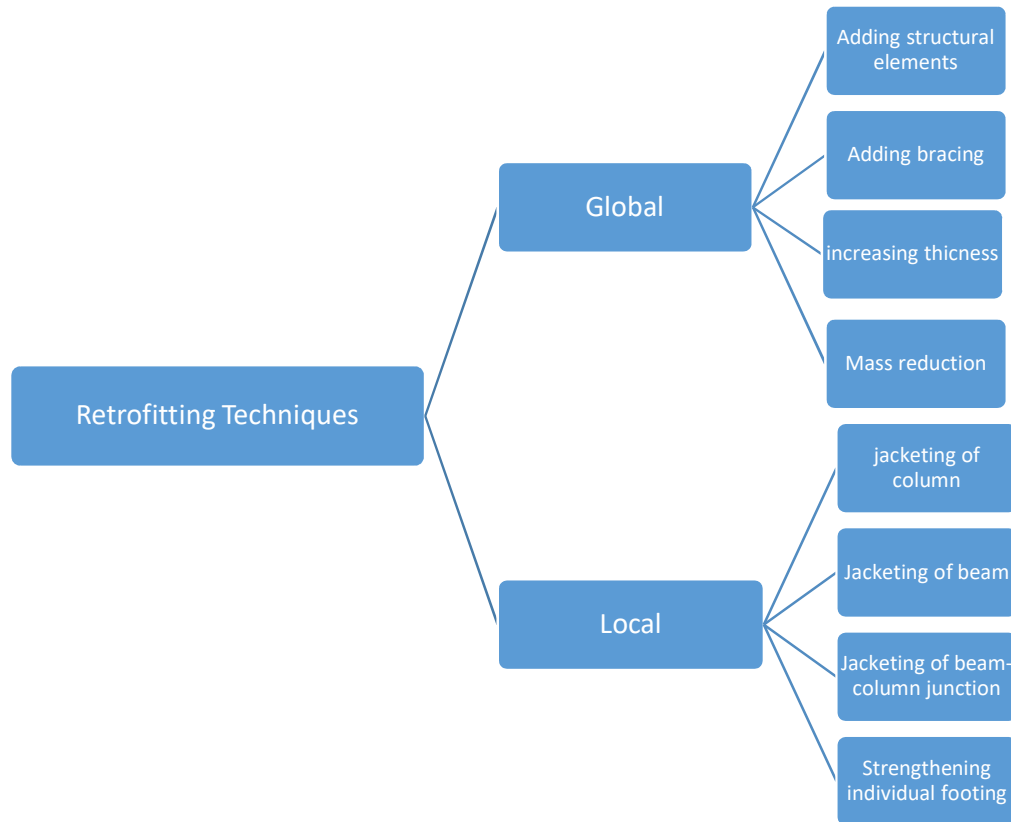
Figure 1.6. The summary of the retrofitting techniques (Abdel Baky et al. 2014).

1.4. Strengthening of RC beams

Many strengthening techniques and materials are used to rehabilitate RC beams. Jacketing is the old and traditional strengthening method enveloping a reinforced concrete from 3 or four faces and sometimes just from one side by using different strengthening materials like reinforced concrete, Steel plates, Lightweight self-compacting concrete, and Fiber-reinforced concrete with other techniques of a binding (Figure 1.7. to Figure 1.10.) jacketing is the most popular technique used for strengthening and repairing building elements (Pravin & Waghmare, 2011).
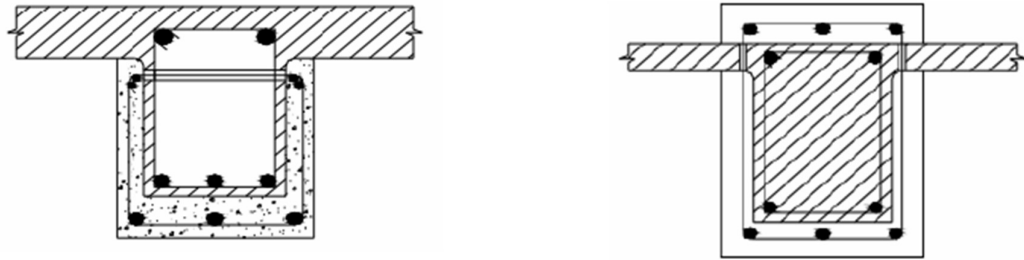
Figure 1.7. Three-side (U-shape) and four-side jacketing of a beam (Pravin and Waghmare 2011)

Figure 1.8. Fixation of the strengthening steel cages on the tensile side (Shehata, Shehata, Santos, & Simo˜es, 2009)
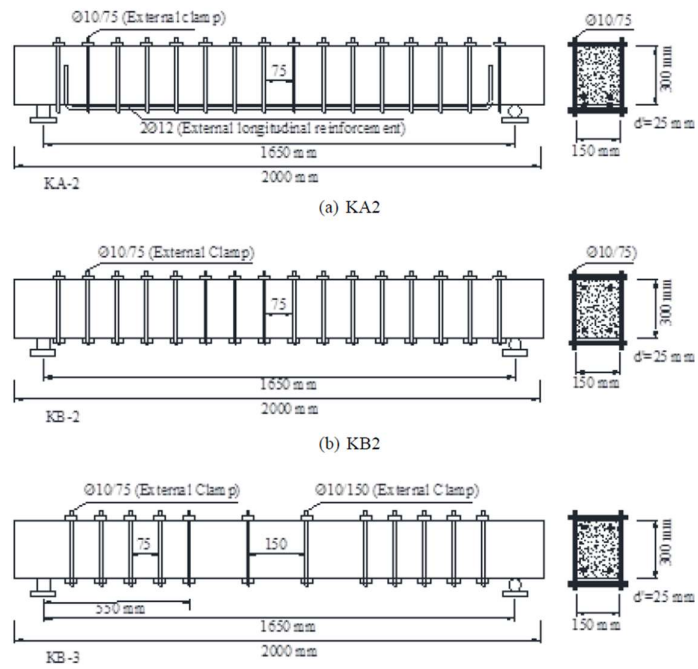
Figure 1.9. Types and shapes of steel member used in strengththening (Demir et al. 2018).

Figure 1.10. The strengthened beams by using CFRP.

1.5. Research Scope, Objectives and Limitations

1.5.1. The scope

The scope of this research is to investigate the behaviour of strengthened RC beams under different types of strengthening methods by using CFRP in a non-linear finite element program (ABAQUS).

1.5.2. The objectives

The objectives of this research are:

1. Determine available elements types in the ABAQUS library according to the ABAQUS user guide and relevant papers in order to model and analyse RC beams strengthened by CFRP layers.
2. Develop three-dimensional non-linear finite element models to simulate the behaviour of simply supported reinforced concrete beams externally strengthened in flexure and shear with CFRP.
3. Verify the finite element models by comparing results obtained from the models with results obtained from experimental tests available in the literature.
4. Use the verified model of RC beams to expand the research results through change some of the parameters to evaluate parameters effects on the behaviour of beams.

1.5.3. Methodology

To achieve the objectives of this research, the following tasks were executed:

01 • Review of available literature related to the research

02 • Development of the Finite Element models using ABAQUS.

03 • Models Verification.

04 • Performing a Parametric Study.

05 • Conducting comparison.

06 • Conclusions and recommendations.
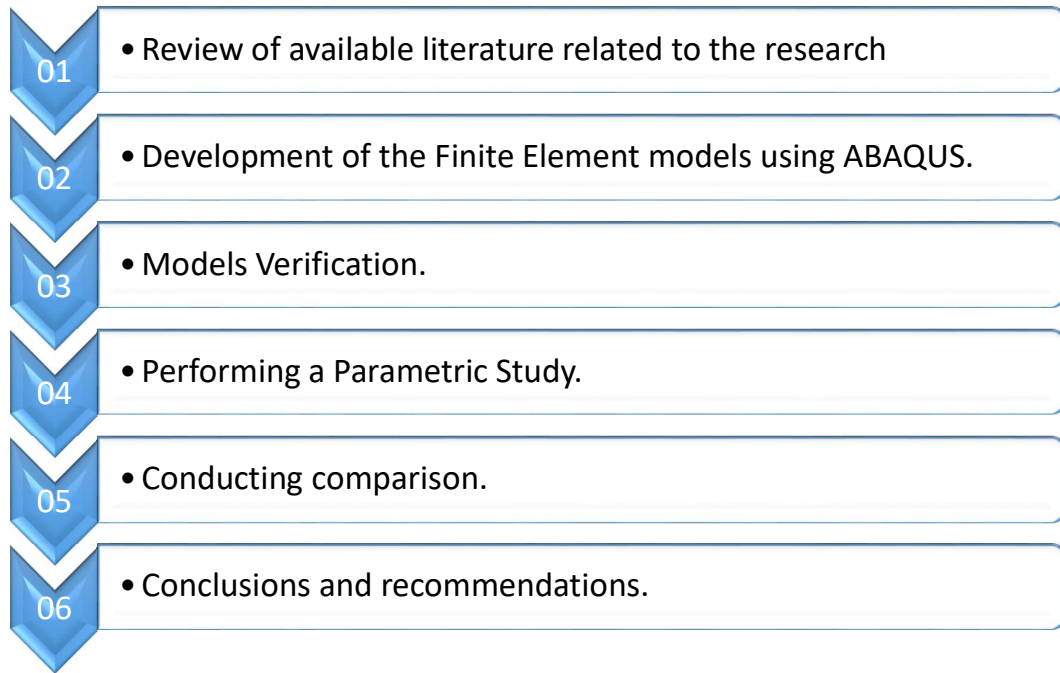
2. LITERATURE REVIEW

2.1. Introduction

FRP's definition , properties , application method, types and matrix resin were reviewed. The application of CFRP for external flexural and shear strengthening of RC beams and literature reviews about finite element analysis of RC beams strengthened with CFRP.

2.2. What is Fiber Reinforced Polymer?

Fiber reinforced polymer (FRP) is a composite material, consist of fibers that are put as layers over each other with the same or different directions embedded in a matrix resin (Abdel Baky et al. 2014). The combination of fiber reinforced polymer and matrix leads to high-performance tensile strength, better than steel and aluminum. The most used types of fibers in civil engineering works are glass, carbon, and aramid. The performance of fiber is related to its length, cross-section, and size to utilize FRP must be designed according to the geometry of an element and loads (Kaufmann 1998). It was illustrated the basic material component which are combine to create a FRP compoisite in Figure 2.1 (Kaw 2006).
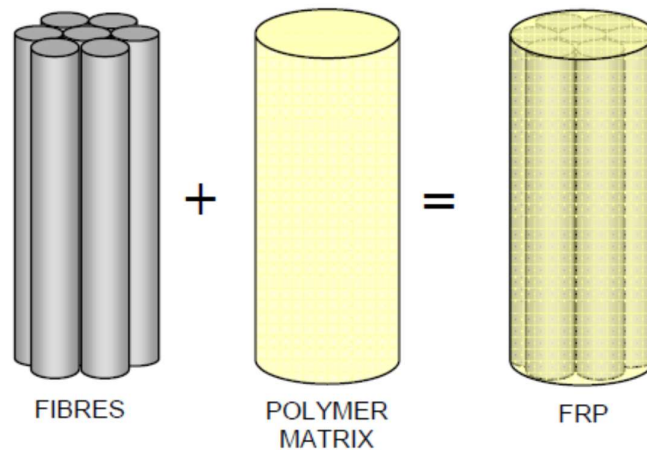
Figure 2.1. Constituents of fiber reinforced polymers materials (Kaw 2006).

2.2.1. Advantages and disadvantages of fiber reinforced polymers

FRP is considered attractive strengthening material due to it has advantages that couldn't be found in other strengthening materials. Some of the most important advantages include (Irwin ve Rahman 2002, Masuelli 2016):

1. Higher-strength to weight ratio.
2. Higher performance.
3. Rehabilitating existing structures and extending their life.
4. Ease of handling and application.

Here are the disadvantages of FRP materials (Masuelli 2016),

1. The price of FRP is high compare to other strengthening techniques.
2. Weak resistance of fire and accident damage.
3. FRP is made of fossil fuel and the un-recycle material.

2.3. Types and Properties of FRP Used for Structural Strengthening

Glass, Carbon and Aramid fiber reinforced polymer are the most commonly used in construction engineering applications (Kaw 2006, Report on Fiber-Reinforced Polymer (FRP) Reinforcement 2015).

2.3.1. Glass fibers

Glass fibers are the most inexpensive and commonly used fibers in a structural application (Hammad 2015). It is characterized by high strength, low cost, and high chemical resistance. Nevertheless, glass fibers have disadvantages, low elastic modulus, and high specific gravity. Therefore, it can allow the large deflection for strengthened members under loads and consider the heavier FRP materials used in structural repair and rehabilitation (Kaw 2006).

2.3.2. Carbon fiber reinforced polymers (CFRP)

CFRP is the most preferred used in structural rehabilitation. Because of CFRP have a high specific strength, low coefficient of thermal, high modulus, and high fatigue strength. However, CFRP have also disadvantages are high cost and low impact resistance (Mugahed Amran et al. 2018).

2.3.3. Aramid fibers

Aramid fibers are the third type of FRP, were selected in this research. It has low density, high tensile strength, and low cost compared to other kinds of FRP. However, the disadvantages of aramid fibers are low compression and degradation in sunlight (Kaw 2006).

Table 2.1. Mechanical properties of several classes of FRP materials (Mugahed Amran et al. 2018).

Reinforcing material	Yield strength (MPa)	Density, (g/cm^3)	Tensile strength (MPa)	Specific gravity	Elastic modulus (GPa)	Strain at break, %
Steel	500–500	7.75–8.05	–	7.8	(200)	–
Glass FRP	600–1400	2.11–2.70	480–1600	1.5–2.5	35–51	1.2–3.1
Basalt FRP	1000–1600	2.15–2.70	1035–1650	2.7–2.89	45–59	1.6–3.0
Aramid FRP	1700–2500	1.28–2.6	1720–2540	1.38–1.39	41–125	1.9–4.4
		1.39–1.45				
Carbon FRP	1755–3600	1.55–1.76	1720–3690	1.0–1.1	120–580	0.5–1.9

Annotation:

- Ultimate tensile strength, f_{fu}
- Tensile Modulus of Elasticity, Ef
- Elongation at Break, εf_u
- The values of fiber volume fraction of FRPs are limited between 0.5 and 0.7.

CFRP and GFRP have a tensile elastic modulus of at least 124 GPa and 39.3 GPa, respectively.

As it is indicated in Table 2.1. the yielding strength of FRP materials are higher than steel bars, in contradictory, the density of FRP materials are lower than steel bars. This result showed that FRP material a major rule in strengthen and rehabilitation RC beams.

2.4. Matrix resins

The resin is the second primary material used in FRP, and it is the interaction agent of several composites. The matrix resins of FRP are divided into thermosetting and thermoplastic. Thermoplastic is not recommended for civil engineering applications because its properties are a low creep and thermal resistance. Thermosetting is recommended to use for civil engineering applications. The types of thermosetting are epoxy, vinyl ester, and polyester (Abdel Baky et al. 2014, Hammad 2015)

2.5. Application of FRP on RC beams

2.5.1. Flexural strengthening

The strengthening method of flexure beams, is through bonded FRP layers at the tension side or on three faces to increase the ultimate carrying capacity and decrease the deflection values. The fibers are oriented along the longitudinal axis of the beams to obtain the perfect performance (Mugahed Amran et al. 2018). Figure 2.2. shows the types of flexural strengthened techniques.

a) CFRP sheets wrapped at ends

b) Anchorage at ends using mechanical anchors

Anchor bolt detail

c) Steel plates positioned along CFRP composite

d) CFRP sheet wrapped along entire span

Beam section
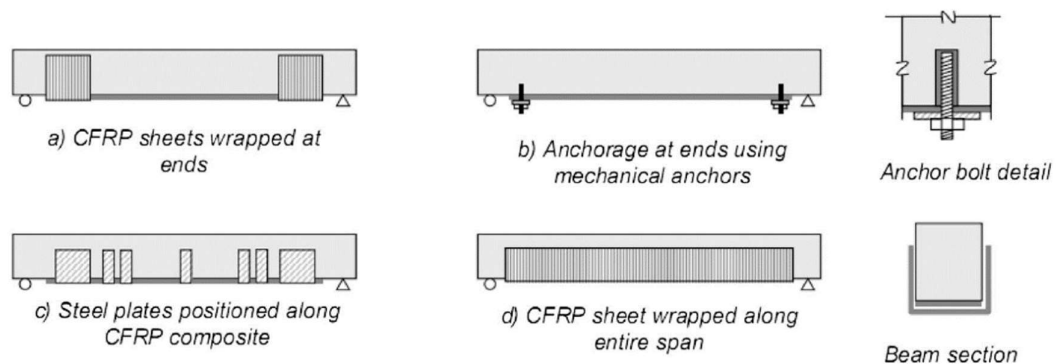
Figure 2.2. The types of flexural strengthening techniques (Amran, et al. 2018).

2.5.2. Shear strengthening

The strengthening method of shear beams, is bonded FRP layers from two, three faces or full wrapped a beam to increase the ultimate load capacity. Figure 2.3. explains how can be strengthened RC beams against shear forces (Ibrahim and Mahmood 2009).
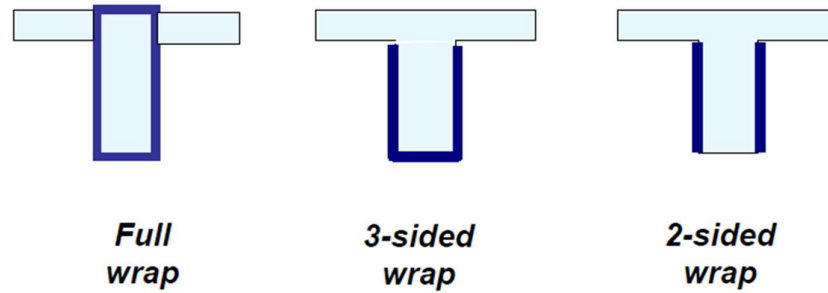
Figure 2.3. Types of strengthening RC beams against shear failure (Ibrahim and Mahmood 2009)

2.5.3. Selecting the suitable type of FRP

Each type of FRP material (e.g. glass fiber sheet, carbon fiber sheet, carbon fiber laminate) has its own advantages and disadvantages. Table 2.2. provides guidelines for selecting the suitable types of FRP materials for each RC structural element.

Table 2.2. Guidelines for selecting the suitable types of FRP materials for each RC structural element (Hammad 2015).

Element	Application	Glass Fibre Sheet (GFS)	Carbon Fibre Sheet (CFS)	Carbon Fibre Laminate (CFL)
	Fibre Direction	Uni-directional	Uni-directional	Uni-directional
	Fibre arrangement	Woven	Straight	Straight
Columns	Confinement	☼ ☼	☼ ☼	NA
	Flexure	☼	☼	☼☼☼☼
	Axial Load	☼☼	☼	☼☼☼☼
	Ductility	☼☼	NA	NA
	Durability	☼☼	☼	NA
Beams	Flexure	NA	☼	☼ ☼
	Shear	NA	☼ ☼	NA
Walls	Shear & flexure	☼ ☼	☼	☼
Slabs	Flexure	NA	☼	☼ ☼
Durability	Spalling	☼ ☼	☼	NA

2.6. Literature Reviews

Ibrahim and Mahmood (2009) worked on FEM of RC beams strength with FRP laminates. They analyzed reinforced concrete beam models externally strengthened with fiber-reinforced polymer (FRP) layers using ANSYS that utilizes the finite element method. The finite element model is developed using a smeared cracking approach for concrete and three-dimensional layers elements for the FRP composites. The direction of fibers was 90° and 45° with the longitudinal axis of beams. All of these beams have low

reinforcement steel against shear forces. The results showed finite element models represented by the load-deflection curve at mid-span had good agreement with the experimental data from the previous research.
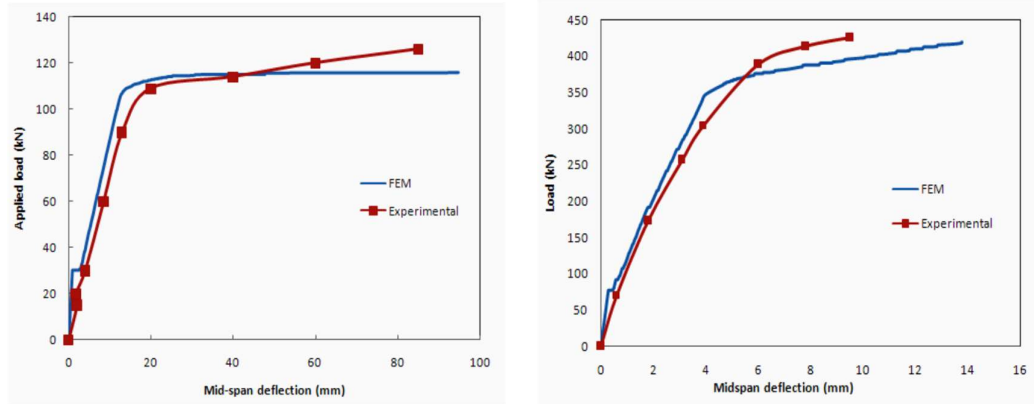
Figure 2.4. The comparison among modelling beams and experimental beams (Ibrahim ve Mahmood 2009).

Mbereyaho and Moyo (2016) studied on non-linear finite element analysis of reinforced concrete beams strengthened with fiber-reinforced plastics (Mbereyaho and Moyo 2016). The purpose of the research was to study the influence of the length CFRP on RC beams' ultimate loading capacity and failure pattern of RC beams by using the ABAQUS program. The finite element model is developed using the concrete damaged plasticity model (CDP) for concrete to obtain the performance of concrete. On the other hand, the steel bars were modeled as a linear elastic-perfectly plastic material model. The interface between concrete and FRP was modeled using a cohesive zone model and CFRP is modeled as an anisotropic elastic model. The results showed that the analyses data is stiffer than the experimental results except for the control beam.

The results showed that finite element models represented by the load-deflection curve at mid-span is in agreement with the previous research's experimental data. The results revealed the relation between FRP length and the loading-carrying capacity of the strengthened reinforced concrete beam. Consequently, whenever the length of FRP increases, the ultimate load capacity of RC beams increases, as shown in Figure 2.5.

18
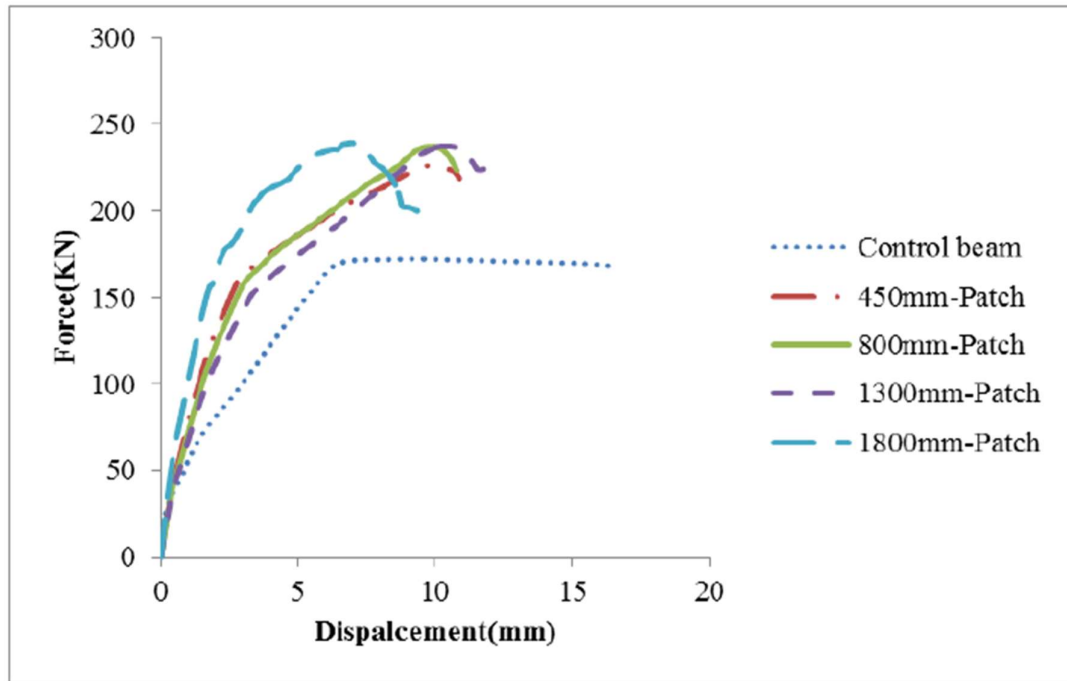
Figure 2.5. The relationships among the length of reinforcement polymer and the obtained maximum loads(Mbereyaho ve Moyo 2016).

Mukhtar et al. (2019) worked on a comparison between experimental and numerical results for the ultimate strength of RC beams strengthened by CFRP. It examines the influence of the thickness of the CFRP layer on the performance of beams comparing by the load-deflection curve and the ultimate load. These samples were simulated using the FE program called ABAQUS. Nonlinear materials' were simulated by using CDP. In this paper, the analytical models behave stiffer than the tested samples because of the fact that the interface between concrete and steel is assumed perfect in analytical models. The thickness of CFRP is must be taken into account because its influences on load carrying capacity and behaviour of beams, as shown in Figure 2.6 (Mukhtar et al. 2019).
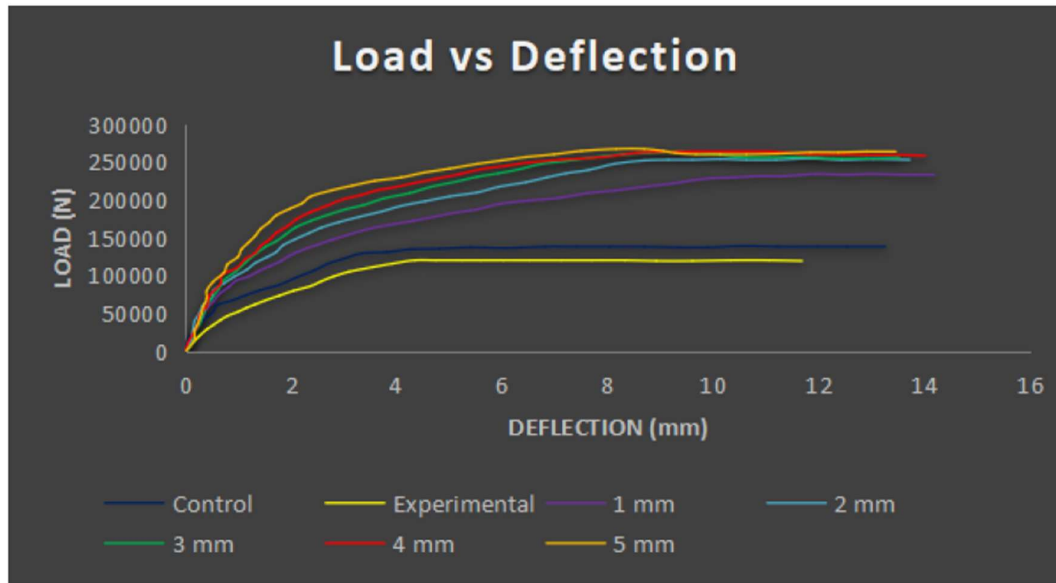
Figure 2.6. The effect of the thickness of fibers on the maximum strength of beams
(Mukhtar et al. 2019).

Hu et al (2004) have focused on some of the influence parameters in order to obtain the optimum ultimate load capacity of rectangular RC beams strengthened with CFRP against shear and flexural failure. The parameters which studied in this paper by researchers were fiber's orientation, reinforcement ratio, number of fibers layers and test types. They divide their tests into two groups according to failure mode of beams. The first group is strengthening RC beams against moment failures and the second group is strengthening RC beams against shear failures. The samples of test were divided into two types according to used reinforcement ratio and every group has two samples. Therefore, the first group has L8 means long beam with high reinforcement ratio and L4 means long beam with low reinforcement ratio. On the other hand, the second group has S8 means short beam with high reinforcement ratio and S4 means short beam with low reinforcement ratio. Then, the samples were strengthened by CFRP and using different types of parameter in ABAQUS and the results of tests were the following. the stiffness of the beams increase when the numbers of layer are increased. The number of FRP layer plays an important role in increase the load capacity of strengthened RC beams as shown in Figure (2-10). The optimum number of layers for strengthening RC beams against

20

moment failure were one layer. It is observed that when the angle of fibers close to 0° the beams have strongest stiffness.
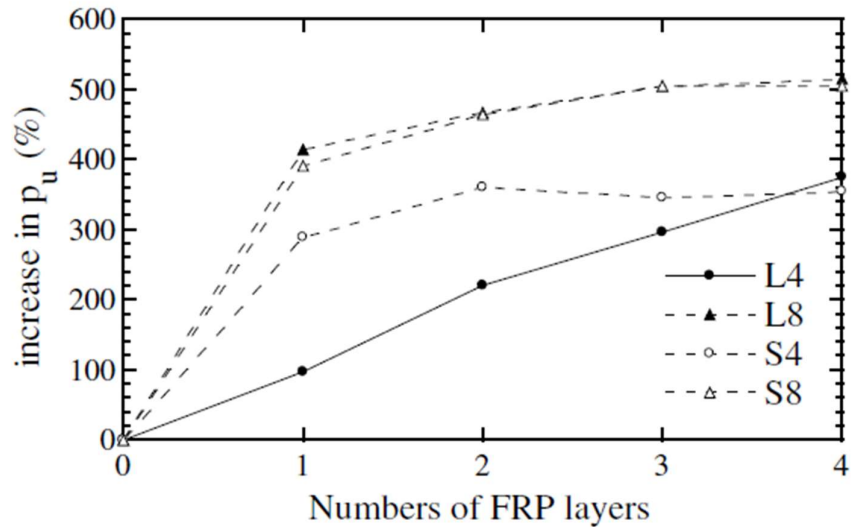
Figure 2.7. The importance influence the number of layers of FRP on maximum strength (Hu et al. 2004).

In the research carried by Hammad (2015), reinforced concrete beams with CFRP were modelled using a finite element program to study the influence the orientation of the layer of CFRP on response of strengthened RC beams in shear. The researchers presented the relation among the orientations of CFRP on load capacity and on deflection at the mid-span of the beams.

The results show that using one layer of CFRP of parallel with longitudinal axis of beam increases the ultimate load carrying capacity of beams by 14% and increases the deflection value up to 135%. That means that first configuration A has more ductility than other types of strengthening. On the other hand, the stiffer type is third configuration which is meaning the ultimate load carrying capacity of beam will increase but the deflection value will be the same. Strengthening RC beams with one vertical layer of CFRP fabric is more ductile than strengthening with one layer of CFRP inclined at an angle 45 and give adequate warning before failure. It is noticed that the failure load of the fourth configuration is more than the second configuration by 34%. However, the value

of deflection at mid-span between second configurations and fourth configuration is very close to each other as shown in Figure 2.8.
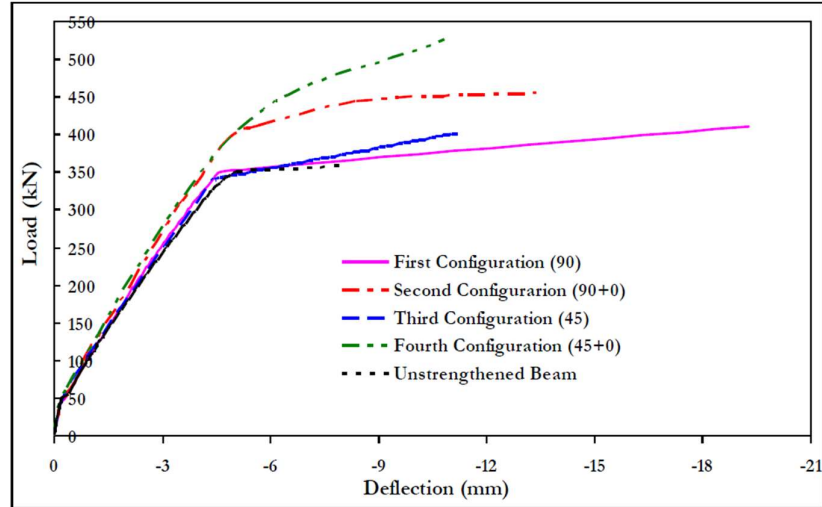
Figure 2.8. The results Load-Deflection curves for control beam and strengthening beams (Hammad 2015).

Abdel Baky et al. (2014) worked on nonlinear FE analysis of RC beams strengthened in flexure with NSM system. A numerical analysis using ADINA is performed to simulate seven RC beams strengthened by near-surface mounted (NSM) CFRP applied externally these beams as a stirrup with different steel reinforcement ratios. Nonlinear material behaviour was simulated using suitable and available models. The obtained results from finite element analysis presented by load-deflection curve at centre of beams showed agreement with the experimental data (Abdel Baky et al. 2014).

The research carried by Hawileh et al. (2015) focused on the development of finite element models for shear deficient RC beams strengthened with NSM CFRP rods under cyclic loading. A numerical analysis ANSYS using was performed to develop models of RC beams strengthened with near-surface mounted (NSM) CFRP applied externally to the beams as a stirrup with different steel reinforcement ratios under cyclic loading. According to the obtained results, modelled strengthened beams' maximum failure load capacity is 3.00% more than the experimental results. In addition, the value of deflection for the modelled strengthened beams is 8.98% over un-modelled strengthened beams. The

NSM approach promised an alternative method for strengthening RC beams. Moreover, the result of the strengthened RC models was in an acceptable agreement range.

In the present study, three dimensional nonlinear finite element models of reinforced concrete beams strengthened with CFRP are developed using ABAQUS, and then, a parametric study with different CFRP strengthening schemes are performed to study the effect of these schemes on the overall response of RC strengthened beams in flexure and shear.

3. THEORITICAL BASICS and MATERIALS

3.1. Introduction

The mechanical properties of concrete, steel reinforcement bars, and carbon fiber reinforcement polymer (CFRP) materials are presented in this chapter. Further, failure criteria and modeling approaches for each material are introduced.

3.2. Concrete

3.2.1. Mechanical Behavior of Concrete

A. Uniaxial compressive stress

The definition of compressive strength of concrete is the value of response of cube or cylinder shaped hardened concrete measured at 28 days by the compression test. Calculating the compression strength of concrete is done through cylinder tests or cube tests. Figure 3.1. shows the obtained curves of the response of concrete specimens (Kaufmann 1998).
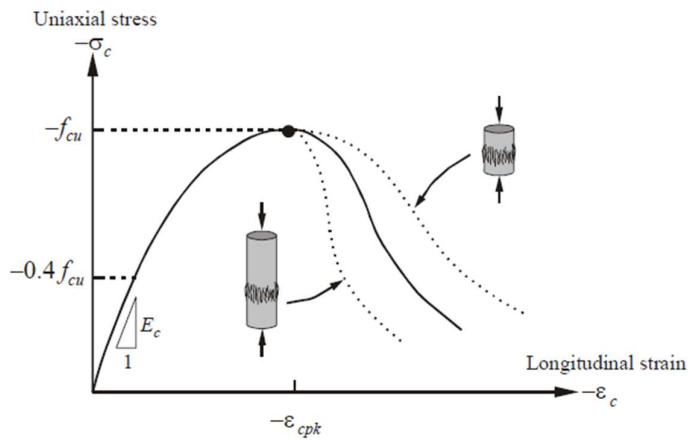
Figure 3.1. Uniaxial compression curve test (Kaufmann 1998).

From figure 3.1. in the beginning, it is noticed that the response of concrete is linear until 40% - 30% of the peak stress (Chong 2004). Then, the concrete behavior starts to be a non-linear reach up to the peak stress and that is because micro-cracking between aggregates and mortar is formed (Hammad 2015). After the peak stress, the specimen comes in the complicated process known as strain softening (Chong 2004). The strain softening is a last branch of the stress-strain curve and the results of the part depend on the length and volume of specimens. For instance, the softening branch of long specimens is sharper than that of short specimens (Hammad 2015).

B. Uniaxial tensile stress

The tensile strength of concrete is very low compare to the compressive strength and it's appreciated about 5-10% of the compressive strength (Chong 2004). To measure a response of tensile strength of concrete is done through direct and indirect tests (Kaufmann 1998). Figure 3.2. illustrates the performance of the specimens under the tensile test. It starts as a linear elastic curve until close to the peak point. Then, the curve's behavior changes to a softer line due to micro-cracking between aggregates and concrete material. After peak point, due to quasi-brittle properties of concrete, the curve of response tensile concrete material does not reduce to zero value suddenly. This is because of the interfacing between aggregates and cement mixture, and the stress transfers in the fracture zone across the opening crack direction until the complete crack is formed, as explained in Figure 3.2. It is noticed that after the peak point the response of long specimens is weaker than the response of short specimens.
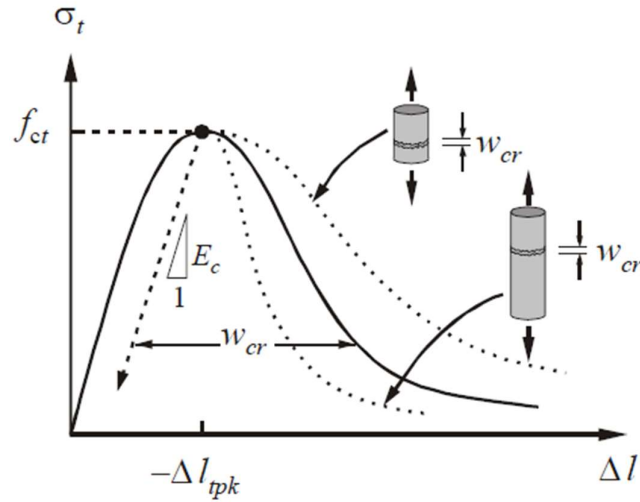
Figure 3.2. Uniaxial tensile behaviour of concrete (Chong 2004).

3.2.2. Finite element modelling of concrete

The concrete stress-strain relation in both compression and tension are illustrated in Figure 3.3. To draw and predict this nonlinear behavior of concrete is done by using various mathematical models. They are the piecewise linear model, linearly elastic-perfectly plastic model, inelastic-perfectly plastic, Hognestad, Kent and Park model. In this thesis, Kent and Park mathematical model has been used for the evaluation of the stress-strain behavior of concrete intension and compression cases as shown in Figure 3.4 (Hafezolghorani et al. 2017, Kotsovos ve Pavlovic 1995, Uzbaş 2014).

1. Elastic Modulus: initial tangent for a stress-strain curve increases with an increase in compressive strength of element until 50% of the ultimate compressive strength of concrete. Therefore, the value of elastic modulus is calculated from (ACI 8.5.1):

$$Ec = 4700\sqrt{fc'} \qquad (3\text{-}1)$$

where fc' is the compressive strength of a cylinder sample at 28 days MPa.
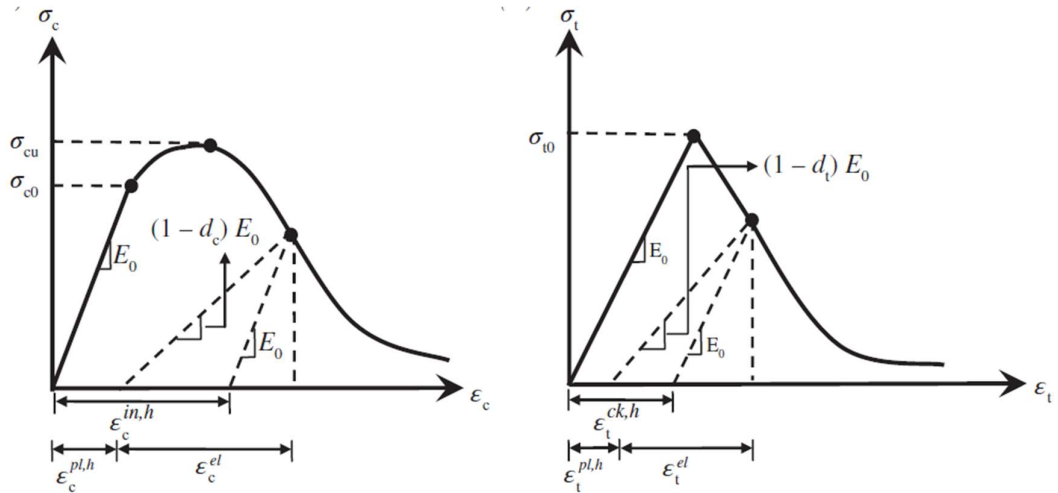
Figure 3.3. Uniaxial Stress-Strain behaviour of (a) concrete compressive and (b) tension strength (Kotsovos ve Pavlovic 1995).
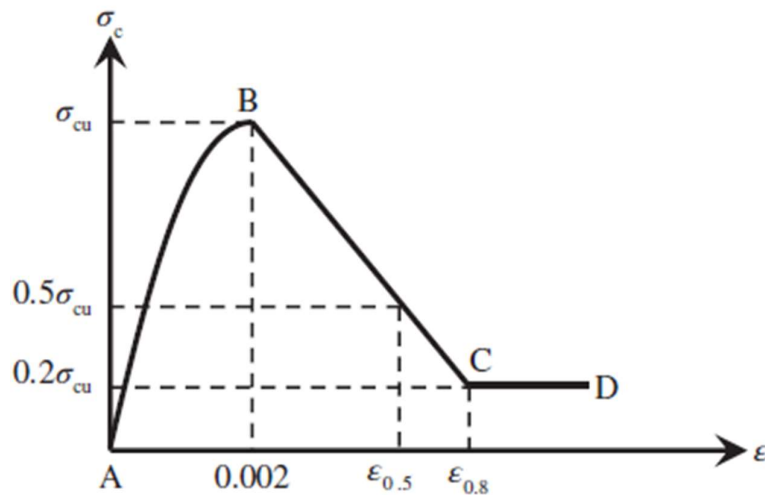
Figure 3.4. Kent and Park Model for confined and unconfined concrete (Uzbaş 2014).

2. To calculate unconfined concrete curve from $0.5*\sigma_{cu}$ to (Point B) it should be used the following equation and :

$$\sigma_c = \sigma_{cu} \left[2 * \left(\frac{\varepsilon_c}{\varepsilon'_c} \right) - \left(\frac{\varepsilon_c}{\varepsilon'_c} \right) {}^{\wedge}2 \right] \qquad (3\text{-}2)$$

3. To complete the curve from point (B to C) should be used this equation:

$$\sigma_c = m * (\varepsilon_c - 0.002) + \sigma_{cu} \qquad (3\text{-}3)$$

4. The softening phase continued until 20% of the unconfined cylinder compressive strength (Point C) was reached.

5. For obtaining the inelastic hardening strain the following equation should be used:

$$\varepsilon_c^{in,h} = \varepsilon_c - \frac{\sigma_c}{E0} \qquad (3\text{-}4)$$

6. To obtain the Compression Damage (dc):

$$d_c = 1 - \frac{\sigma_c}{\sigma_{cu}} \qquad (3\text{-}5)$$

7. Finally, ABAQUS automatically convert cracking strain to plastic strain according to the following Eq.:

$$\varepsilon_c^{\sim pl} = \varepsilon_c^{\sim in} - \left(\frac{d_c}{1-d_c}\right) * \frac{\sigma_c}{E_0} \qquad (3\text{-}6)$$

3.2.3. Cracks of concrete in finite element method

Finite element method (FEM) uses a numerical method to simulate and analyze the non-linear behavior of reinforced concrete elements. FEM should be agreed with an accurate representation of concrete cracking to achieve perfect modeling for the sample (Hammad 2015). According to ABAQUS User's Guide, classifies three approaches to simulate concrete material, and these approaches are Concrete Smeared Cracking, Cracking Model for Concrete and Concrete Damaged Plasticity (CDP) (ABAQUS User's Guide 2014)

A. Concrete smeared cracking

Cracking of concrete starts at any location when the concrete stresses reach one of the failure surfaces. This model is used for applications in which the concrete is exposed to essentially monotonic straining. The model exhibits concrete material either cracking or compressive crushing. Compressive yield surface controls the plastic straining of concrete in compression cases. The critical aspect of behaviour is cracking (ABAQUS User's Guide 2014).
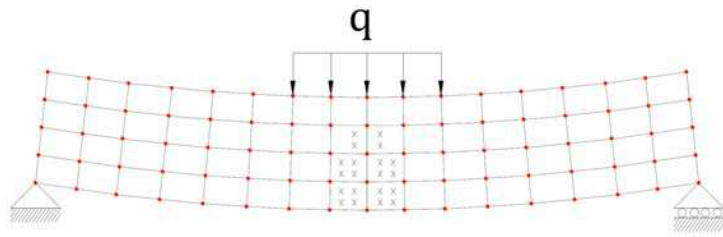
Figure 3.4. Smeared crack model (Chong 2004).

B. Cracking model for concrete

Cracking model assumes the behavior of concrete material in compression is as linear elastic behavior. It is prepared for applications in which the tensile cracking is dominated.(ABAQUS User's Guide 2014)

C. Concrete damaged plasticity

Concrete damaged plasticity (CDP) is dependent on the suggestions of scalar damage and is prepared for applications that the concrete material is exposed to arbitrary loading conditions and cycling loading. Concrete acts in a brittle manner and the main failure mechanisms are cracking in tension and crushing in compression (V.Chaudhari ve A. Chakrabarti 2012). The importance of this model is based on the deterioration of the concrete elastic stiffness by motivating the values of plastic straining in tension and compression cases. The required data and inputs of materials are obtained from the tensile and compression test of concrete (ABAQUS User's Guide 2014).

3.3. Steel Reinforcement

3.3.1. Mechanical behavior of steel reinforcement

The response of steel reinforcement is linear until the peak stress. Then, the reinforcement behavior starts to be a non-linear reach up to the ultimate tensile strain. At ultimate tensile strain, the reinforcement begins to neck, and strength reduced. The required parameters

of steel reinforcement to simulate in Finite element program are (E_S) elastic modulus, (f_y) the yield strength, (ε_u) the strain at peak strength, (f_u) the peak strength, (ε_{max}) the strain at which fracture occurs, and (f_s) the capacity prior to steel fracture.
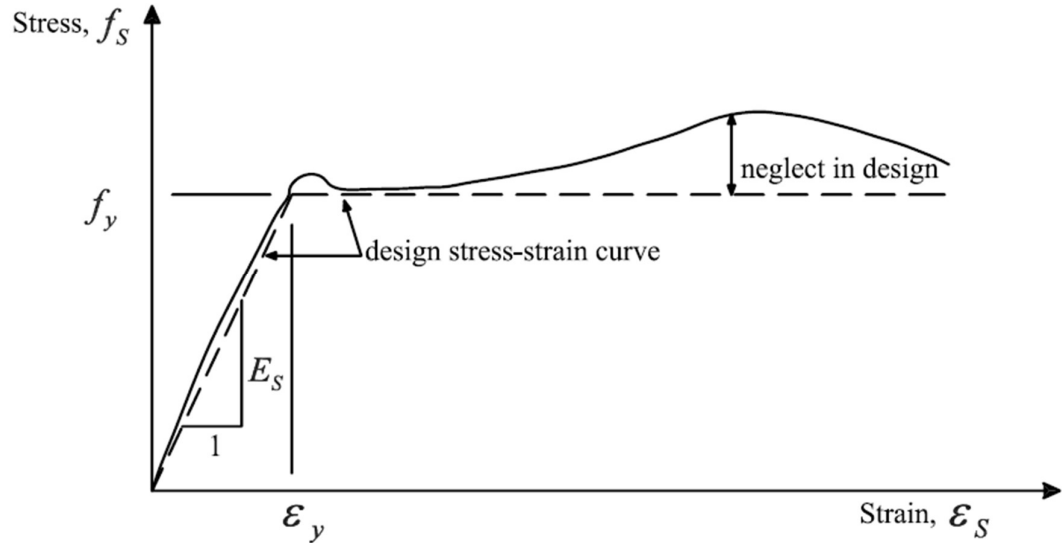
Figure 3.5. Tensile stress-strain curve for typical hot rolled reinforcement steels bars (Shidada 2011).

3.3.2. Approaches of modeling steel reinforcement bars

According to ABAQUS User's Guide there are three approaches to simulate reinforcement materials; and these are Smeared Steal Approach, Embedded Steel Approach and Discrete Steel Approach (ABAQUS User's Guide 2014).

A. Smeared approach

Smeared steel approach is assumed to be smeared over concrete elements at a particular angle of orientation as shown in Figure 3.7.a. The smeared steel approach method divides the stiffness of RC elements into the stiffness of concrete and steel, and a certain amount contributes each type of stiffness. For RC structures with densely distributed

reinforcement, this type of formulation is considered valuable. (ABAQUS USER'S GUIDE, 2014)

B. Embedded approach

The embedded steel approach considers each reinforcing bar like an axial member incorporated into the concrete element by the principle virtual work as shown in Figure 3.7.b. There is a compatibility between the displacement of embedded steel and the displacement of the concrete element. The significant advantage of the embedded steel formulation is the reinforcing steel can be defined arbitrarily regardless of the mesh shape and size of the concrete base element (ABAQUS User's Guide 2014, Hammad 2015).

C. The Discrete approach

The last approach, is based on spate elements to represent the reinforcing steel as shown in Figure 3.7.c. This approach greatly facilitates the inclusion of bond-slip effects between steel and concrete elements and the steel truss elements. A major disadvantage of this approach is must be an overlap between the mesh boundary of the concrete element and the direction and location of the steel reinforcement (ABAQUS User's Guide 2014).
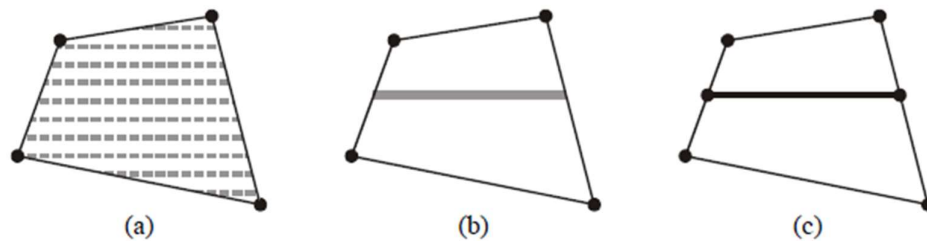
Figure 3.6. The approaches of modelling of steel reinforcement bars: (a) Smeared approach. (b) Embedded approach. (c) Discrete approach (Chong 2004)

3.4. Fiber Reinforced Polymer (FRP)

3.4.1. Mechanical behavior of FRP

Fiber reinforced polymer (FRP) is a composite material consists of fibers and matrix resin. These composed materials are considered heterogeneous materials. The properties of FRP depend on the following these factors (Masuelli 2016):

1. Fiber length and orientation within the matrix.
2. The relative proportions of fiber and matrix.
3. The mechanical properties of the fiber, matrix and resin.
4. The method of manufacture.

The typical stress-strain relations of fibers, matrix and FRP materials are shown in Figure 3.8. Consequently, the relation of FRP is linear elastic up to failure and don't have any yielding behavior like reinforcement steel. Figure 3.9. illustrates the comparison between behavior both of FRP materials and normal reinforcement steels based on stress-strain behavior.
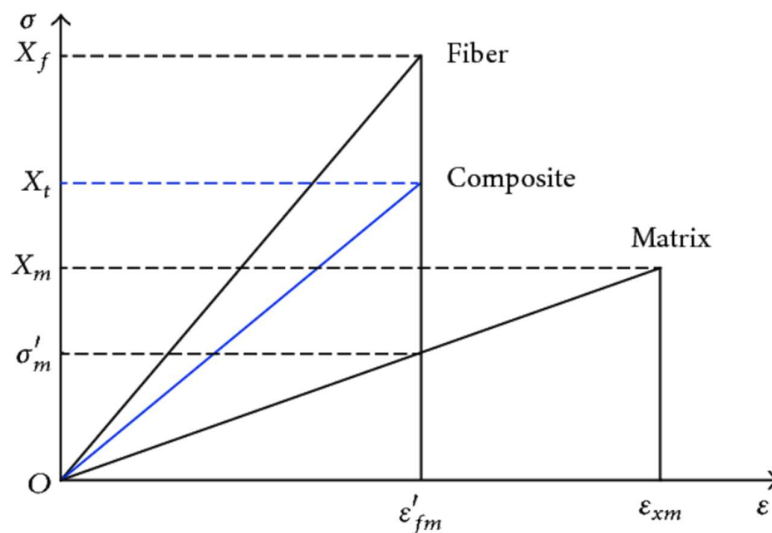
Figure 3.7. Stress-Strain relationships for fibers, matrix and FRP (Wu et al. 2014)
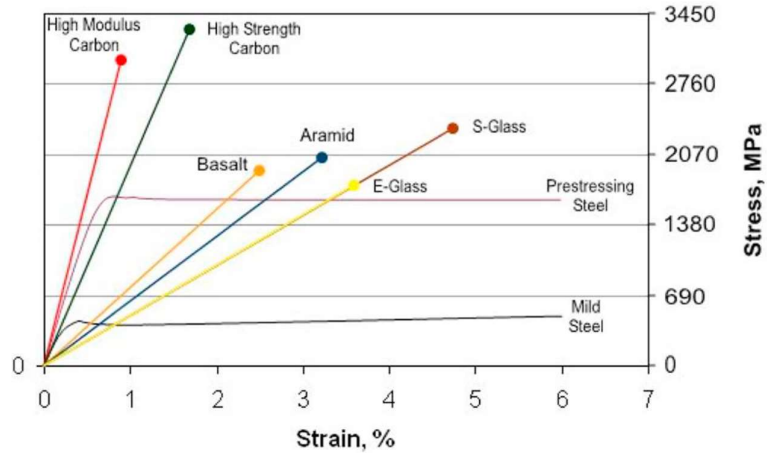
Figure 3.8. The behaviour of reinforcement bars and FRP based on stress-strain relationships (Mugahed Amran et al. 2018).

Table 3.1. Compare among the most common mechanical properties of steel, GFRP, BFRP, AFRP and CFRP respectively (Mugahed Amran et al. 2018).

Reinforcing material	Yield strength (MPa)	Density, (g/cm³)	Tensile strength (MPa)	Specific gravity	Elastic modulus (GPa)	Strain at break, %
Steel	500–500	7.75–8.05	–	7.8	(200)	–
Glass FRP	600–1400	2.11–2.70	480–1600	1.5–2.5	35–51	1.2–3.1
Basalt FRP	1000–1600	2.15–2.70	1035–1650	2.7–2.89	45–59	1.6–3.0
Aramid FRP	1700–2500	1.28–2.6 1.39–1.45	1720–2540	1.38–1.39	41–125	1.9–4.4
Carbon FRP	1755–3600	1.55–1.76	1720–3690	1.0–1.1	120–580	0.5–1.9

3.4.2. Finite element modeling of FRP

FRP materials are classified as elastic orthotropic material and the damage of this material initiates without significant plastic deformation. Hashin's failure criteria are recommended from ABAQUS User's Guide to simulate FRP materials. Hashin's criterion is developed its prediction ability through the quadratic interaction criterion between the different tractions. Hashing criterion introduces six criteria for initiation of tension and compression damage for fiber and matrix and at the interface level(Chaht et al. 2019). The damage model is defined by providing the longitudinal and transverse tensile and compression strengths of CFRP and the longitudinal and transverse shear strengths (Mohammed Ali Kadhim ve Hadi Adheem 2018). These criteria of damage have the following general forms (Chaht et al. 2019):

33

1- It assumes that the damage is characterized by progressive degradation of material stiffness.

2- FRP has six different criteria of damage modes are

    a. Tensile fiber failure (Rupture):

$$\sigma_{11} \geq 0 \left(\frac{\sigma_{11}}{X_T}\right)^2 + \frac{\sigma_{12}^2 + \sigma_{13}^2}{S_{12}^2} = \begin{cases} \geq 1 \; failure \\ < 1 \; no \; failure \end{cases} \tag{3-7}$$

    b. Compressive fiber failure (Buckling):

$$\sigma_{11} < 0 \left(\frac{\sigma_{11}}{X_C}\right)^2 = \begin{cases} \geq 1 \; failure \\ < 1 \; no \; failure \end{cases} \tag{3-8}$$

    c. Tensile matrix failure (Cracking):

$$\sigma_{22} + \sigma_{33} > 0 \frac{(\sigma_{22}+\sigma_{33})^2}{Y_T^2} + \frac{\sigma_{23}^2 - \sigma_{22}\sigma_{33}}{S_{23}^2} + \frac{\sigma_{12}^2 + \sigma_{13}^2}{S_{12}^2} = \begin{cases} \geq 1 \; failure \\ < 1 \; no \; failure \end{cases} \tag{3-9}$$

    d. Compressive matrix failure:

$$\sigma_{22} + \sigma_{33} < 0 \left[\left(\frac{Y_C}{2S_{23}}\right)^2 - 1\right]\left(\frac{\sigma_{22}+\sigma_{33}}{Y_C}\right) + \frac{(\sigma_{22}+\sigma_{33})^2}{4S_{23}^2} + \frac{\sigma_{23}^2 - \sigma_{22}\sigma_{33}}{S_{23}^2} + \frac{\sigma_{12}^2 + \sigma_{13}^2}{S_{12}^2} =$$

$$\begin{cases} \geq 1 \; failure \\ < 1 \; no \; failure \end{cases} \tag{3-10}$$

    e. Inter-laminar tensile failure (Crashing) :

$$\sigma_{33} > 0 \left(\frac{\sigma_{33}}{Z_T}\right)^2 = \begin{cases} \geq 1 \; failure \\ < 1 \; no \; failure \end{cases} \tag{3-11}$$

    f. Inter-laminar compressive failure:

$$\sigma_{33} < 0 \left(\frac{\sigma_{33}}{Z_C}\right)^2 = \begin{cases} \geq 1 \ failure \\ < 1 \ no \ failure \end{cases} \qquad (3\text{-}12)$$

4. RESULTS and DESCUSSION

4.1. Introduction

A numerical analysis using ABAQUS is performed to simulate RC beams strengthened by CFRP. The first one was for flexure strengthening (Balamuralikrishnan ve Jeyasehar 2009), and the second one was for shear strengthening (Alagusundaramoorthy 2002).

After that, the obtained results from modelling beams were verified with experimental results of beams based on Load-Deflection curves and the values of loads and deflection at failure. The validated finite element model, parametric studies was performed using ABAQUS to investigate the effect of the following parameters on the behavior of strengthened beams: number of layers, layer length and jacketing methods.

4.2. Description of Experimental Beams

In this section, the dimension of flexure beams, shear beams samples and the name of them are presented. Each type of them has a control beams model and a strengthened beam model.

4.2.1. Flexure beam

In this thesis, the dimension of flexure control beam was taken from the samples of (Balamuralikrishnan ve Jeyasehar 2009) to simulate in ABAQUS program. The details of control and strengthened beam models are presented.

A. Control beams

The total length of the beam is 3200 mm, the width of 125 mm and the height of 250 mm. The spacing between the centerline of supports are 2900 mm. The beam is exposed to two static loads through two loading plates, the clear distance between loading plates is 900 mm and the type of test is four-point bending test.

RC beams are illustrated in Figure 4.1. The reinforcement steel bars at compression side are 2Ø10 mm, and at tension side are 2Ø12 mm, the diameter of stirrups is 6mm, and the space between them are 150mm.
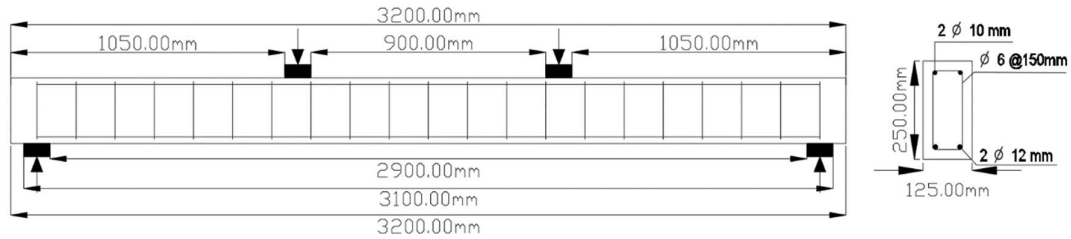
Figure 4.1. Description of the flexure control beam model (Balamuralikrishnan ve Jeyasehar 2009).

B. Flexure strengthened beam

The control beam was externally strengthened with 0.18 mm thickness of CFRP layers. Different methods of strengthening techniques were used as at the tensile side, U-shaped, and different lengths of CFRP on RC beams to enhance RC beams. Figure 4.2. shows the details of the different strengthening methods for flexure beams.
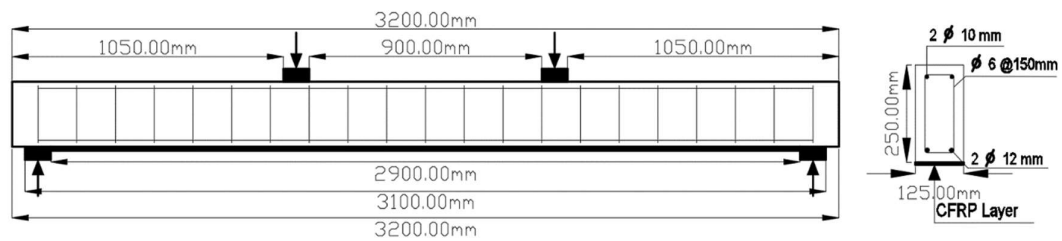
Longitudinal Section   Cross Section

a) Flexure beam strengthened at tensile side.
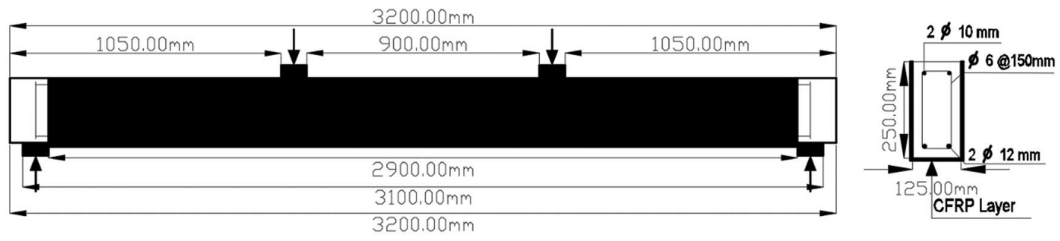
Longitudinal Section   Cross Section

b) Flexure beam strengthened by using jacketing method.
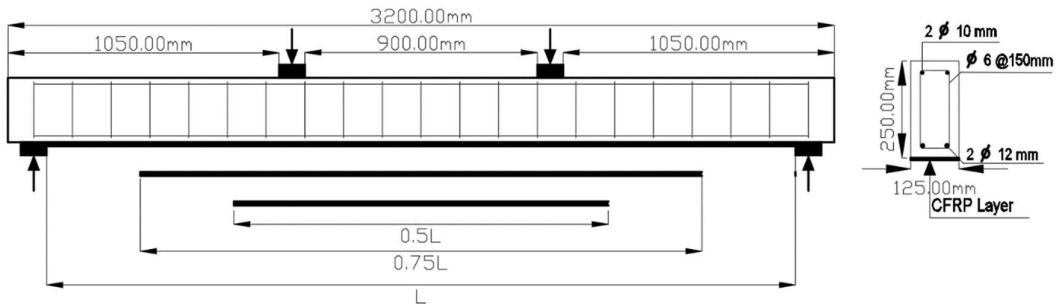
Longitudinal Section   Cross Section

c) Flexure beam strengthened by changing Length of Fibers.

Figure 4.2. Description of flexure strengthened beam model (Balamuralikrishnan ve Jeyasehar 2009).

4.2.2. Shear beam

In this thesis, the dimension of shear control beam was depended on the samples of (Alagusundaramoorthy 2002) in dimension, material properties and type of tests.

A. Shear control beam

The total length of the beam is 2130 mm, the width of 230 mm and the height of 380 mm. The spacing between the centerline of supports is 1810 mm. The details of the shear RC

beam are illustrated in Figure 4.3. The reinforcement steel bars at compression side is 2Ø10 mm and tension steel bars of the beam is 2Ø25 mm, the diameter of stirrups is 6 mm, and the space between them is 300 mm.

Longitudinal Section   Cross Section
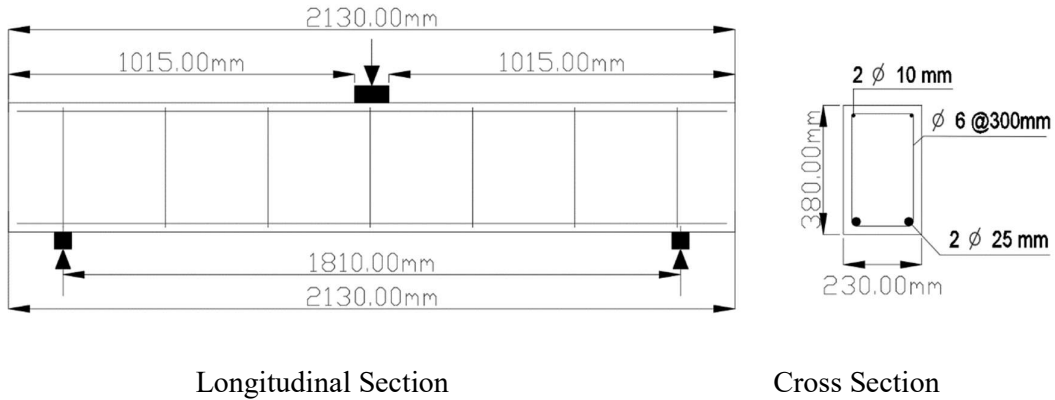
Figure 4.3. Description of control shear model (Alagusundaramoorthy 2002)

B. Shear strengthened beam

The control beam was strengthened with 0.18 mm thickness of CFRP layers. Different methods of strengthening were applied on RC beams as U-shaped and wrapped method of CFRP to enhance RC beams. Figure 4.4. shows the details of strengthened shear beams.
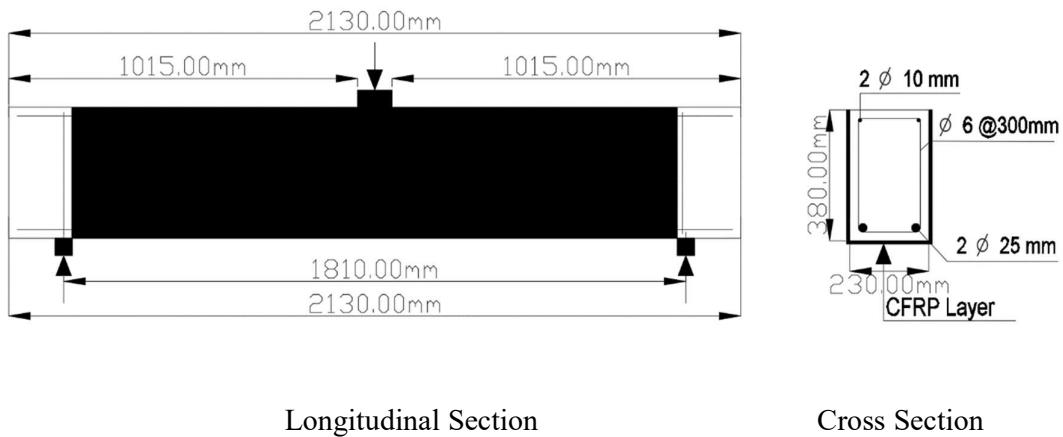
Longitudinal Section   Cross Section
a)   Shear beam strengthened at three side.

Longitudinal Section   Cross Section
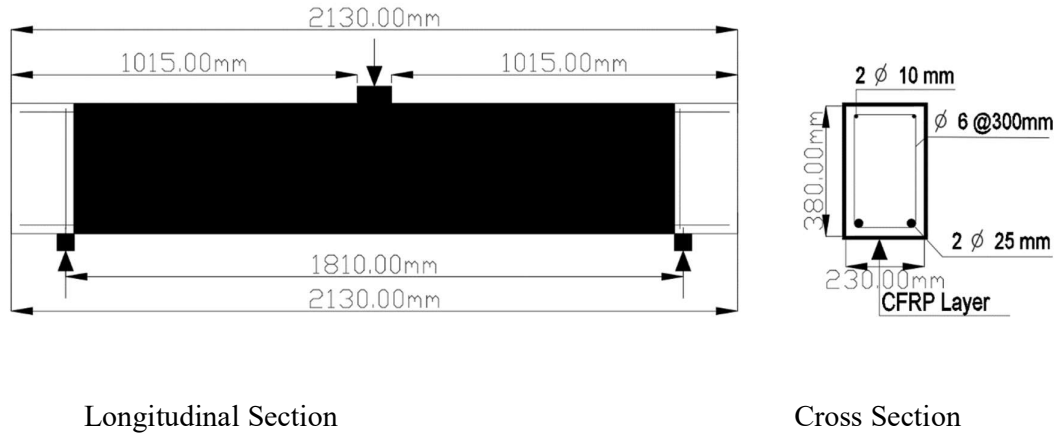
b) Shear beam strengthened by completely CFRP wrapping.

Figure 4.4. Description of Shear Strengthened Beam Model (Alagusundaramoorthy 2002)

4.3. Modelling Assumptions

As it is known, concrete and steel materials are non-homogeneous materials, and thus to simulate these complex materials some assumptions should be suggested to obtain realistic results. In this study, the following assumptions are considered for flexure beam model and shear beam:

1. The main materials of beam, concrete and steel are considered homogenous materials in modelling program.
2. The bonding between concrete and steel reinforcement is perfect.
3. The value of Poisson's ratio throughout the testing period is assumed constant.
4. The bond between concrete and CFRP layers are perfect.

4.4. Description of Materials Modelling Types in ABAQUS

This section explains the types of materials (concrete, steel reinforcement, loading plates, supports plates and carbon fiber reinforced polymer) are used in ABAQUS. The types of

modelling elements are selected based on recommendations of ABAQUS User's Guide and previous researches (Hammad 2015, Ibrahim ve Mahmood 2009).

4.4.1. Concrete

C3D8R was used to model concrete material in the ABAQUS program. It consists of cube shape has eight nodes with three degrees of freedom. The node has capable to simulate and calculate plastic deformation, crushing and cracking values. Figure 4.5. shows the shape and nodes location for C3D8R element to model concrete beams in ABAQUS (ABAQUS User's Guide 2014).
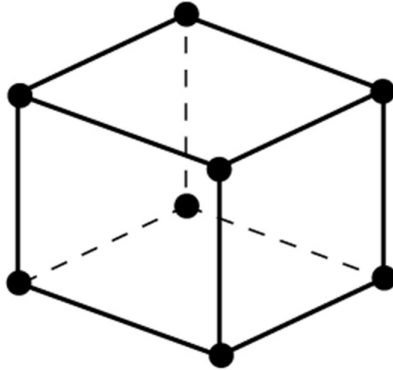
Figure 4.5. C3D8R's geometry (ABAQUS User's Guide 2014).

4.4.2. Reinforcement steel bars

C3D8R and T3D2 were used to simulate the longitudinal reinforcement steel bars in shear and flexure beams. The reinforcement steel stirrups in flexure and shear beams were simulated by T3D2 in the ABAQUS program. C3D8R consists of cube shape has eight nodes with three degrees of freedom in each its node. The node has capable to simulate and calculate plastic deformation, crushing and cracking values (ABAQUS User's Guide 2014). The reason for using C3D8R models in simulating the longitudinal bars of shear beams is to get accurate results. The experiment was done with the T3D2 to simulate the longitudinal bars, but the results were not correct.

T3D2 is used to model reinforcement steel bars in flexure beams. T3D2 supports loading only along the centerline of the element and can simulate and calculate plastic deformation, creep, rotation, large deformation, and significant strain capabilities. Figure 4.6. shows the shape and node location for this element to model reinforcement bars in ABAQUS (ABAQUS User's Guide 2014).
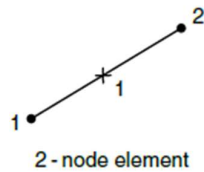
Figure 4.6. The element using to model steel bars (ABAQUS User's Guide 2014)

4.4.3. Modelling types of loading and supporting steel plates

C3D8R was used to model loading plates and supporting plates in the ABAQUS program. C3D8R consists of cube shape has eight nodes with three degrees of freedom in each of its node. The node can simulate and calculate plastic deformation, crushing and cracking values (ABAQUS User's Guide 2014).

4.4.4. Carbon fiber reinforcement polymer (CFRP)

S4R is used to model carbon fiber reinforcement polymer in the ABAQUS program. It is a 4-node general-purpose shell, reduced integration with hourglass control, finite membrane strains. Figure 4.7. shows the shape and node location for this element to model Carbon Fiber Reinforcement Polymer in ABAQUS (ABAQUS User's Guide 2014).
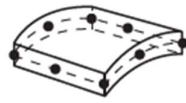
Figure 4.7. Shell S4R geometry (ABAQUS User's Guide 2014)

Table 4.1. The element types are used for modelling of flexure and shear beams in the program.

Material Type	ABAQUS Element
Reinforced Concrete	C3D8R
Steel Reinforcement (Longitudinal / Stirrups)	C3D8R/T3D2
Loading and Supporting Steel Plates	C3D8R
Carbon Fiber Reinforced Polymer (CFRP)	Shell S4R

4.5. Material Properties

4.5.1. Constitutive model of concrete

C3D8R element is used to model concrete material. The C3D8R requires a linear at elastic and nonlinear damaged plasticity of material properties to selection failure criteria of concrete.

A. Linear isotropic properties of concrete

Linear isotropic of concrete is the initial tangent for a stress-strain curve that starts from zero value until 50% of the ultimate compressive stress of concrete. The elastic modulus of elasticity determines the slope of the line based on equation (3-1), the value of (Ec) for flexure beam was 26.6 MPa and 30 MPa for shear beam, and value of Poisson's ratio (v) was assumed to be 0.2 for flexure and shear beam.

B. Nonlinear isotropic properties

The nonlinear curve is the second part of the stress-strain curve of concrete material, Kent and park mathematical model has been used to calculate the coordinates points of the nonlinear curve. Equations (3-2) to (3-6) were used to calculate values of the nonlinear curve of concrete material.

Figure 4.8. and 4.9. show the stress-strain relationship of concrete material and table 4.2 and 4.3 show the used values in the ABAQUS program to modelling the concrete material in flexure beam and shear beam models respectively. The curve starts at 50% of the compressive strength of concrete. Equation (3-2) was used to calculate the maximum compressive strength of concrete. From Eq. (3-3) to (3-6) were calculated stress and strain values from starting point to softening phase which continue to 20% of maximum compressive strength of concrete. After ultimate compressive strength, the perfectly plastic behaviour of concrete was assumed. The values of nonlinear concrete were input by using concrete damaged plasticity CDP approach in ABAQUS program.
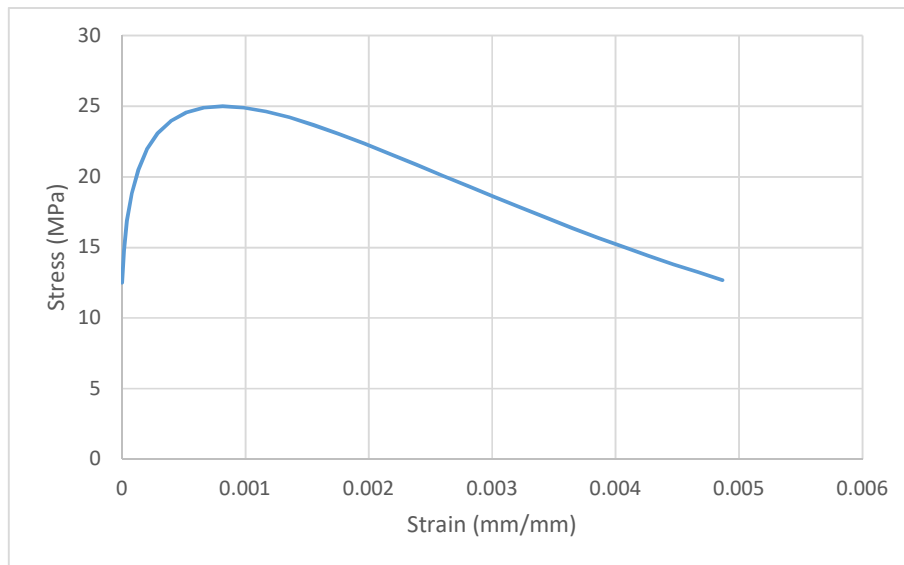
Figure 4.8. Stress-strain curve of concrete material for flexure beam model.
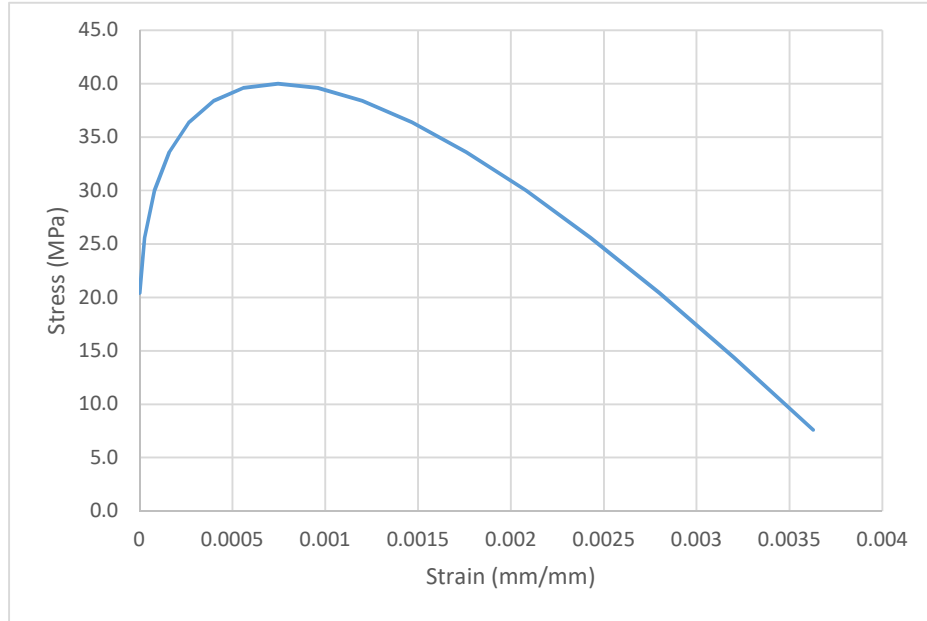
Figure 4.9. Stress-strain curve of concrete material for shear beam model.

Table 4.2. The used values in the ABAQUS program to modelling the concrete material.

Material's parameter	B 25	Plasticity parameter	
		Dilation angle	35
Concrete Elasticity		Eccentricity	0.1
		fb0/fc0	1.16
E (GPa)	23.5	K	0.667
Poisson Ratio	0.2	viscosity Parameter	0
Concrete compressive behavior		Concrete compression damage	
Yield Stress	Inelastic Strain	Damage Parameter C	Inelastic Strain
12.5	0	0.00	0
14.8	1.50E-05	0.00	1.50E-05
16.9	4.00E-05	0.00	4.00E-05
18.8	7.90E-05	0.00	7.90E-05

Concrete compressive behavior		Concrete compression damage	
Yield Stress	Inelastic Strain	Yield Stress	Inelastic Strain
20.5	1.32E-04	0.00	1.32E-04
21.9	0.000202	0.00	0.000202
23.1	0.00029	0.00	0.00029
23.9	0.000396	0.00	0.000396
24.5	0.00052	0.00	0.00052
24.9	0.000661	0.00	0.000661
25.0	0.000816	0.00	0.000816
24.9	0.000985	0.00	0.000985
24.6	0.001166	0.01	0.001166
24.2	0.001356	0.03	0.001356
23.7	0.001553	0.05	0.001553
23.0	0.001756	0.08	0.001756
22.4	0.001964	0.11	0.001964
21.6	0.002174	0.14	0.002174
20.9	0.002386	0.17	0.002386
20.1	0.002598	0.20	0.002598
19.3	0.002811	0.23	0.002811
18.5	0.003023	0.26	0.003023
17.8	0.003235	0.29	0.003235
17.1	0.003445	0.32	0.003445
16.4	0.003653	0.35	0.003653
15.7	0.00386	0.37	0.00386
15.0	0.004065	0.40	0.004065
14.4	0.004268	0.42	0.004268
13.8	0.004469	0.45	0.004469
13.2	0.004669	0.47	0.004669
12.7	0.004866	0.49	0.004866
12.2	0.005062	0.51	0.005062
11.7	0.005257	0.53	0.005257

Concrete compressive behavior		Concrete compression damage	
Yield Stress	Inelastic Strain	Yield Stress	Inelastic Strain
11.2	0.005449	0.55	0.005449
10.8	0.005641	0.57	0.005641
10.4	0.00583	0.59	0.00583
10.0	0.006019	0.60	0.006019
9.6	0.006206	0.62	0.006206
9.2	0.006392	0.63	0.006392
8.9	0.006576	0.64	0.006576
8.6	0.00676	0.66	0.00676
8.3	0.006942	0.67	0.006942
8.0	0.007124	0.68	0.007124
7.7	0.007304	0.69	0.007304
7.5	0.007448	0.70	0.007448
3	0	0	0
1.664354	0.000281	0.445215	0.000281
1.179148	0.000507	0.606951	0.000507
0.923358	0.000718	0.692214	0.000718
0.76383	0.000923	0.74539	0.000923
0.654173	0.001124	0.781942	0.001124
0.573836	0.001324	0.808721	0.001324
0.512265	0.001522	0.829245	0.001522
0.463463	0.00172	0.845512	0.00172
0.423761	0.001917	0.858746	0.001917
Concrete tensile behavior		Concrete tension damage	
Yield Stress (MPa)	Cracking strain	Damage Parameter	Cracking strain
2.4	0	0	0
1.331483	0.000262	0.445215	0.000262
0.943318	0.000473	0.606951	0.000473

Yield Stress (MPa)	Cracking strain	Damage Parameter	Cracking strain
0.738687	0.00067	0.692214	0.00067
0.611064	0.00086	0.74539	0.00086
0.523338	0.001048	0.781942	0.001048
0.459069	0.001235	0.808721	0.001235
0.409812	0.00142	0.829245	0.00142
0.37077	0.001604	0.845512	0.001604
0.339009	0.001788	0.858746	0.001788

Table 4.3. Material properties of concrete for ABAQUS shear beam model.

Material's parameter	B 40	Plasticity parameter	
		Dilation angle	31
Concrete Elasticity		Eccentricity	0.1
		fb0/fc0	1.16
E (GPa)	25.7	K	0.667
Poisson Ratio	0.2	viscosity Parameter	0
Concrete compressive behavior		Concrete compression damage	
Yield Stress	Inelastic Strain	Damage Parameter	Inelastic Strain
20.4	0	0.00	0
25.6	2.67E-05	0.00	2.67E-05
30.0	8.00E-05	0.00	8.00E-05
33.6	1.60E-04	0.00	1.60E-04
36.4	2.67E-04	0.00	2.67E-04
38.4	0.0004	0.00	0.0004
39.6	0.00056	0.00	0.00056
40.0	0.000746667	0.00	0.000746667
39.6	0.00096	0.01	0.00096
38.4	0.0012	0.04	0.0012
36.4	0.001466667	0.09	0.001466667
33.6	0.00176	0.16	0.00176
30.0	0.00208	0.25	0.00208
25.6	0.002426667	0.36	0.002426667
20.4	0.0028	0.49	0.0028

Concrete compressive behavior		Concrete compression damage	
Yield Stress	Inelastic Strain	Damage Parameter	Inelastic Strain
14.4	0.0032	0.64	0.0032
7.6	0.003626667	0.81	0.003626667
Concrete tensile behavior		Concrete tension damage	
Yield Stress (MPa)	Cracking strain	Damage Parameter	Cracking strain
4	0	0	0
0.04	0.001333333	0.99	0.001333333

4.5.2. Reinforcement steel

The stress-strain curve response of steel bars is characterized by the same values in tension and compression cases. The stress-strain curve is divided into two different parts, the linear elastic and non-linear plastic parts. Steel reinforcement response starts by linear curve until close up to (f_y). Then, the response of steel material changes from linear to non-linear curve and the value of stain begin increasing with stability value of stress until reach to failure load. In ABAQUS program, It is defined as a one-dimensional wire and with metal plasticity models to describe the behavior of the rebar materials. To achieve this important procedure, for flexure beams model, T3D2 is used to model the longitudinal reinforcement and stirrups but for shear beams model, C3D8R is used to model the longitudinal reinforcement bars and T3D2 to model the stirrups. The Elastic-perfectly plastic model is used in the ABAQUS program to describe reinforcement bars' behavior in tension and compression. Figure 4.10. shows the stress-strain curve for reinforcement bars. Table 4.4 and 4.5 explain the material properties of steel reinforcement used in ABAQUS for flexure and shear beams.
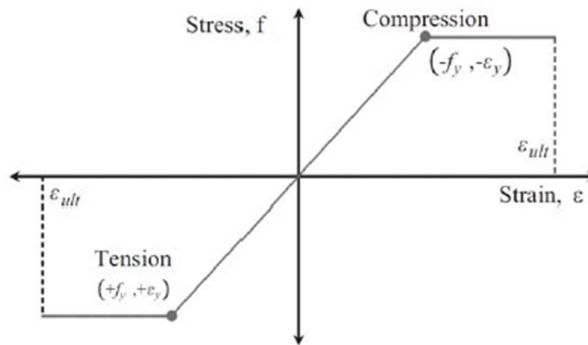
Figure 4.10. The stress-strain curve for reinforcement bars.

Tables 4.4. The material's properties of steel reinforcement used in ABAQUS for flexure.

Name of Element	Element Type	Material Properties	
		Linear Isotropic	
		E	200,000 MPa
		Poisson's Ratio	0.3
(Longitudinal Reinforcement)	T3D2		
		Plastic Isotropic	
		Yield Stress	420 MPa
		Plastic Strain	0
		Linear Isotropic	
		E	200,000 MPa
		Poisson's Ratio	0.3
Stirrups	T3D2		
		Plastic Isotropic	
		Yield Stress	420 MPa
		Plastic Strain	0

Table 4.2. Reinforcement bars properties for shear beam in ABAQUS.

Name of Element	Element Type	Material Properties	
(Longitudinal Reinforcement)	C3D8	Linear Isotropic	
		E	200,000 MPa
		Poisson's Ratio	0.3
		Plastic Isotropic	
		Yield Stress	420 MPa
		Plastic Strain	0
Stirrups	T3D2	Linear Isotropic	
		E	200,000 MPa
		Poisson's Ratio	0.3
		Plastic Isotropic	
		Yield Stress	420 MPa
		Plastic Strain	0

4.5.3. Properties of supporting and loading steel plates

Steel plates were used as support and loading plates in ABAQUS program. C3D8R is the type of modelling element which used to model the supports and steel plates. Tables 4.6. explains the properties of materials for supports and loading steel plates which used in ABAQUS program.

Table 4.3. Properties of materials for supports and loading steel plates which used in ABAQUS.

Name of Element	Element Type	Material Properties	
Loading and supporting steel plates	C3D8R	Linear Isotropic	
		E	200,000 MPa
		Poisson's Ratio	0.3

4.5.4. Properties of carbon fiber reinforced polymer (CFRP)

S4R was used to model carbon fiber reinforced polymer (CFRP) for strengthening flexure and shear beams in the ABAQUS program. The CFRP composite strip was modeled as a lamina model to define the elastic moduli and shear moduli and Poisson's ratio in two directions. Hashin's failure criteria was used to define the properties of CFRP in ABAQUS program. The Hashin's failure criteria is calculated by Computer Aided Design Environment for Composites (CADEC), Autodesk Helius Composite, Composite Design and simulation software (CDS 3.1) and Automated System for Composite Analysis (ASCA). Composite Design and simulation software (CDS 3.1) is used to obtain the parameters of Hashin's failure criteria.

Parameters needed to define the material model for CFRP in ABAQUS flexure beam and shear beam models are shown in Tables 4.7. and 4.8.

Table 4.7. The values of CFRP used in ABAQUS.

Name of Element	Element Type	Material Properties	
CFRP for Flexure Beams	S4R	Linear Orthotropic	
		Longitudinal modulus (E1)	285000 MPa
		Transverse in-plane modulus (E2)	22800 MPa

Name of Element	Element Type	Material Properties	
CFRP for Flexure Beams	S4R	Transverse out-plane modulus (E3)	22800 MPa
		Major in-plane Passion's ratio	0.3
		Out-of-plane Passion's ratio	0.25
		Out-of-plane Passion's ratio	0.25
		In-plane shear modulus (Gxy)	13570 MPa
		Out-of-plane shear modulus (Gyz)	7860 MPa
		Out-of-plane shear modulus (Gxz)	13570 MPa
		Layer No.1	
		Thickness	0.18 mm
		Orientation	0 degree
Hashin's Failure Criteria			
Property			Value
Longitudinal Tensile Strength			2050
Longitudinal Compressive Strength			1200
Transverse Tensile Strength			62
Transverse Compressive Strength			190
Longitudinal Shear Strength			81
Transverse Shear Strength			81
Longitudinal Tensile Fracture Energy			45
Longitudinal Compressive Fracture Energy			45
Transverse Tensile Fracture Energy			0.6
Transverse Compressive Fracture Energy			0.6

Table 4.8. The values of CFRP used in ABAQUS.

Name of Element	Element Type	Material Properties	
CFRP for Shear Beams	S4R	Linear Orthotropic	
		Longitudinal modulus (E1)	228000 MPa
		Transverse in-plane modulus (E2)	15200 MPa

Name of Element	Element Type	Material Properties	
CFRP for Shear Beams	S4R	Transverse out-plane modulus (E3)	15200 MPa
		Major in-plane Passion's ratio	0.3
		Out-of-plane Passion's ratio	0.45
		Out-of-plane Passion's ratio	0.25
		In-plane shear modulus (Gxy)	9120 MPa
		Out-of-plane shear modulus (Gyz)	5241.4 MPa
		Out-of-plane shear modulus (Gxz)	9120 MPa
		Layer No.1	
		Thickness	0.30 mm
		Orientation	0 degree
Hashin's Failure Criteria			
Property			Value
Longitudinal Tensile Strength			1950
Longitudinal Compressive Strength			1080
Transverse Tensile Strength			62
Transverse Compressive Strength			170
Longitudinal Shear Strength			95
Transverse Shear Strength			95
Longitudinal Tensile Fracture Energy			68
Longitudinal Compressive Fracture Energy			68
Transverse Tensile Fracture Energy			0.2
Transverse Compressive Fracture Energy			0.2

4.6. Meshing of Samples

The type and size of meshing play an essential role in the analysis and results of samples. Therefore, for flexure beams, meshing was rectangular and the dimension was 20 mm. For shear beams the type of meshes were used rectangular and irregular meshes shapes to obtain the perfect performance of analytical data (ABAQUS User's Guide 2014). Figure 4.11. shows meshes of the reinforced concrete beam, support plates and loading plates for flexure beam
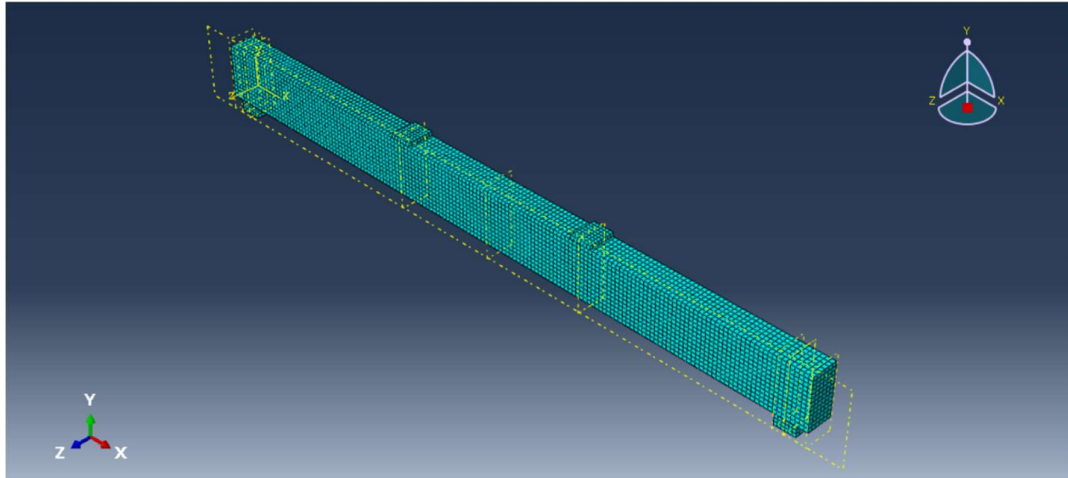
Figure 4.11. The meshing of the concrete beam and steel plates - flexure beam model.

Figure 4.12. shows meshes of shear reinforced concrete beam, support plates and loading plates for shear beam.
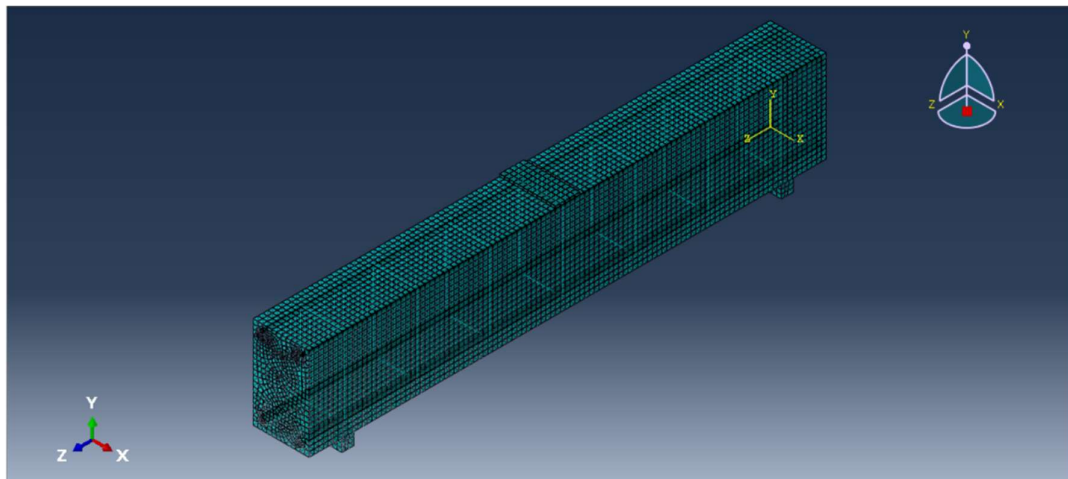

Figure 4.12. The meshing of the concrete beam and steel plates - shear beam model.

Figures 4.13. and 4.14. illustrate meshes of reinforcement steel modeled in ABAQUS for flexure beam.
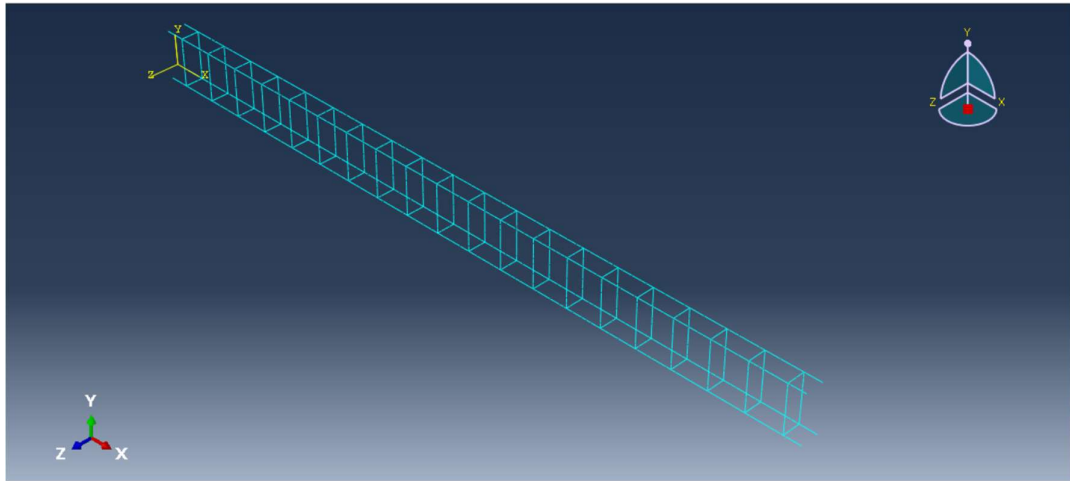
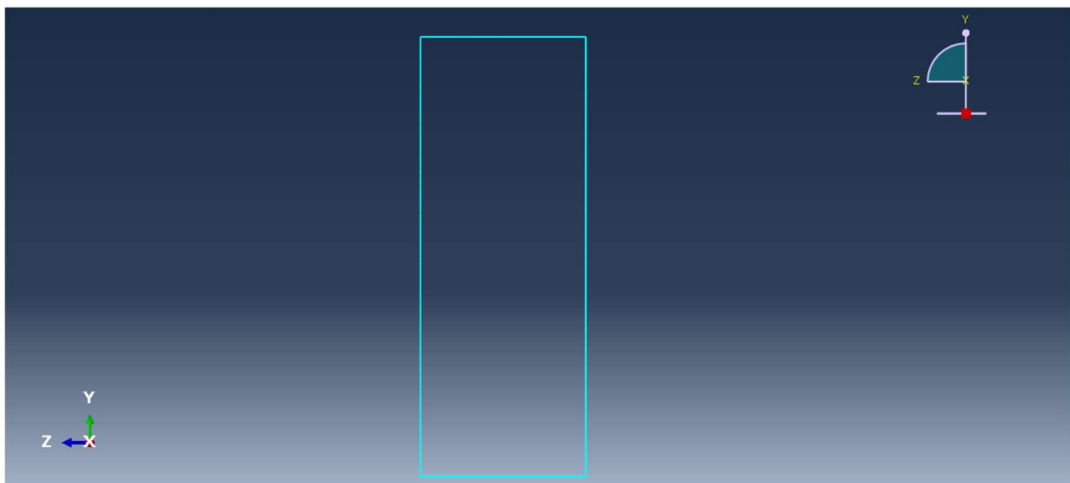**Figure 4.13.** Meshing of reinforcement for flexure beam model.

Figure 4.14. Meshing of stirrups reinforcement steel for flexure beam model

Figures 4.15. the meshes of reinforcement steel modeled in ABAQUS for shear beam model.
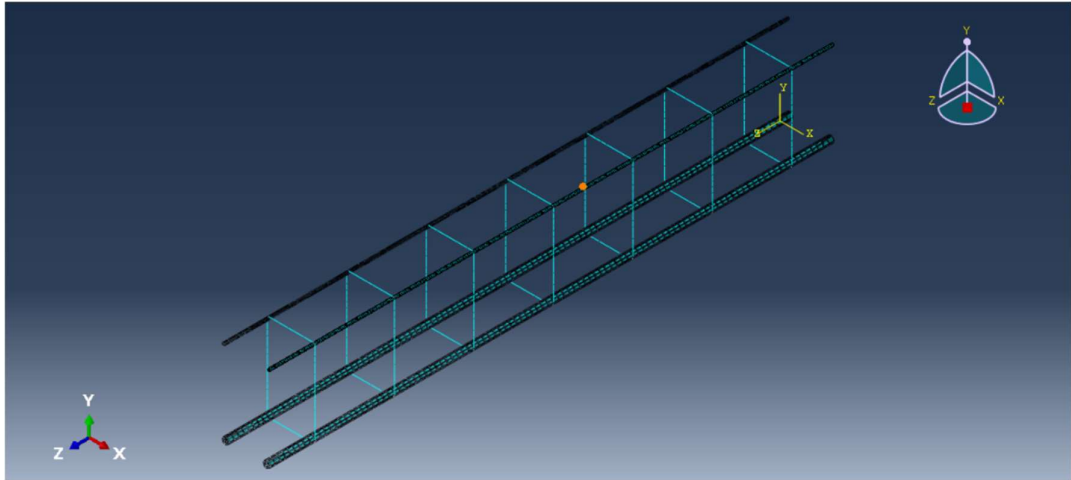
Figure 4.15. Reinforcement configuration for shear beam.

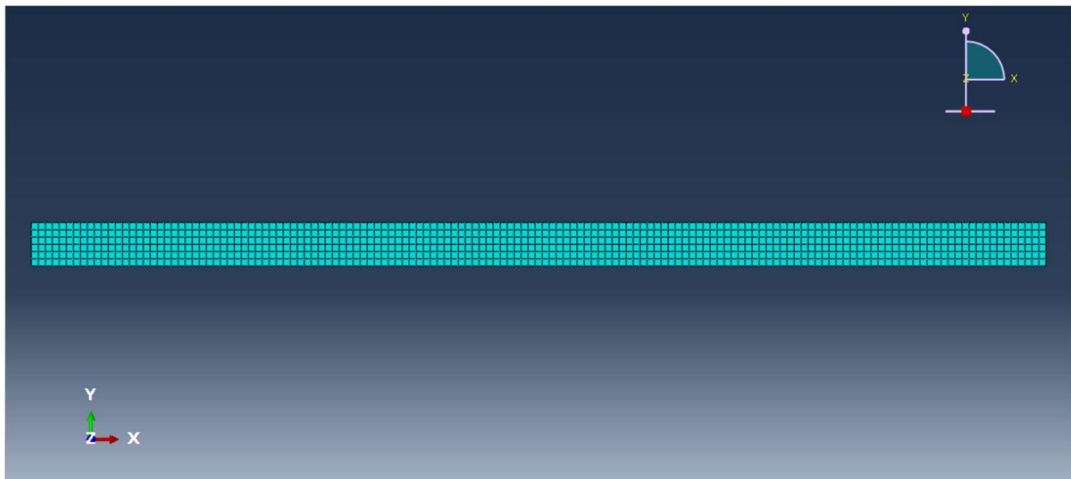Figures from 4.16. to 4.18. show the meshing of CFRP fabric layer in ABAQUS for flexure and shear beam model.

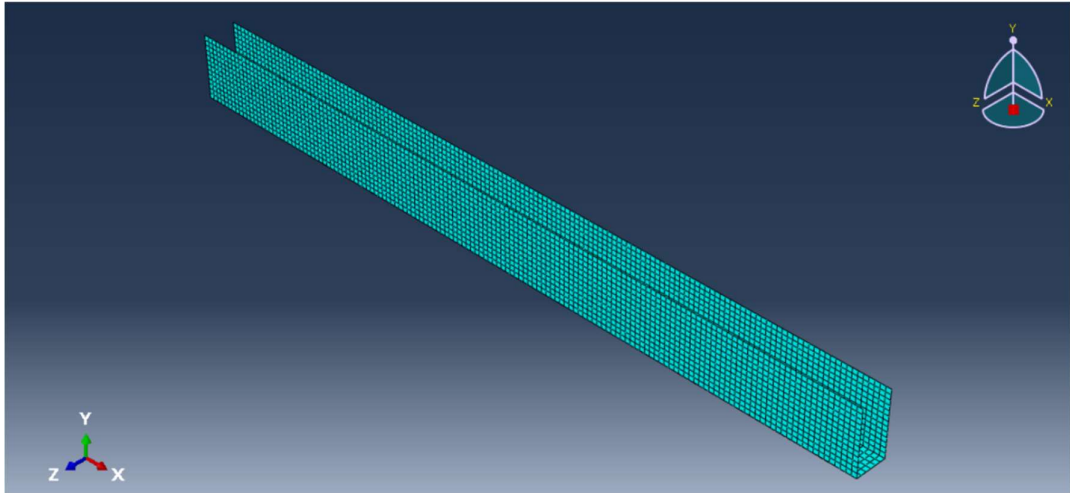**Figure 4.16.** Meshing of CFRP layer in ABAQUS for flexure beam.

Figure 4.17. The meshing of CFRP layer in ABAQUS for flexure and shear beam model.
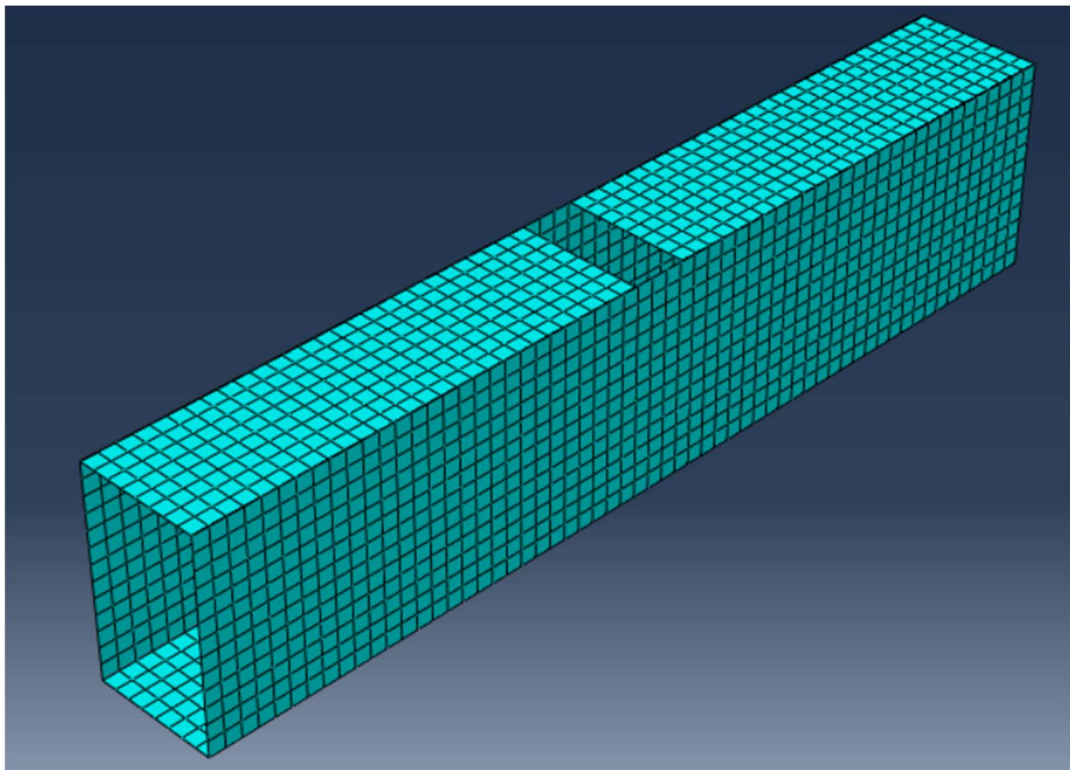

Figure 4.18. The meshing of CFRP layer in ABAQUS for shear beam model.

Figures 4.19. and 4.20. show the meshing of all model components: concrete beam, steel loading, supporting plates, steel reinforcement, and CFRP layer, for flexure beam and shear beam models.
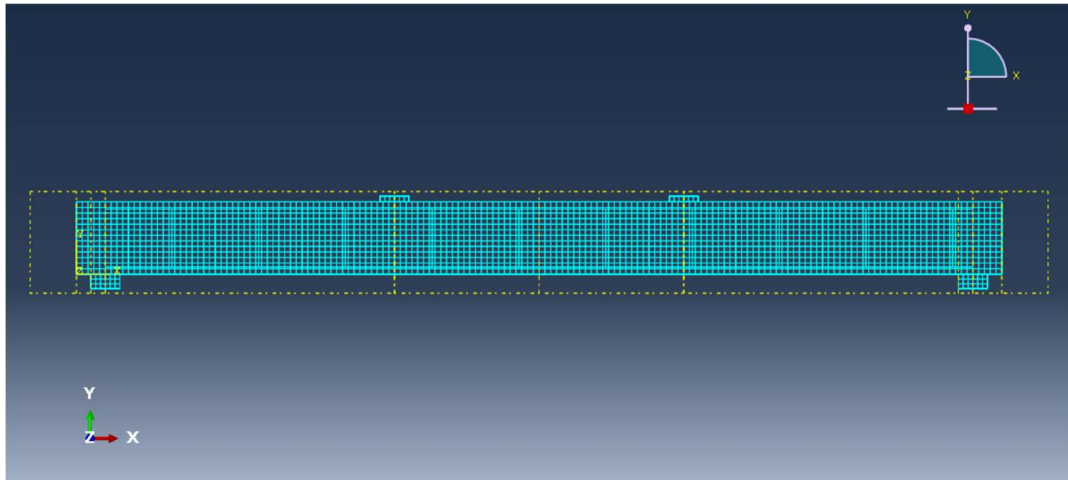

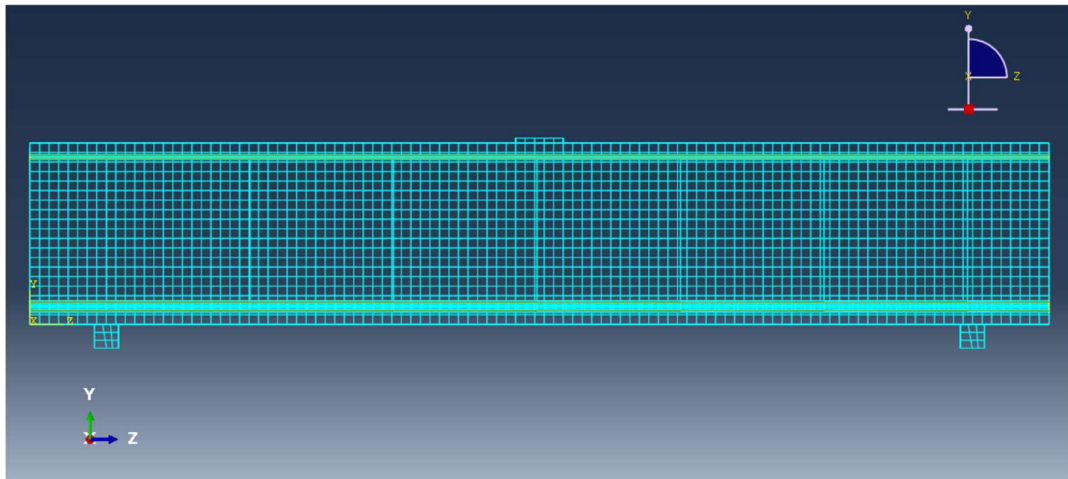**Figure 4.19.** The overall meshing of the flexure beam.

Figure 4.20. The overall meshing of the shear beam.

4.7. Boundary Conditions and Applied loads

Displacement boundary conditions are needed to constrain the model and to get a unique solution and to ensure that the model acts the same way as the experimental beam;

boundary conditions need to be applied at points of symmetry, and where the supports and loadings exist.

4.7.1. Support plates

Type of Supports plates (pin and roller) was selected according to experimental data (Alagusundaramoorthy 2002, Balamuralikrishnan ve Jeyasehar 2009). For pin supports, were given constraint in the Y-axis, Z-axis and free in X-axis and rotation. Roller support was given constraint in the Y-axis and free in X-axis, Z-axis and rotation. Figures 4.21. and 4.22. show the types of supports selected for flexure and shear beam.
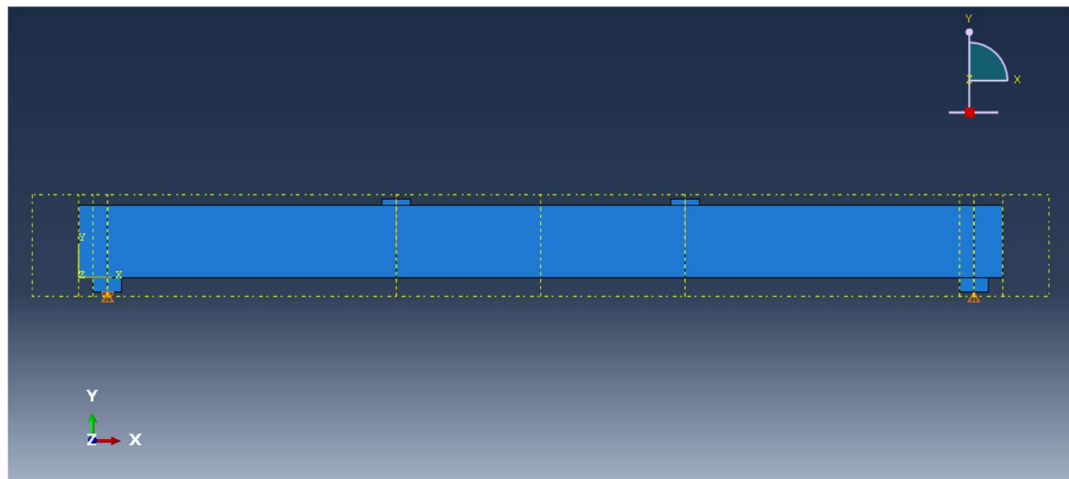

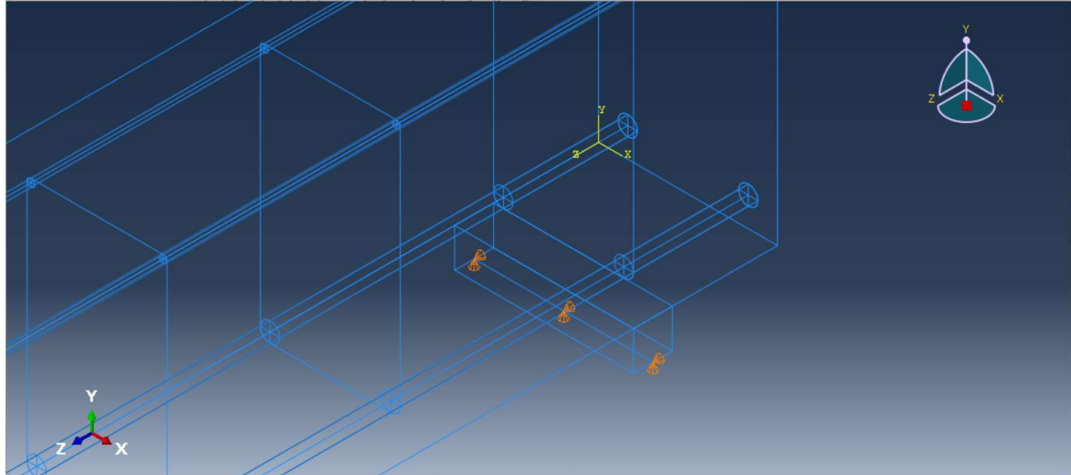**Figure 4.21.** Supports of flexure beams.

Figure 4.22. Supports of shear beams.

4.7.2. Static applied loads

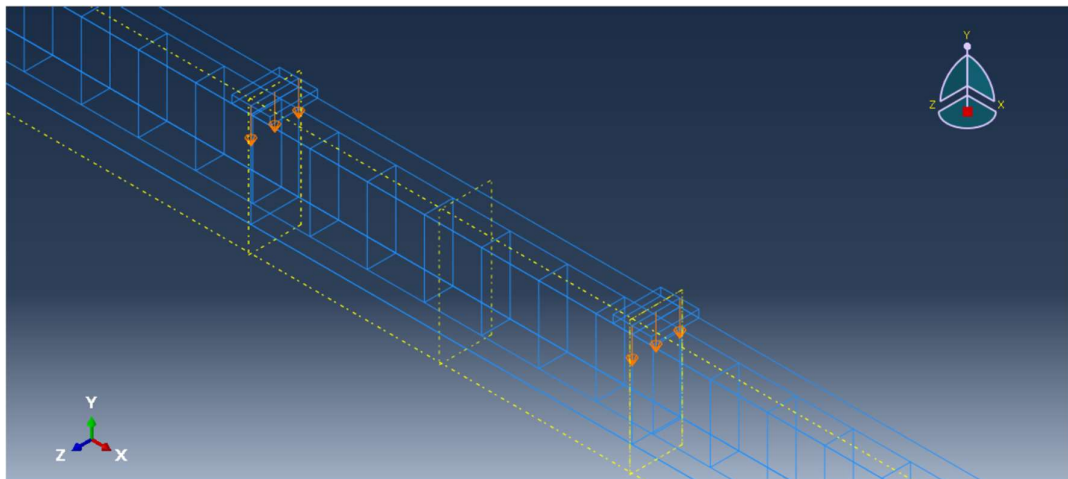Static loads was applied on the center lines of plates as shown in Figures 4.23. and 4.24.

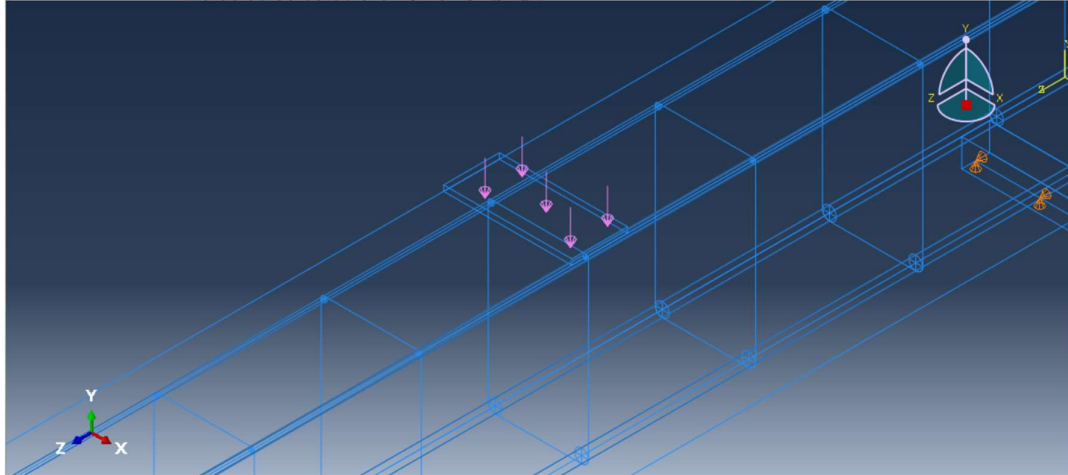**Figure 4.23.** Loading Plate for Flexure Beam.

Figure 4.24. Loading Plate for Shear Beam.

4.7.3. Creating job analysis of samples

The relevant job should be established to solve any finite element's problem. After this step, the extracted answer is visualized analytically and graphically.

4.8. Validation of ABAQUS Finite Element Models

The finite element models developed for flexure and shear beams were verified by comparing results from the FE analysis with experimental test data. The verification process was based on the following criteria load-mid span deflection curves, crack pattern, ultimate load capacity and deflection at failure.

4.8.1. Load - mid span deflection curves of beams

A. Flexure beam

A comparison of the load-deflection curve for the flexure control beam and strengthened beam as reported in the experimental investigation show in figure 4.25. (Balamuralikrishnan & Antony Jeyasehar, 2009).
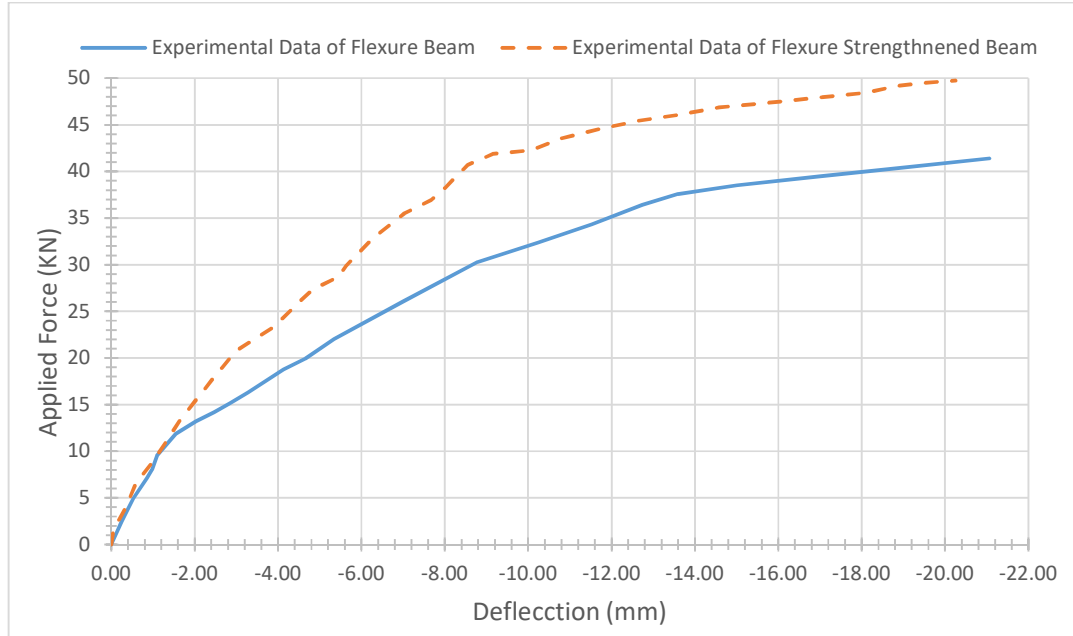
Figure 4.25. Comparison of experimental load-deflection curves for flexure beam.

Flexure control beam

Figure 4.26. shows that the load-deflection curve obtained from the finite element analysis agrees well with the experimental data for the flexure control beams. However, the analytical results were stiffer than the experimental results as shown in Figure 4.26. This is due to the simulation programs assumes the interaction between concrete and steel bars is perfect consequently, could be noticed this results in the diagrams of the tests. The first cracking of finite analysis is 11 KN, which is lower than the load of 15 KN from the experimental results by -26.6%. The maximum ultimate carrying capacity of 48.9 KN from the model is higher than the ultimate carting capacity of 41.25 KN from the experimental data by 18.54 %. The maximum deflection of the control beam is 21.03 mm and the maximum deflection of the strengthening modeling beam is 21.06 mm by 0.12%
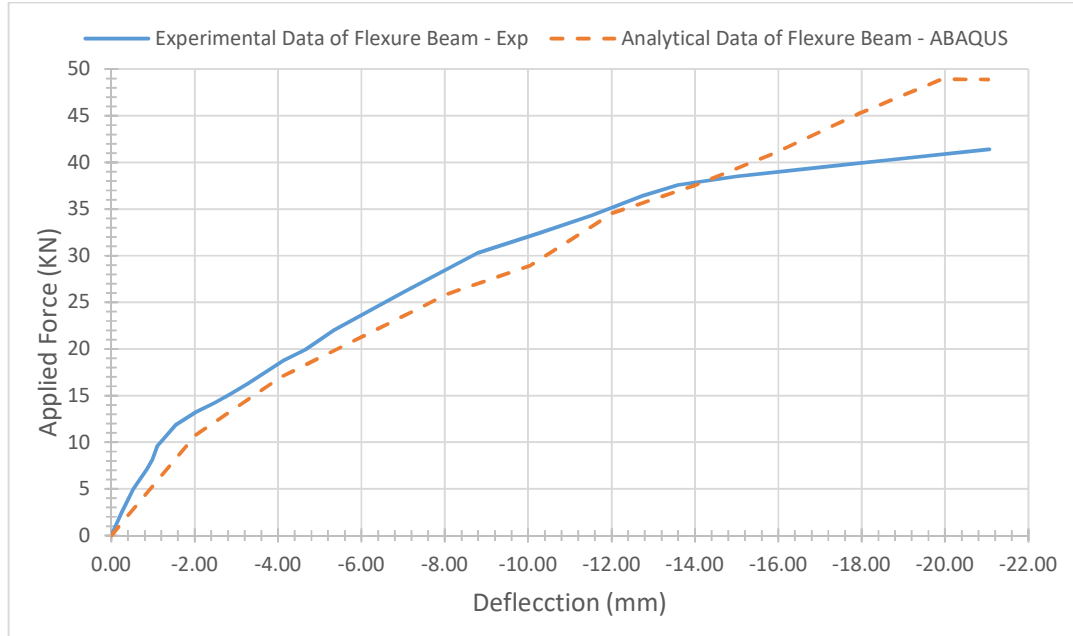
Figure 4.26. The differences between experimental and analytical data for flexure beam.

Flexure strengthened beam

Figure 4.27. shows that the load-deflection curve obtained from the finite element analysis agrees well with the experimental data for the flexure strengthened beams. The analytical results were softer than the experimental results until 41.08 KN. Then, the stiffness of analytical data was stiffer than experimental results and could be noticed in the diagrams of the tests Figure 4.27. The first cracking of finite element samples is 10.9 KN, which is lower than the load of 10 KN from the experimental results by -9.00%. The maximum ultimate carrying capacity of 58.9 KN from the model is higher than the ultimate carting capacity of 49.5 KN from the experimental data by 18.54 %. Therefore, the maximum deflection of the experimental control beam is 19.92 mm, and the maximum deflection of the strengthening modeling beam is 20.25 mm by 1.63%.
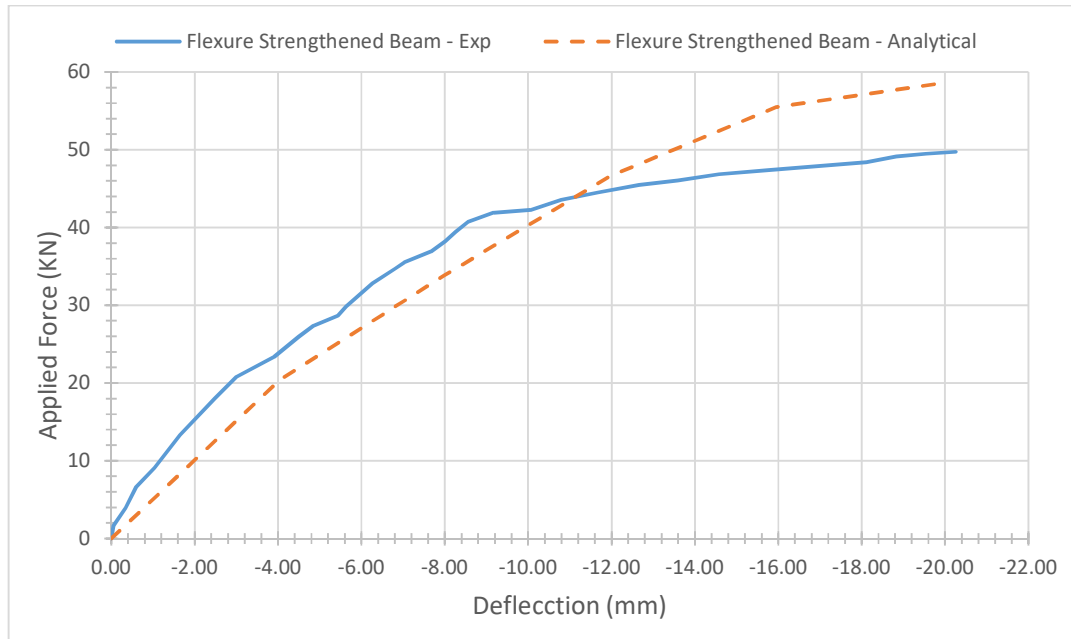
64

Figure 4.27. Comparison of experimental and analytical results of flexure strengthened beam.

B. Shear beam

A Comparison of the load-deflection curve for the shear control beam and strengthened beam reported in the experimental investigation shows in figure 4.28. (Alagusundaramoorthy, Harik, & Choo, 2002).
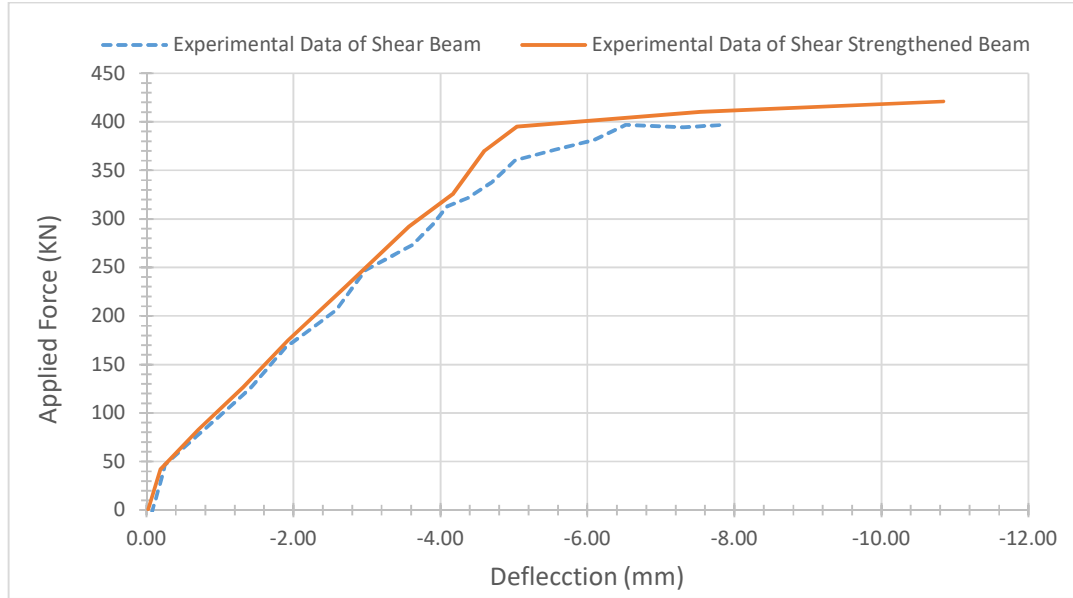
Figure 4.28. Comparison of experimental load-deflection Curves for shear Beam.

Shear control beam

The analytical results were almost close to experimental results as indicated in Figure 4.29. The maximum ultimate carrying capacity of 396.25 KN from the model is close to the ultimate carting capacity of 398.25 KN from the experimental data by -0.5 %. The maximum deflection of the control beam is 6.42 mm and the maximum deflection value of the strengthening modeling beam is 7.88 mm by 18.53%

Figure 4.29. Comparison of experimental and analytical results of shear control beam.

Strengthening shear beam

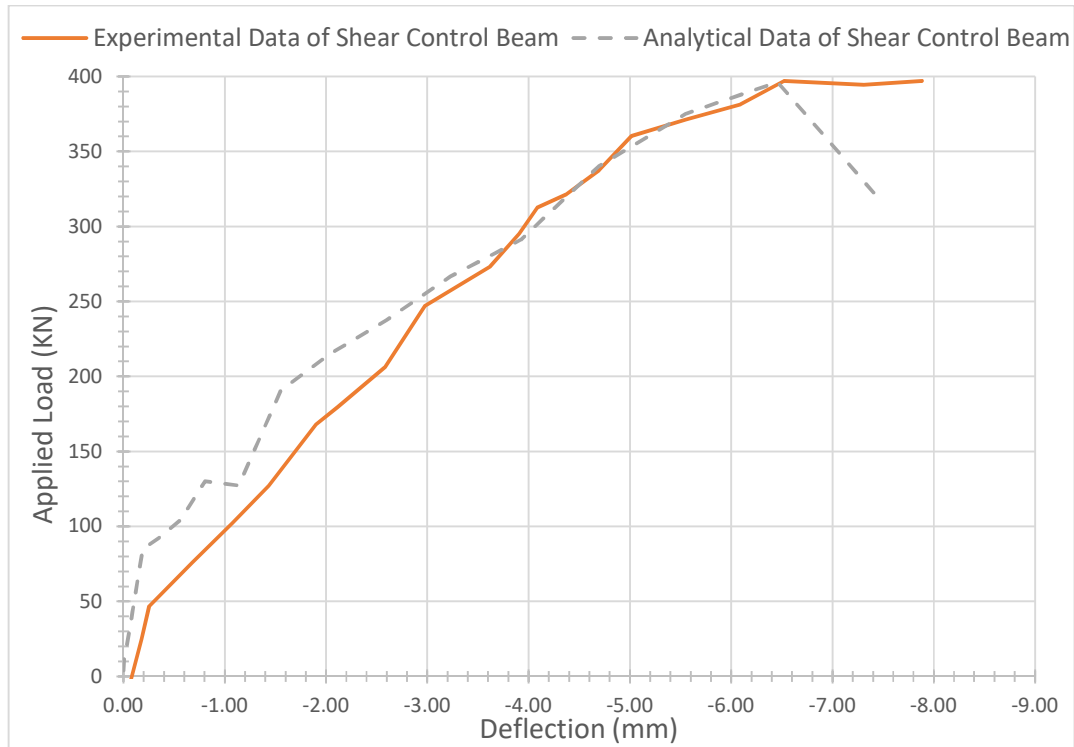Figure 4.30. shows that the load-deflection curve obtained from the finite element analysis agrees well with the experimental data for the shear strengthened beams. The analytical results are stiffer than experimental results but the experimental curve behavior is more ductility than the analytical beam, as shown in Figure 4.30. The maximum ultimate carrying capacity of 421.21 KN from the model is higher than the ultimate carting capacity of 421.20 KN from the experimental data by -0.5 %. Therefore, the maximum deflection value of the control beam is 10.84 mm and the maximum deflection of the strengthening modeling beam is 8.28 mm by 23.6%
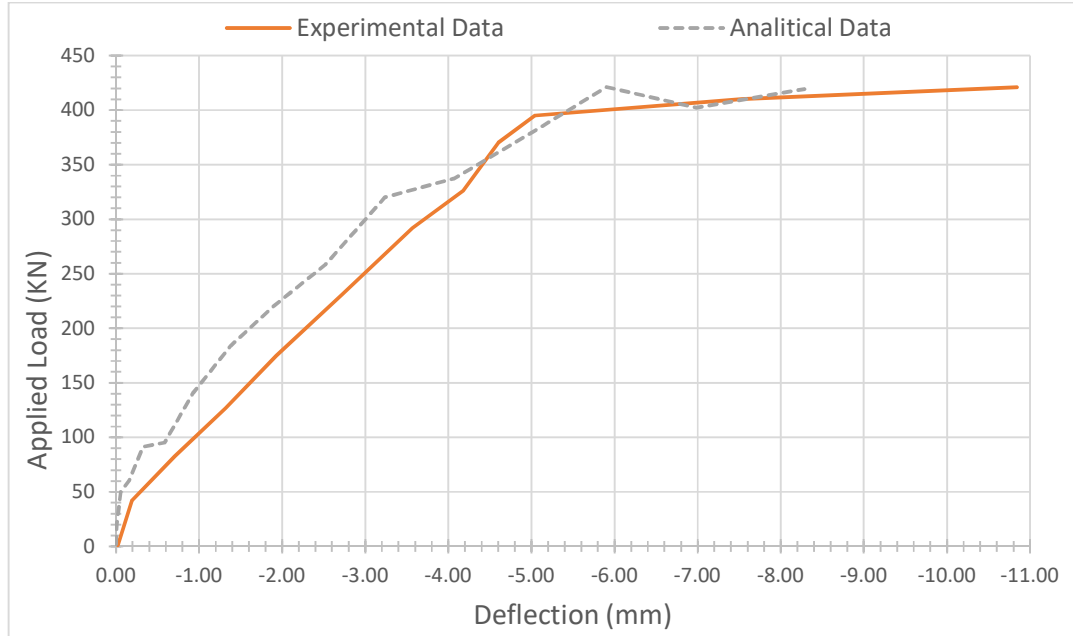
Figure 4.30. Comparison of Experimental and analytical results of shear strengthened beam.

4.8.2. Crack patterns

In ABAQUS, stresses and strains are calculated at integration points of the concrete solid elements. A cracking sign is represented by a different color that appears when principal tensile stress exceeds the ultimate tensile strength of the concrete or principal compressive stress reaches up to the ultimate compressive strength of concrete. The cracking sign appears perpendicular to the direction of the principal stress. Figures from 4.31 to 4.34. showed that evolutions of crack patterns developing for each beam at different loading steps.
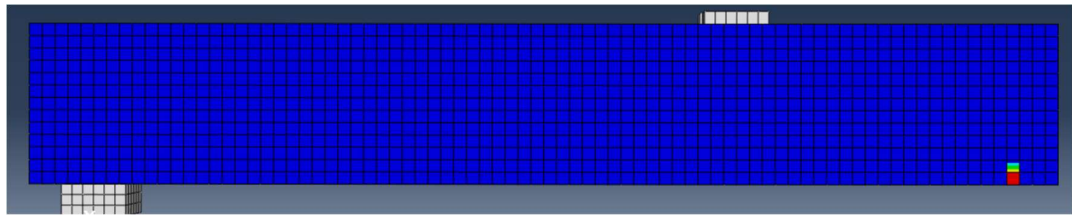
A. Crack pattern for flexure beam

The changing of cracks color at different load steps for the modeling of flexure control and strengthened beams were shown in figure 4.31. and 4.32. Flexural cracks occurred early at mid-span. When applied loads increase, vertical flexural cracks spread horizontally from the mid-span to the support. Increasing applied loads induces additional

diagonal and flexural cracks. Finally, compressive cracks appeared at nearly the last applied load steps. The appearance of the cracks defines the failure mode for the beams.

Flexure control beam

The increasing crack pattern of the flexure control beam are shown in figure 4.31, (a), (b), (c), (d) and (e).

a) Crack Pattern at 10.9 KN
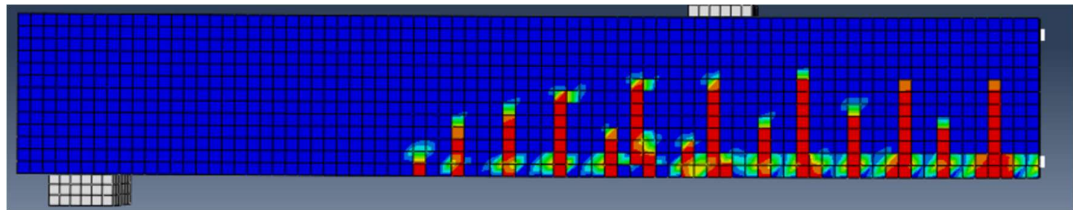
b) Crack Pattern at 21.5 KN

c) Crack Pattern at 41.02 KN

d) Crack Pattern at 48.5 KN

e) Experimental Crack Pattern at Failure Load (49.5 KN)

Figure 4.31. Crack propagations of flexure control beam.

Comparing crack pattern obtained from the finite element analysis ABAQUS at the last converged load step with failure photographs from the actual beam, shows that the crack pattern from ABAQUS and the actual beam agree very well. The flexure control beam failed in flexure at the mid-span, with yielding of the steel reinforcement, followed with a compression failure at the top of the beam.

Flexure strengthened Beam

The increasing crack pattern of the flexure strengthened beam are shown in Figure 4.32., (a), (b), (c) and (d).

a) At Load 16 KN
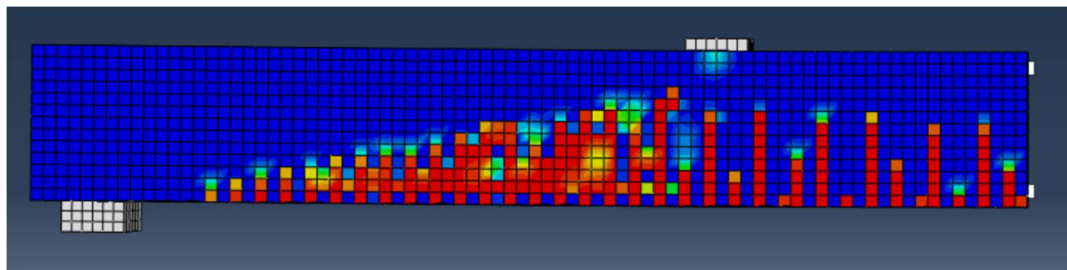
b) At Load 29.8 KN
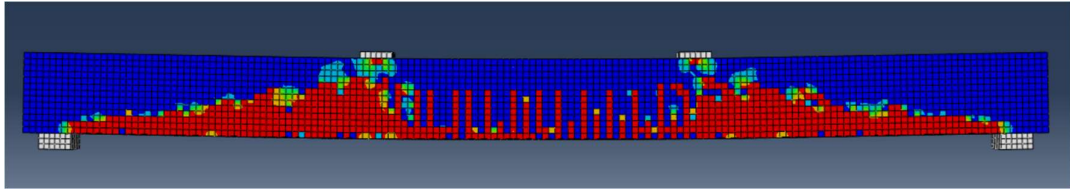
c) At Load 60 KN

d) Experimental Crack Pattern at Failure Load (49.5 KN)

Figure 4.32. Crack propagations of flexure strengthened beam.

Comparing crack pattern of flexure strengthened beam from ABAQUS at last load step with a photograph of the experimental strengthened beam's crack pattern, shows the crack patterns are very good. The flexure strengthened beam failed in flexure at the mid-span with the yielding of the steel reinforcement.

B. Crack pattern for shear beam

The propagation of cracks at different load steps for modeling of shear control and strengthened beams is shown in Figures 4.33. and 4.34. Flexural cracks occur early at mid-span. When applied loads increase, vertical flexural cracks spread horizontally from the mid-span to the support. At a higher applied load, diagonal tensile cracks appear. Finally, compressive cracks appear at nearly the last applied load steps. The appearance of the cracks defines the failure mode for the beams.
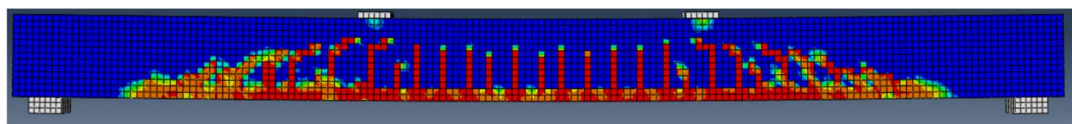
Shear control beam

The increasing propagation crack pattern of the shear control beam is shown in the figure 4.33., (a), (b), (c), (d), (e), (f) and (g).
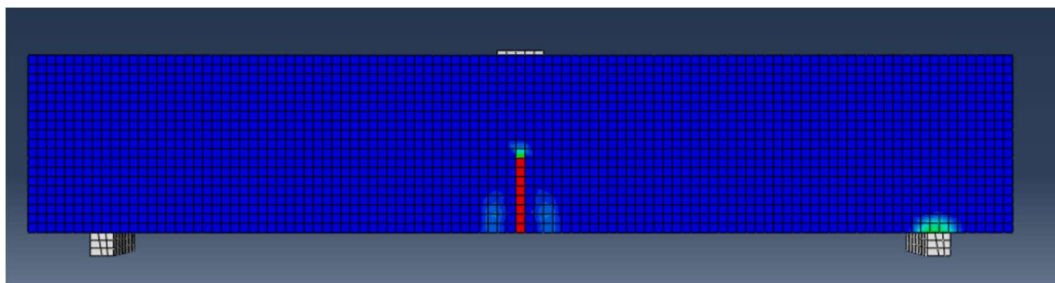
a) Crack Pattern at 50 KN
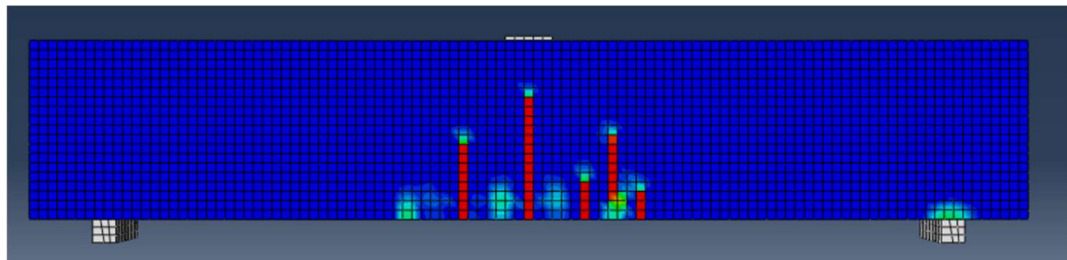
b) Crack Pattern at 135 KN

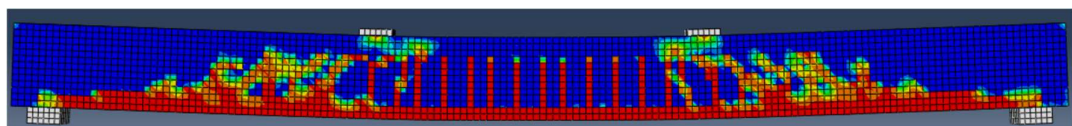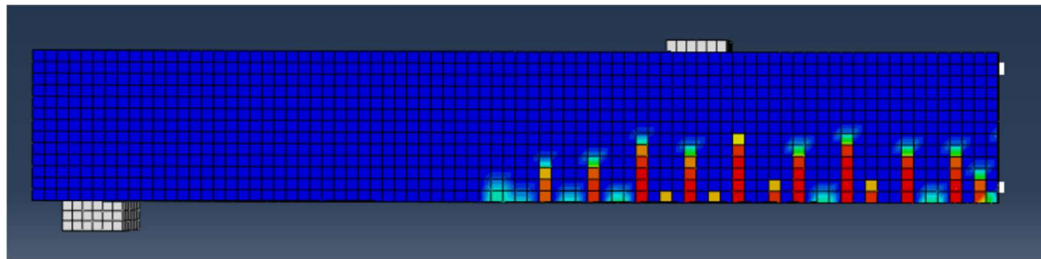c) Crack Pattern at 190 KN
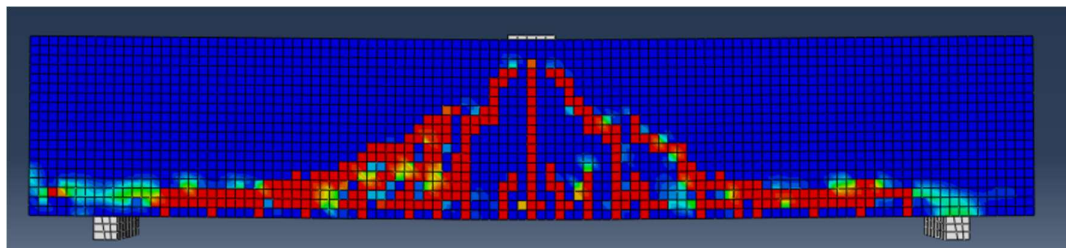
d) Crack Pattern at 290 KN
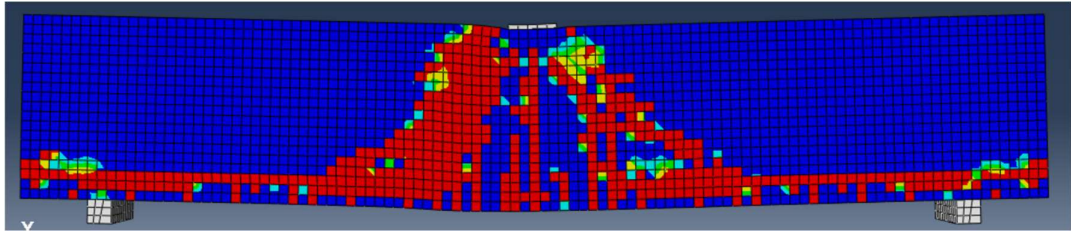
e) Crack Pattern at 385 KN
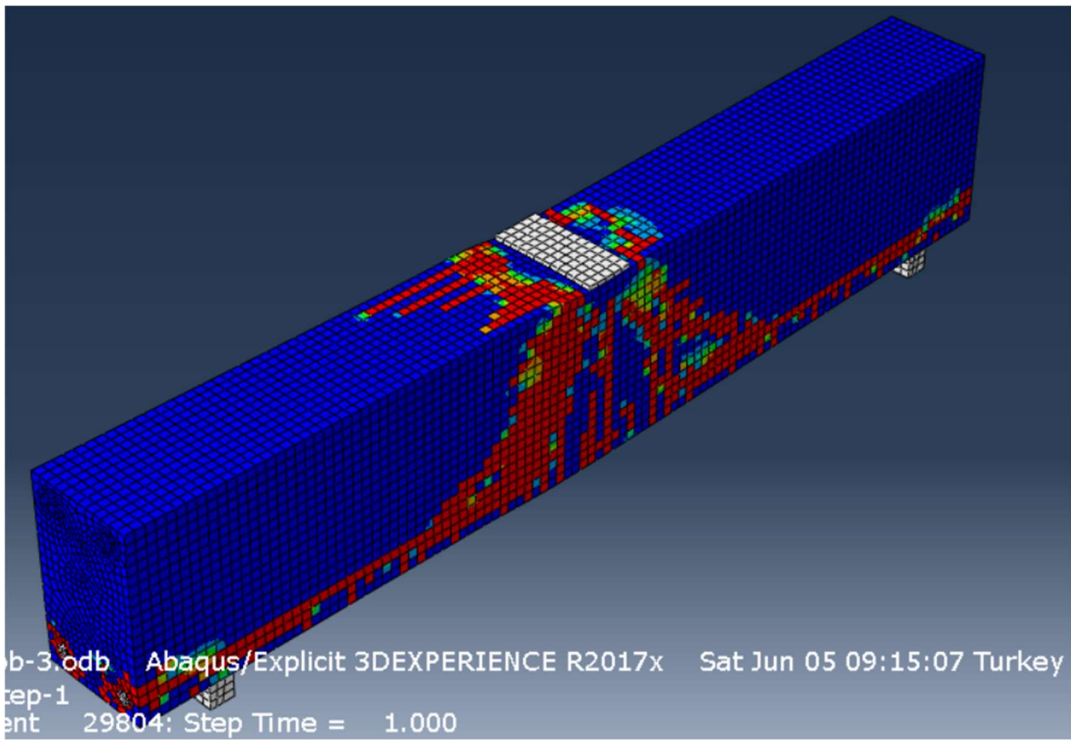
f) Crack Pattern at 398 KN
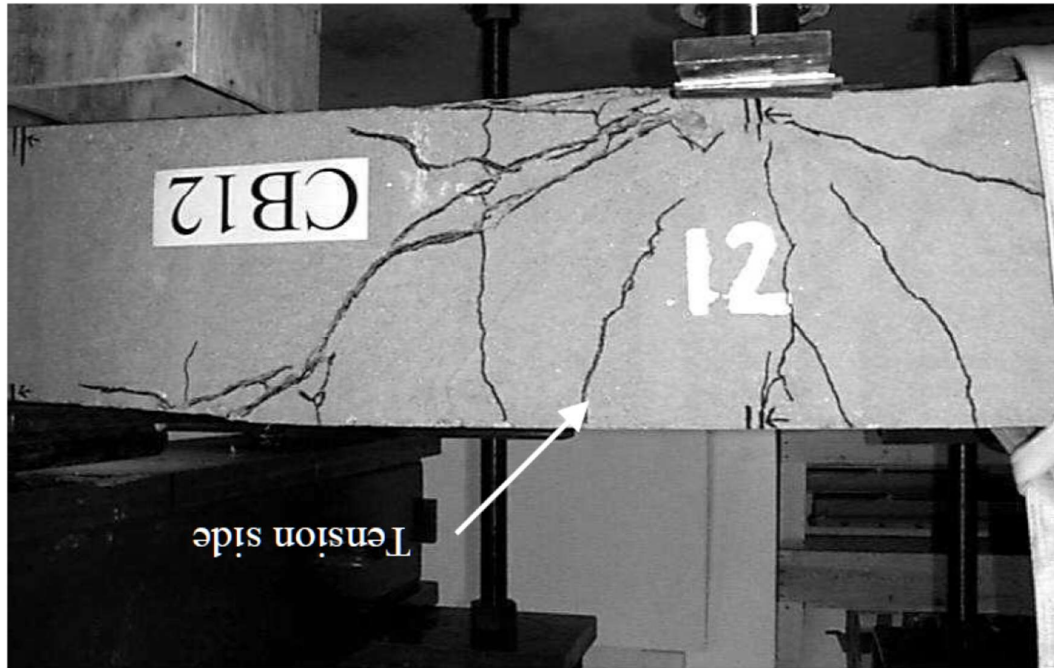
g) Experimental crack pattern at failure load (397 KN)

Figure 4.33. Crack propagation of shear control beam.

The obtained crack pattern of shear control beam from ABAQUS with the photograph of the crack pattern of the experimental control beam agree very well. Diagonal tensile cracks propagates from the loading area towards to supports.

Shear strengthened beam

The increasing propagation crack pattern of the shear strengthened beam are shown in figure 4.34., (a), (b), (c), (d), (e) and (f).
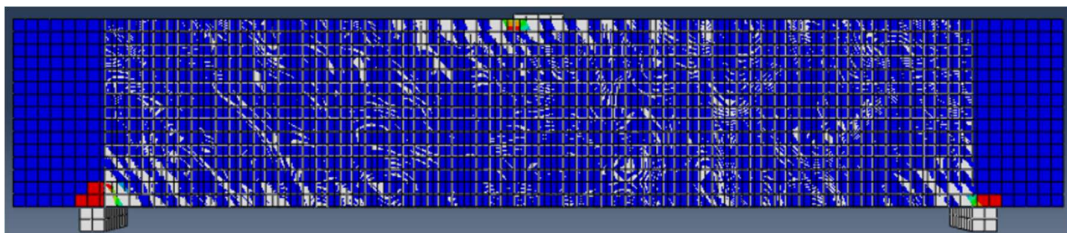
a) Crack Pattern at 20 KN.
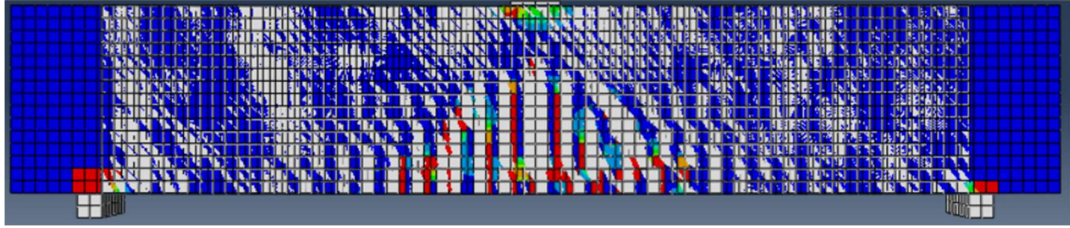
b) Crack Pattern at 183 KN.
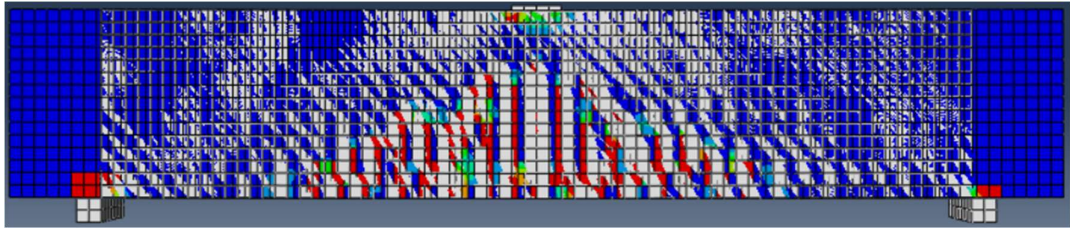
c) Crack Pattern at 258 KN.
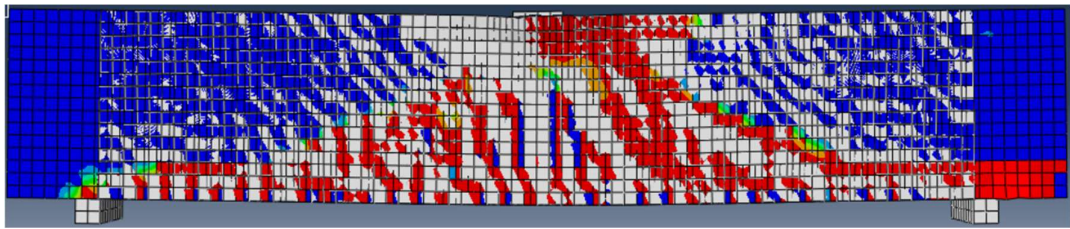
d) Crack Pattern at 337 KN.
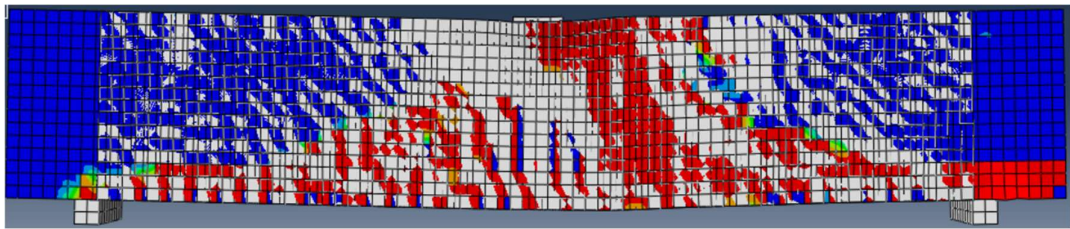
e) Crack Pattern at 421 KN.
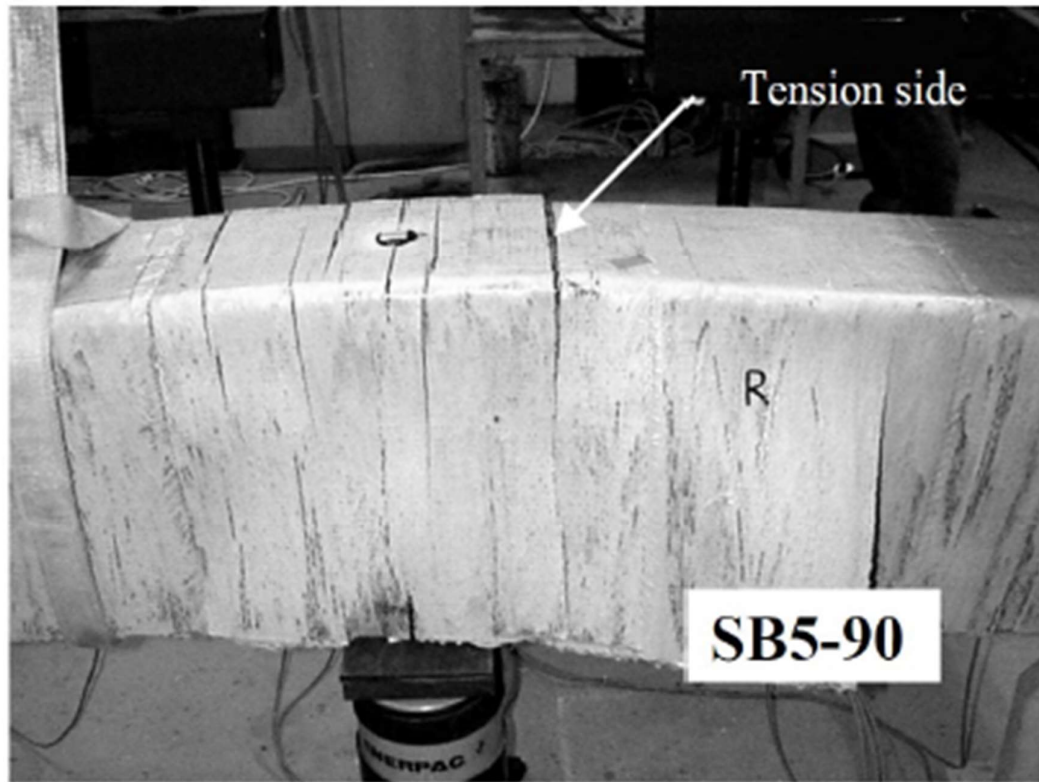
f) Experimental Crack Pattern at Failure Load (397 KN)

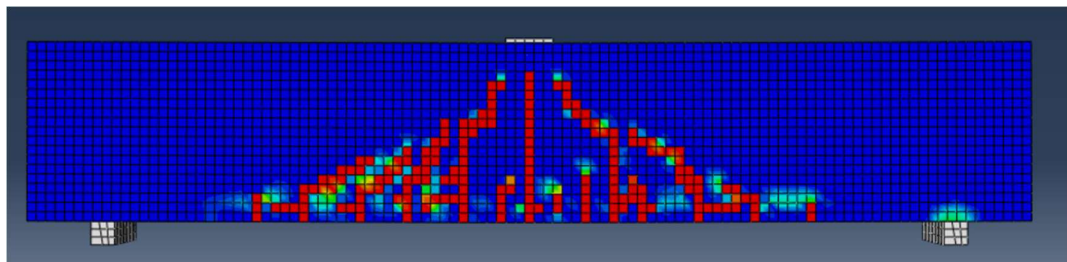**Figure 4.34.** Crack propagation of shear strengthened beam.

As reported in the experimental investigation, (Alagusundaramoorthy 2002), shear strengthened beam was failed in a shear-compression failure mode. The obtained crack pattern of shear strengthened beam from ABAQUS and the photograph of crack pattern of the actual strengthened beam agree very well.

4.8.3. Loads and deflection values of beams

Table 4.9. and 4.10. show a comparison between experimental and finite element models with ultimate carrying capacity and deflection values of the control and strengthened beams.

Table 4.9. A comparison between failure loads of experimental and ABAQUS results.

	Failure Load (KN)		
Beams	Experimental Results	Analytical Results	Difference (%)
Flexure Control Beam	41.25	48.9	18.5%
Flexure strengthened Beam	49.5	58.6	18.4%
Shear Control Beam	397	396.5	-0.1%
Shear strengthened Beam	421	421	0.0%

Table 4.10. A comparison between deflection values of experimental and ABAQUS results.

	Deflection (mm)		
Beams	Experimental Results	Analytical Results	Difference (%)
Flexure Control Beam	21.13	21.03	-0.5%
Flexure strengthened Beam	20.13	19.9	-1.1%
Shear Control Beam	8.1	8.76	8.1%
Shear strengthened Beam	10.86	8.28	-23.61%

4.9. Parametric Study (Analytical Results)

After modelling of experimental beams were verified, the modelling of flexure and shear beams used to expand the range of research through change some of parameters such as number of layers, Length of FRP and jacketing strengthening method of RC beams.

4.9.1. Effect of number of CFRP layers on flexure beam at tension side

Figure 4.35. showed that a comparison of the load-deflection curve resulted from FEA using ABAQUS for the flexure beam strengthened at the tensile side with a different number of CFRP layers. As shown in the figure, the additional layers of CFRP to the control beam increased the stiffness and ultimate loading capacity for all cases but decreased mid-span deflection at failure.
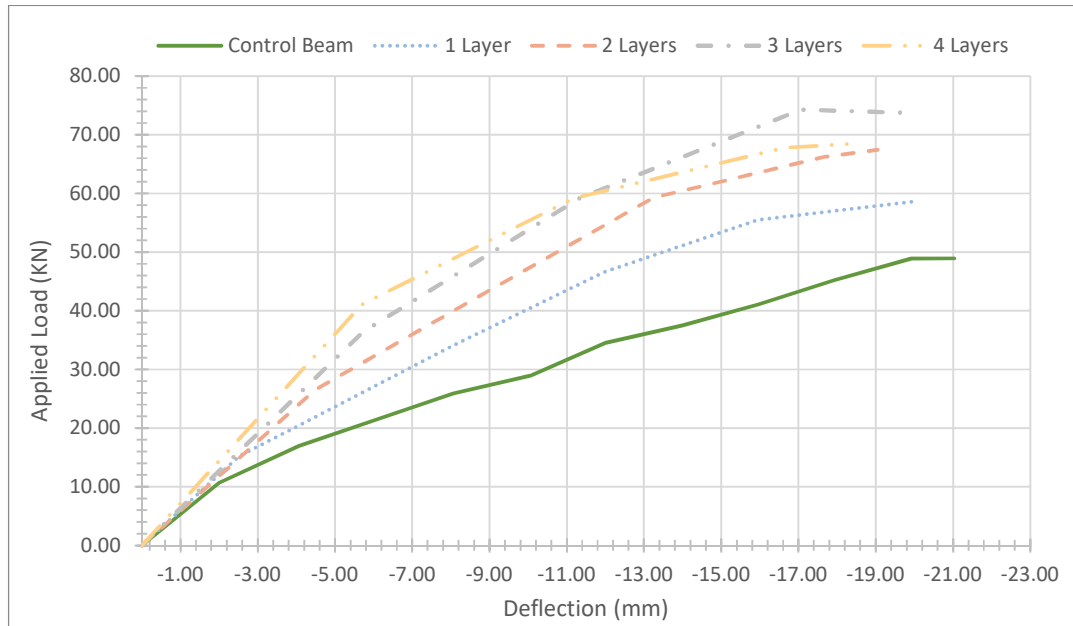
Figure 4.35. The Effect of increasing number of CFRP layers bonded to the flexure beam–load deflection curves.

Table 4.11. A comparison of the effect of additional CFRP layers on the beam ultimate load and mid-span deflection as resulted from FE analysis using ABAQUS.

Beam	Failure Load (KN)	Increased Strength (%)	Mid-Span Deflection at Failure (mm)	Decreased Deflection at Failure (%)
Control Beam	48.9	-	21.035	-
Strengthened Beam (one Layer)	58.57	19.78%	19.93	-5.25%
Strengthened Beam (two Layers)	67.4	37.83%	19.05	-9.44%
Strengthened Beam (three Layers)	74.68	52.72%	17.06	-18.90%
Strengthened Beam (Four Layers)	68.46	40.00%	18.35	-12.76%

From figure 4.35. and table 4.11., using one layer of CFRP at tensile side parallel with the longitudinal axis of the beam, the ultimate load capacity of the strengthened beams was increased by 19.78% but the deflection value of the beam at failure was decreased by 5.25%. While, using two layers of CFRP at tensile side parallel with the longitudinal axis of the beam, the ultimate load capacity of the strengthened beams was increased by 37.83 % and the deflection value of the beam at failure was decreased by 9.44 %. When, using three layers of CFRP at tensile side parallel with the longitudinal axis of the beam, the ultimate load capacity of the strengthened beams was increased by 52.72 % but the deflection value of the beam at failure was decreased by 18.90 %. Therefore, using four layers of CFRP at tensile side parallel with the longitudinal axis of the beam, the ultimate load capacity of the strengthened beams was increased by 40.00 % and the deflection value of the beam at failure was decreased by 12.76 %.

The results mean that the RC beam strengthened by three layers at tension side of CFRP less ductile than beam was strengthened by four layers.

4.9.2. Effect of changing length of CFRP layers on flexure beam

Figure 4.36. shows a comparison of loading-deflection curve obtained from FEA using ABAQUS for the flexure beam, strengthened at tensile side with a different length of CFRP layers over RC beams. As shown in the figure, the bonding of different length of CFRP layer to the beam increases stiffness and ultimate loading capacity, and decreases mid-span deflection at failure.
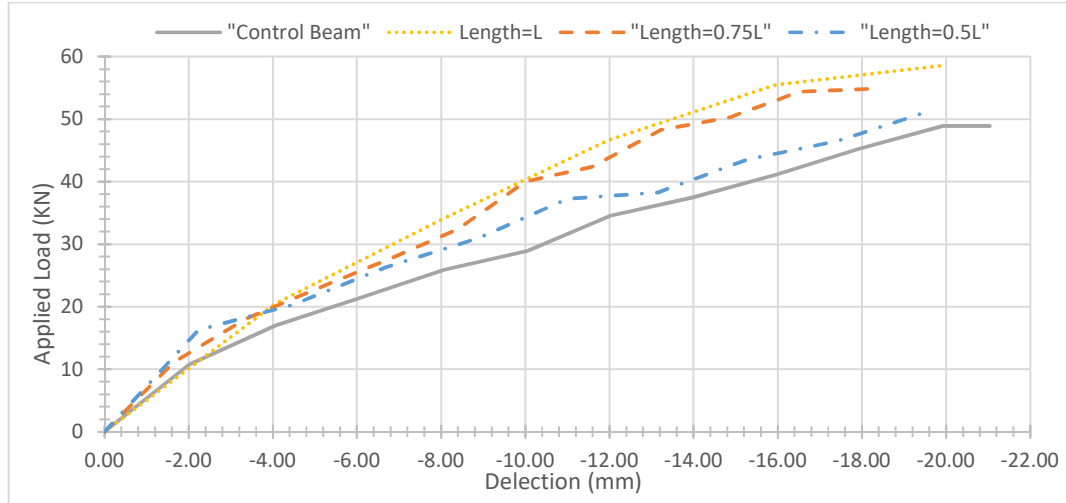
Figure 4.36. Effect of changing length of CFRP layers on flexure beam.

Table 4.12. A comparison of the effect of additional CFRP layers on the beam ultimate loading and mid-span deflection as resulted from FE analysis using ABAQUS.

Beam	Failure Loading (KN)	Increased Strength (%)	Mid-Span Deflection at Failure (mm)	Deflection Value at Failure (%)
Control Beam	48.9	-	21.035	-
Strengthened Beam (Length =50%L)	51.2	4.7%	19.58	-6.9%
Strengthened Beam (Length =70%L)	53.24	8.88%	18.14	-13.76%
Strengthened Beam (Length = L)	58.57	19.78%	19.95	-5.16%

As it is shown in figure 4.36. and table 4.12., increasing the ultimate carrying capacity of the strengthened beam with full length of CFRP at tensile side of beam is 19.78% and the deflection value decreasing by 5.16%. While, increasing the ultimate carrying capacity of the strengthened the control beam with 75% of full length of CFRP layers is 8.88% and decreasing the deflection value of strengthened beam at failure is 5.87%. However, increasing the ultimate carrying capacity of the strengthened the control beam with 50% of full length of CFRP layers is 4.91% and decreasing in deflection value of beam at

80

failure is 17.28%. Length of fibers when uses 50% of beam span length, the increase in ultimate loading capacity of beam becomes worthless.

4.9.3. Effect of using U-shape of CFRP layers on flexure beam

Figure 4.37. shows a comparison of the load-deflection curve of analytical flexure strengthened RC beams from ABAQUS by using a U-shape method with a different number of CFRP layers. As shown in the figure, the additional layers of CFRP to the control beam increases the stiffness and ultimate capacity of beams for all cases. However, mid-span deflection value at failure decreases for all cases except strengthened beam with one layer.
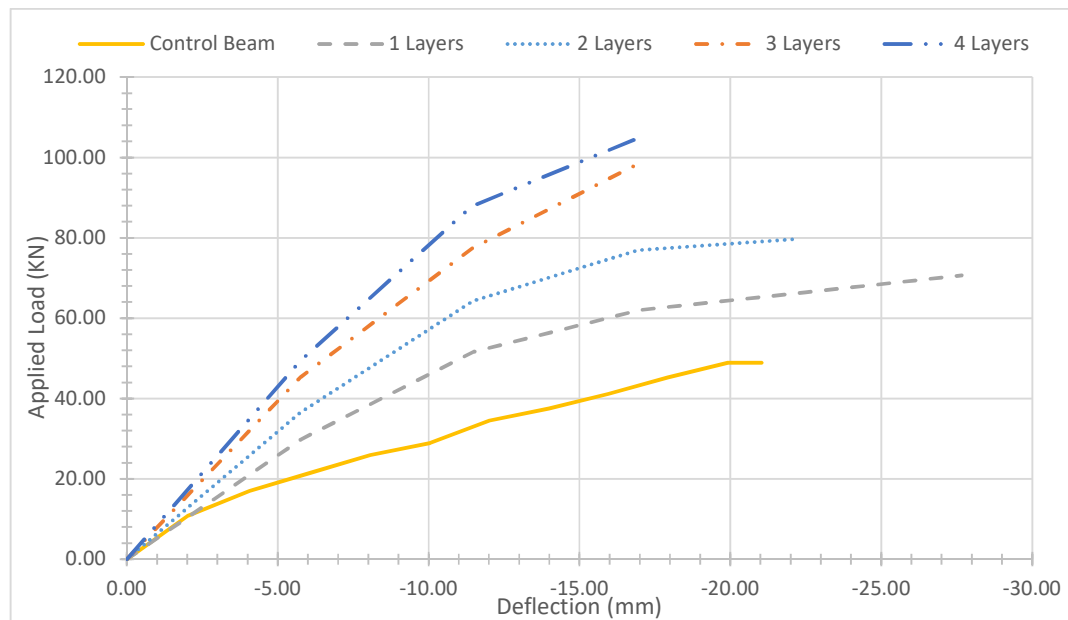

Figure 4.37. Effect of increasing number of CFRP layers bonded to the flexure beam.

Table 4.13. A comparison of the effect of additional CFRP layers on the beam ultimate load and mid-span deflection as resulted from FE analysis using ABAQUS.

Beam	Failure Load (KN)	Increased Strength (%)	Mid-Span Deflection at Failure (mm)	Deflection at Failure (%)
Control Beam	48.9	-	21.035	-
Strengthened Beam (one Layer)	70.64	44.46%	27.663	31.51%
Strengthened Beam (two Layers)	79.65	62.88%	22.13	5.21%
Strengthened Beam (three Layers)	98.2	100.82%	16.8	-20.13%
Strengthened Beam (Four Layers)	104.4	113.50%	16.81	-20.09%

From figure 4.37. and table 4.13., using one layer of CFRP at tensile side parallel with the longitudinal axis of the beam, the ultimate carrying capacity of the strengthened beams increased by 44.46% but the deflection value of the beam at failure increased also by 31.51%. While, using two layers of CFRP at tensile side parallel with the longitudinal axis of the beam, the ultimate carrying capacity of the strengthened beams increased by 62.88 % but the deflection value of the beam at failure increased by 5.21 %. When, using three layers of CFRP at tensile side parallel with the longitudinal axis of the beam, the ultimate carrying capacity of the strengthened beams increased by 100.82 % but the deflection value of the beam at failure decreased by 20.13 %. Therefore, using four layers of CFRP at tensile side parallel with the longitudinal axis of the beam, the ultimate carrying capacity of the strengthened beams increased by 113.5 % but the deflection value of the beam at failure decreased by 20.09 %.

This implies that the RC beam strengthened by a single layer and two layers of CFRP more ductile than beam was strengthened by a three and four layers and give warning before failure.

4.9.4.   Effect of using U-shape of CFRP layers on shear beam

Figure 4.38. shows a comparison of the load-deflection curve as resulted from ABAQUS for the shear beam, strengthened by using a U-shape with a different number of CFRP layers. As shown in the figure, the additional layers of CFRP to the control beam increases the stiffness and ultimate capacity of beams for all cases. However, mid-span deflection at failure decreases in all cases except strengthened beam with one layer and three layers.
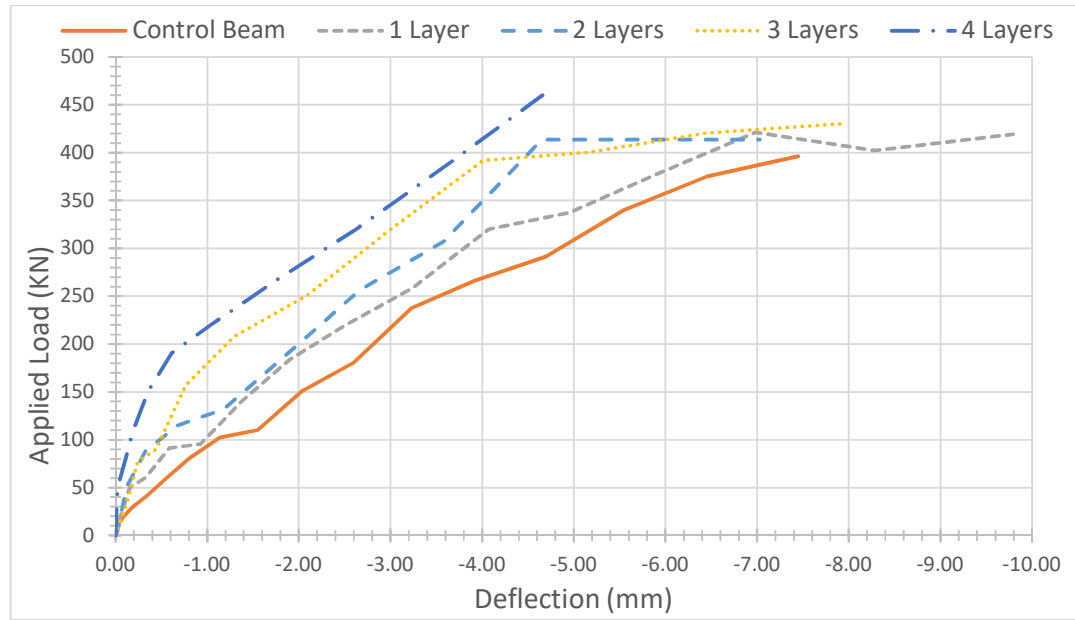
Figure 4.38. Effect of increasing number of CFRP layers bonded to shear beams.

Table 4.14. A comparison of the effect of additional CFRP layers on the beam ultimate load and mid-span deflection as resulted from FE analysis using ABAQUS.

Beam	Failure Load (KN)	Increased Strength (%)	Mid-Span Deflection at Failure (mm)	Deflection value at Failure (%)
Control Beam	396.25	-	7.45	-
Strengthened Beam (one Layer)	419.25	5.80%	9.8	31.54%

Beam	Failure Load (KN)	Increased Strength (%)	Mid-Span Deflection at Failure (mm)	Deflection value at Failure (%)
Strengthened Beam (two Layers)	413.56	4.37%	7.02	-5.77%
Strengthened Beam (three Layers)	430.56	8.66%	7.95	6.71%
Strengthened Beam (Four Layers)	460.04	16.10%	4.65	-37.58%

From figure 4.38. and table 4.14., using one layer of CFRP parallel with the longitudinal axis of the beam, the ultimate carrying capacity of the strengthened beams increased by 5.80% and the deflection value of the beam at failure increased also by 31.51%. While, using two layers of CFRP, the ultimate carrying capacity of the strengthened beams increased by 4.37 % but the deflection value of the beam at failure decreased by 5.77 %. When, using three layers of CFRP, the ultimate carrying capacity of the strengthened beams was increased by 8.66 % but the deflection value of the beam at failure was decreased by 6.71 %. Therefore, using four layers of CFRP, the ultimate carrying capacity of the strengthened beams increased by 16.10 % but the deflection value of the beam at failure was decreased by 37.58 %.

From the obtained results, the RC beam strengthened by four layers of CFRP more brittle than beam was strengthened by a single, two or even three layers and don't give warning before failure.

4.9.5. Effect of using wrapped strengthening method of CFRP layers on shear beam

Figure 4.39. shows a comparison of the load-deflection curve resulted from ABAQUS for the shear beam, strengthened by using wrapped method with a different number of CFRP layers. As shown in the figure, the additional layers of CFRP to the control beam increases the stiffness and ultimate capacity of beams for all cases.
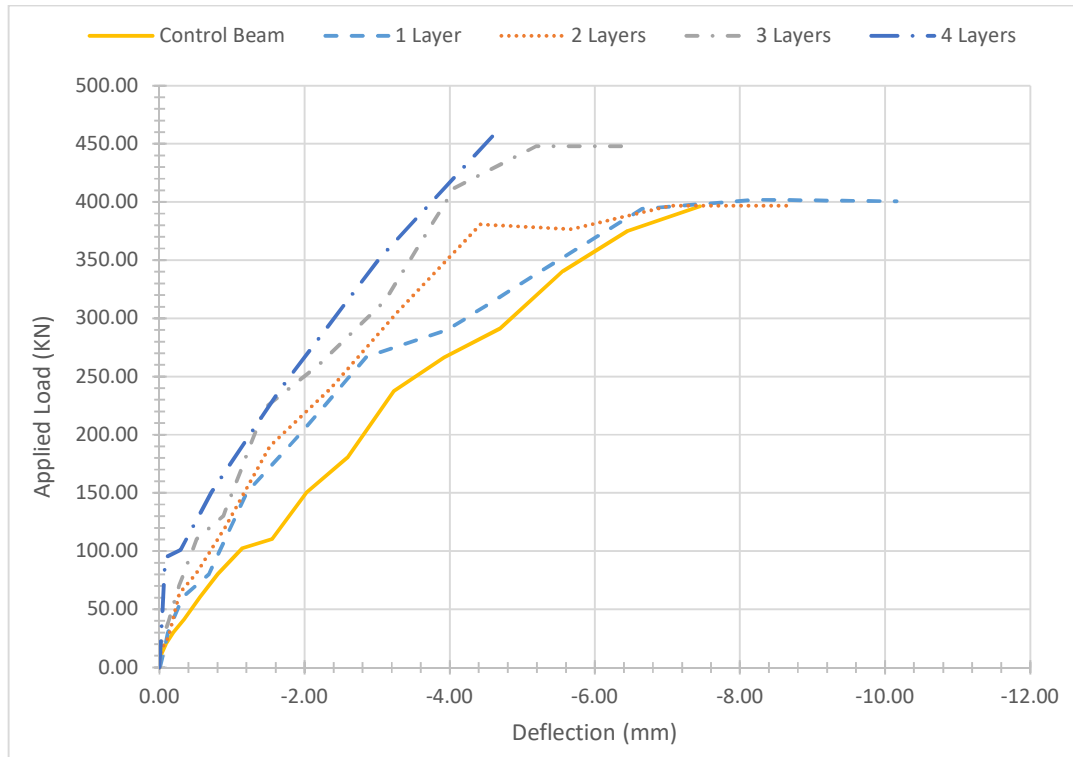
Figure 4.39. Effect of increasing number of CFRP layers bonded to the shear beam Load Deflection Curves.

Table 4.15. A comparison of the effect of additional CFRP layers on the beam ultimate load and mid-span deflection as resulted from FE analysis using ABAQUS.

Beam	Failure Load (KN)	Increased Strength (%)	Mid-Span Deflection at Failure (mm)	Deflection value at Failure (%)
Control Beam	396.25	-	7.45	-
Strengthened Beam (one Layer)	400.64	1.11%	10.15	36.24%
Strengthened Beam (two Layers)	397	0.2%	8.64	15.97%
Strengthened Beam (three Layers)	447.94	13.04%	6.46	-13.29%

85

Beam	Failure Load (KN)	Increased Strength (%)	Mid-Span Deflection at Failure (mm)	Deflection value at Failure (%)
Strengthened Beam (Four Layers)	461.83	16.55%	4.66	-37.45%

From figure 4.39. and table 4.15., using one layer of CFRP, the ultimate carrying capacity of the strengthened beams increased by 1.11% but the deflection value of the beam at failure increased also by 36.24%. While, using two layers of CFRP, the ultimate carrying capacity of the strengthened beams increased by 0.2 % but the deflection value of the beam at failure increased by 15.97 %. When, using three layers of CFRP, the ultimate carrying capacity of the strengthened beams increased by 13.04 % but the deflection value of the beam at failure decreased by 13.29 %. Therefore, using four layers of CFR, the ultimate carrying capacity of the strengthened beams increased by 16.55 % but the deflection value of the beam at failure decreased by 37.45 %.

The results mean that the RC beam strengthened by a single layer and two layers of fully-wrapped of CFRP more ductile than beam was strengthened by three or four layers and give warning before failure.

4.9.6. Effect of jacketing methods on RC Beams

A. Flexural Critical Beam

From Figures (4.40 to 4.43) it can be noticed that the additional layers of CFRP to the control beam increases the stiffness and ultimate loading capacity of beams for all cases. The ultimate loading capacity of RC beams strengthened by U-shape of CFRP is bigger than the ultimate loading capacity of RC beams strengthened at tension side. The difference between the ultimate loading capacities obtained from two methods gets much bigger when the number of CFRP layers increases.
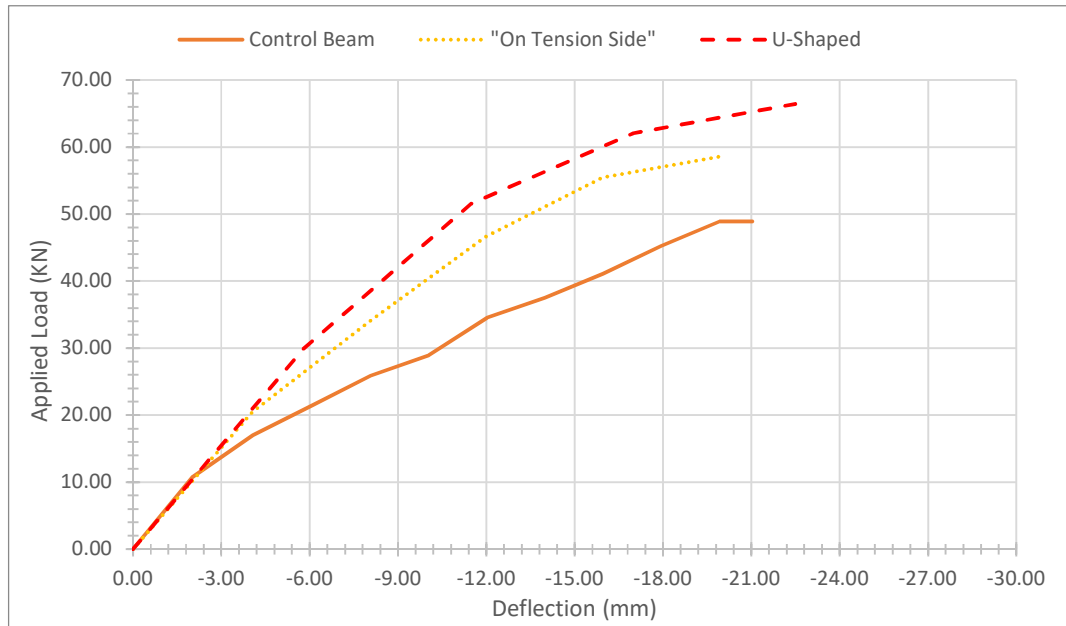
Figure 4.40. Effect of changing the jacketing method of flexural beam for single layer.

Figure 4.41. Effect of changing the jacketing method of flexural beam for two layers.

Figure 4.42. Effect of changing the jacketing method of flexural beam for three layers.

Figure 4.43. Effect of changing the jacketing method of flexural beam for four layers.

88

B. Shear Critical Beam

From Figures (4.44 to 4.47) it can be deduced that, the additional layers of CFRP to the control beam increases the stiffness and ultimate load capacity of beams for all cases. The differences between values of ultimate load capacity of RC beams strengthened by using U-shape method and RC beams strengthened wrapped method of CFRP are worthless. It is also noticed that when four layers of CFRP is used, the behaviour of the beam becomes brittle.

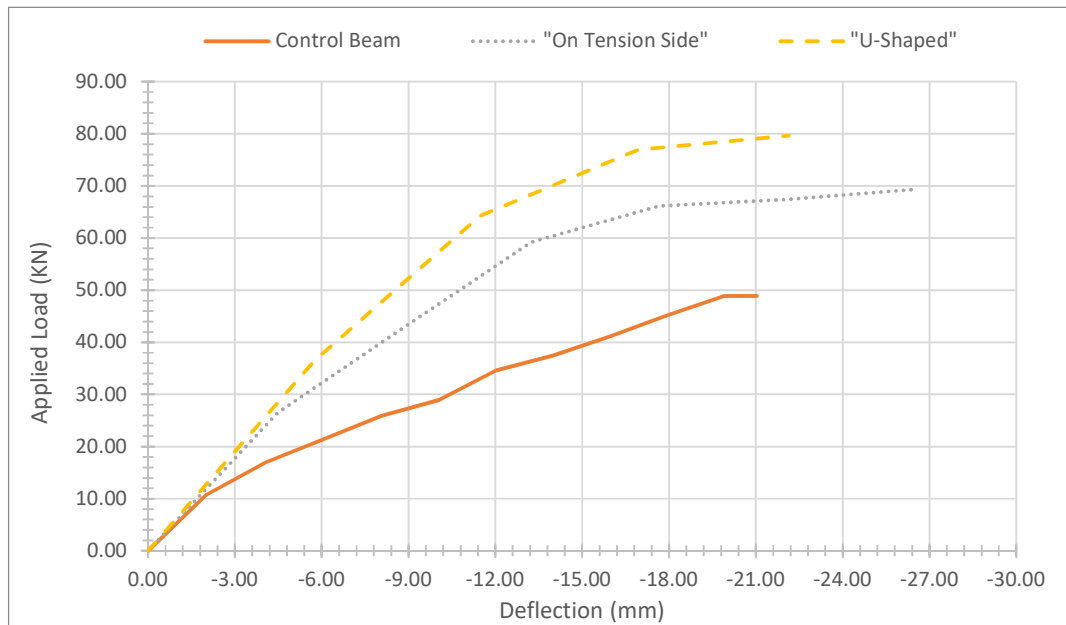**Figure 4.44**. Effect of changing the jacketing method of shear beam for a single layer.
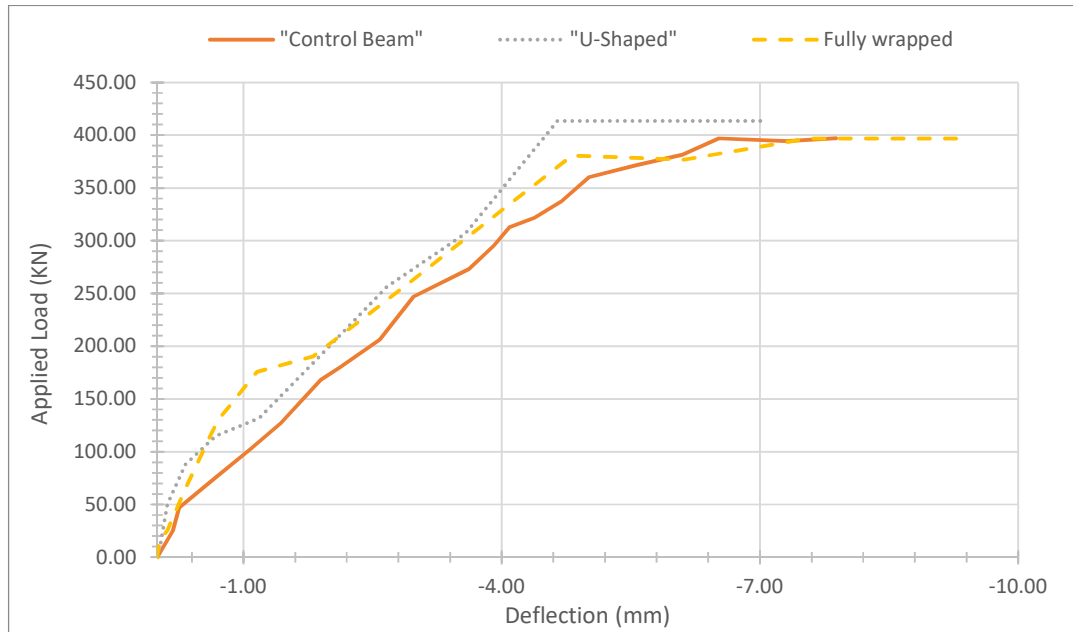
Figure 4.45. Effect of changing the jacketing method of shear beam for two layers.
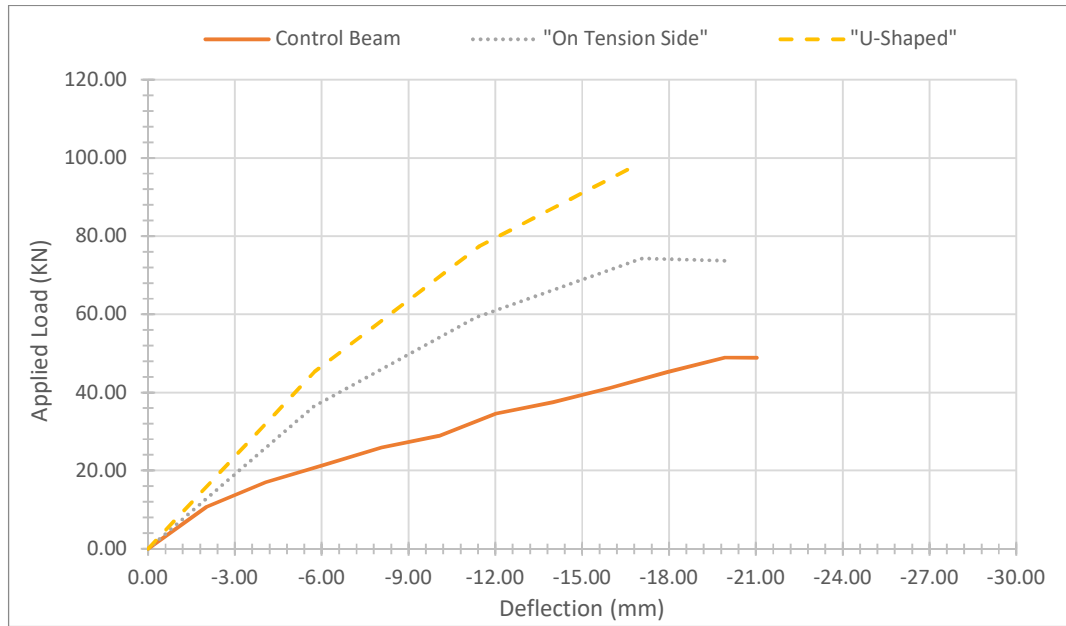

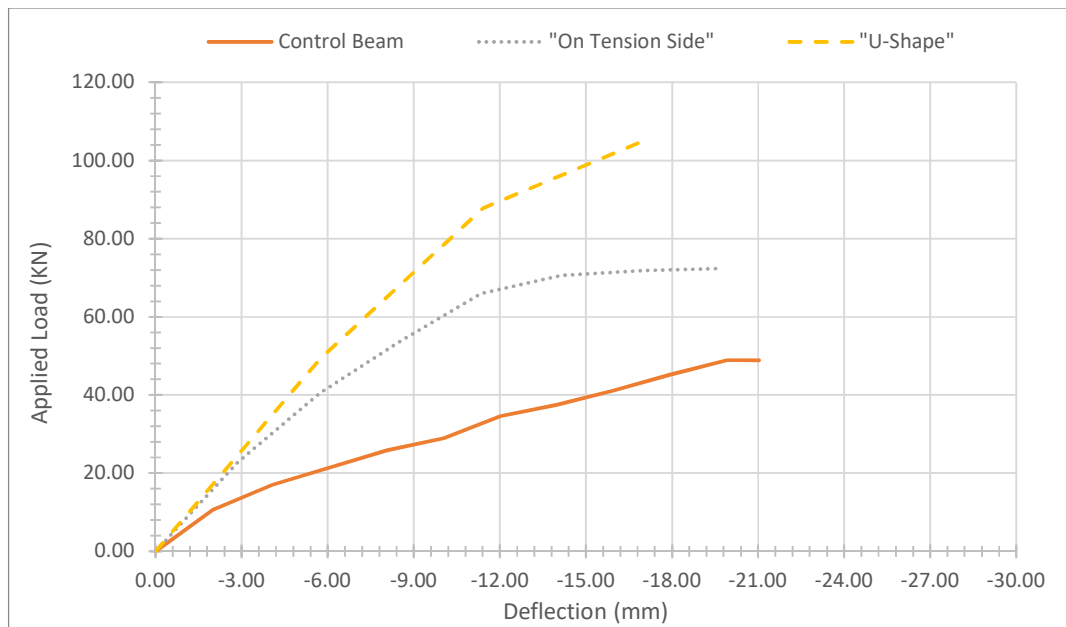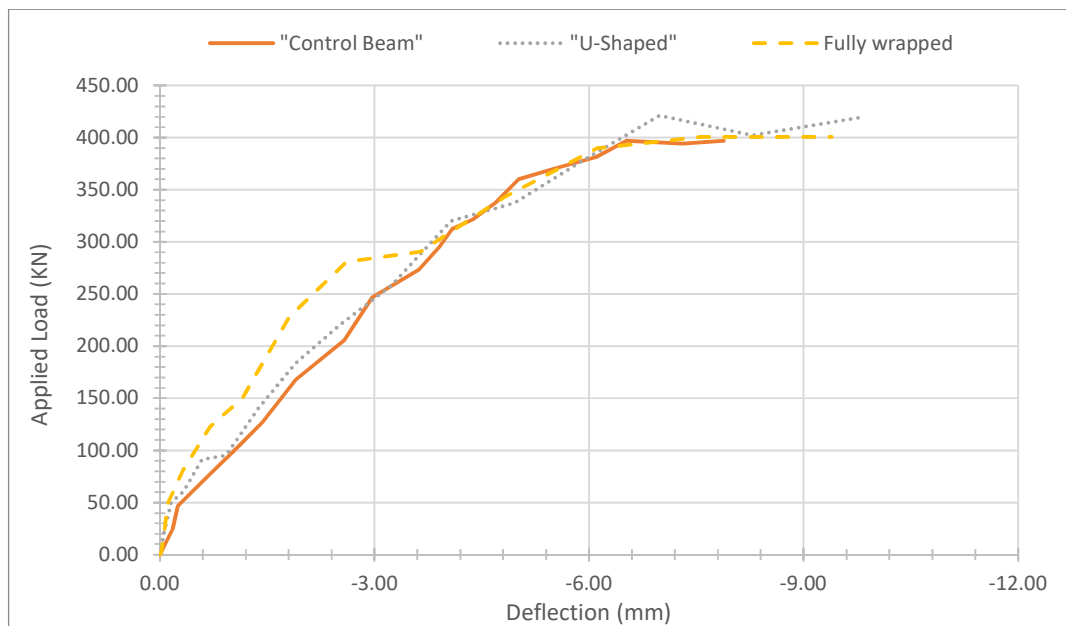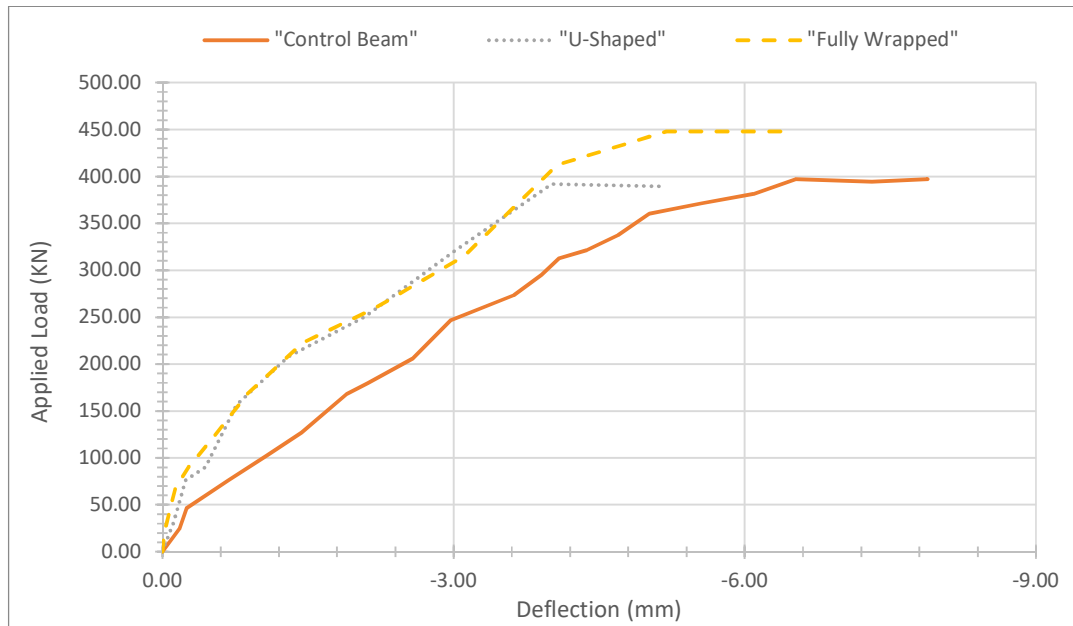**Figure 4.46**. Effect of changing the jacketing method of shear beam for three layers.

90
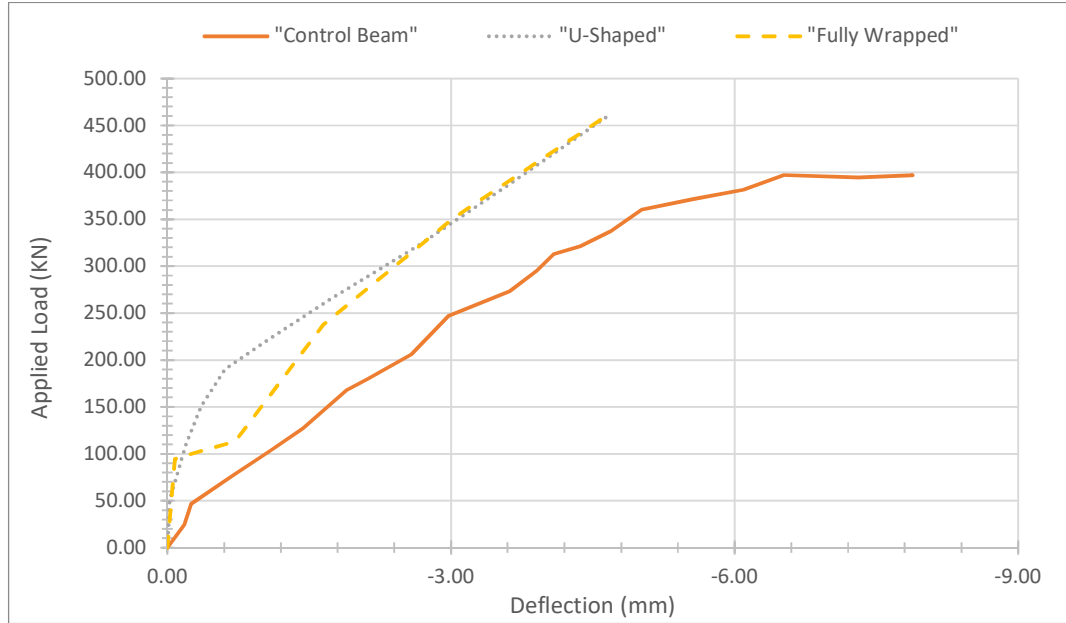
Figure 4.47. Effect of changing the jacketing method of shear beam for four layers.

4.9.7. Effect of changing the orientation of CFRP layers

- **Flexure Beam**

As it is shown in Figure 4.48 and 4.49. strengthening the flexure control beam with one U–wrap CFRP layer parallel with the longitudinal and the second layer inclined at an angle of 90° with the beam axis, increases the beam ultimate load by 129.52% and increases the mid-span deflection at failure by 32.62%. While, strengthening the control beam with two U–wrap CFRP layers parallel with the beam axis increases the beam ultimate load by 92.44% and increases the mid-span deflection at failure by 28.82%.

The results mean that the RC beam strengthened by one U–shaped CFRP layer parallel with the longitudinal and the second layer inclined at an angle of 90° with the beam axis is more ductile and has a higher load capacity than RC beam strengthened by two layers of CFRP parallel with the longitudinal axis of beam.

91
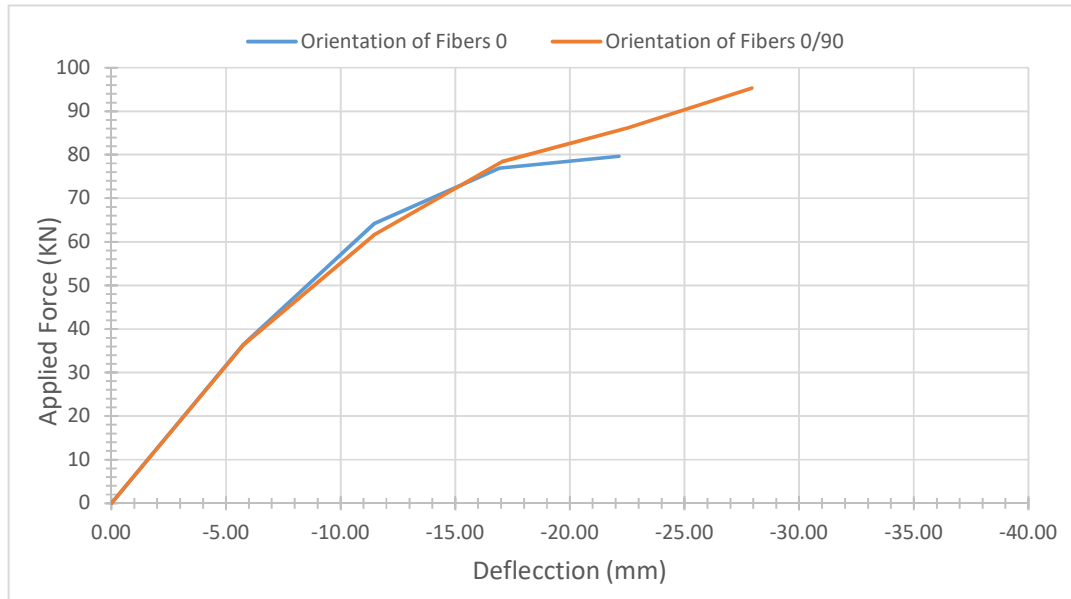
Figure 4.48. Effect of changing the orientation of CFRP layers in flexure beams.

- **Shear Beam**

As it is shown in Figure 4.48 and 4.49. strengthening the shear control beam with one fully–wrapped of CFRP layer parallel with the longitudinal and the second layer inclined at an angle of 90° with the beam axis, increases the beam ultimate load by 31.92% and decreases the mid-span deflection at failure by 12.35%. While, strengthening the control beam with two U–wrap CFRP layers parallel with the beam axis increases the beam ultimate load by 4.7% and decreases the mid-span deflection at failure by 13.35%

From the obtained results, strengthening the shear control beam with one fully–wrapped of CFRP layer parallel with the longitudinal and the second layer inclined at an angle of 90° with the beam axis has a higher load capacity and more efficient than beam was strengthened two layers of CFRP parallel with the longitudinal axis of beam.
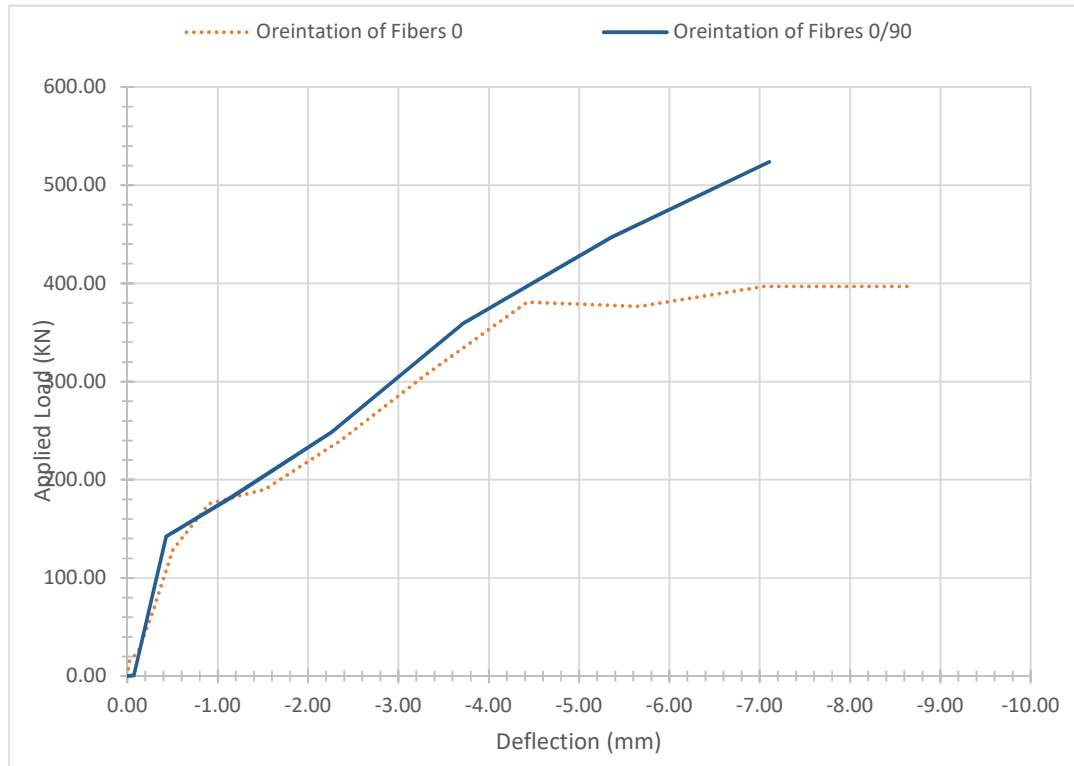
Figure 4.49. Effect of changing the orientation of CFRP layers in shear beams.

5. CONCLUSIONS and RECOMMANDATIONS

In this thesis, the influence of different parameters on the performance of the beams strengthened with CFRP is investigated using finite element models analyzed in ABAQUS program. The conclusions derived from the results of finite element analyses are presented below.

5.1. Conclusions

1. Results of finite element analyses performed in ABAQUS are verified with previously published experimental results of un-strengthened and strengthened RC beams. Therefore, the models developed in ABAQUS can be confidently used in the analysis of RC Beams externally strengthened with CFRP.

2. For un-strengthened control beams, the ultimate loads obtained from analytical models are higher than the experimental results in both flexure critical and shear critical cases. Because it was assumed that the interaction between reinforcement bars, concrete and CFRP layers are perfect.

3. For flexural critical beams strengthened only at the tensile side over the full length, the maximum increase in the ultimate load capacity is obtained when three layers of fibers are used. In this case the flexural strength of the beam increases 52.72% and the mid-span deflection at failure reduces 18.90% compared to un-strengthened control beam.

4. As for the effect of the length of the CFRP that is used only on the tension side on the beam behavior, results showed that using CFRP over the full length of the beam yields better results compared to using it over the length of 50% and 75% of the beam length. In full length case ultimate strength of beam increased by 19.78% while the deflection value was decreased by 5.16% compared to control beam.

5. To study the effect of jacketing method on flexural beams, CFRP sheets are applied on only the tension side of the beam in one set and they are applied on three sides (U shape) of the beam in another set. In both sets, the length and the number of CFRP layers varied too. Results showed that the maximum strength is

obtained from the beams which have the four layers of CFRP on three sides over the full length of the beam. In this case the ultimate strength is increased 113.50% compared to control beams. In the same case the deflection value was decreased by 20.09%.

6. Strengthening the shear critical beam with four layers of U-shaped CFRP increases the shear strength of the beam by 16.10% and decreases the beam mid-span deflection by 37.58%.

7. Strengthening the control shear beam with four layer of wrapped CFRP the shear strength of the beam by 16.55% and decreases the beam mid-span deflection by 37.45%.

8. Strengthening the control beam with one layer of U-wrap CFRP layer parallel with the longitudinal axis and the second layer inclined at an angle of 90° with an additional layer of CFRP layer is more efficient than strengthening RC with two layers of U-wrap CFRP layers parallel with the longitudinal axis of the beam.

5.2. Recommendations

1. It is recommended to use another strengthening FRP materials as a glass or aramid fiber reinforced polymer to study its influence on behavior of RC beams.

2. In this study, the bond between concrete and CFRP was assumed to be perfect. The behavior of the concrete-CFRP bond and de-bonding issues can be studied analytically to get more precise results especially regarding failure modes.

3. In this study, environmental factors that may affect the efficiency of RC beams strengthened with CFRP as seasonal temperature variation, creep and shrinkage were not considered.

REFERENCES

ABAQUS User's Guide. ABAQUS 6.14 Analysis User's Guide 2014., IV:, 1128.

Abd, I., Malik, E., Conceic, L., Luisa, M., Simo, D. F. 2009. Strengthening of reinforced concrete beams in flexure by partial jacketing. Materials and Strucctures, (42):, 495–504. https://doi.org/10.1617/s11527-008-9397-3

Abdel Baky, H., Kotynia, R., Neale Kenneth W. 2014. Nonlinear FE analysis of RC beams strengthened in flexure with NSM CFRP systems. , (June 2008):, 1–12.

Alagusundaramoorthy, P. 2002. Shear Strength of R/C beams Wrapped with CFRP Fabric, Frankfort.

Balamuralikrishnan, R., Jeyasehar, C. A. 2009. Flexural Behavior of RC Beams Strengthened with Carbon Fiber Reinforced Polymer (CFRP) Fabrics. The Open Civil Engineering Journal, 3(1):, 102–109. https://doi.org/10.2174/1874149500903010102

Chaht, F. L., Mokhtari, M., Benzaama, H. 2019. Using a Hashin criteria to predict the damage of composite notched plate under traction and torsion behavior. Frattura ed Integrita Strutturale, 13(50):, 331–341. https://doi.org/10.3221/IGF-ESIS.50.28

Chong, K. T. 2004. Numerical modelling of time-dependent cracking and deformation of reinforced concrete structures. PhD Thesis, University of New South Wales, Sydney, Australia, (December)

Demir, A., Ercan, E., Demir, D. D. 2018. Strengthening of reinforced concrete beams using external steel members. Steel and Composite Structures, 27(4):, 453–464. https://doi.org/10.12989/scs.2018.27.4.453

Emmons, P. 1994. Concrete Repair and Maintenance Illustrated, PH Emmons.pdf, Kingston, : Construction Publishers and consultants.

Hafezolghorani, M., Hejazi, F., Vaghei, R., Jaafar, M. S. Bin, Karimzade, K. 2017. Simplified damage plasticity model for concrete. Structural Engineering International, 27(1):, 68–78. https://doi.org/10.2749/101686616X1081

Hammad, M. R. 2015. Non-linear Finite Element Analysis of Reinforced Concrete Beams Strengthened with Carbon Fiber - Reinforced Polymer (CFRP) Technique. Masters' Thesis the Islamic University of Gaza, 98.

Hu, H. T., Lin, F. M., Jan, Y. Y. 2004. Nonlinear finite element analysis of reinforced

concrete beams strengthened by fiber-reinforced plastics. Composite Structures, 63(3–4):, 271–281. https://doi.org/10.1016/S0263-8223(03)00174-0

Ibrahim, A. M., Mahmood, M. S. 2009. Finite element modeling of reinforced concrete beams strengthened with FRP laminates. European Journal of Scientific Research, 30(4):, 526–541.

Irwin, R., Rahman, A. 2002. FRP Strengthening of Concrete Structures - Design Constraints and Practical Effects on Construction Detailing. NZ Concrete Society Conference, (1):, 14.

Jumaat, M. Z., Kabir, M. H., Obaydullah, M. 2006. A Review of The Repair Concrete Beams. Journal of Applied Science Research, 2(6):, 317–326.

Kaufmann, W. 1998. Strength And Deformations of Structural Concrete Subjected to In-Plane And Normal Forces (Vol. 24). Retrieved from https://doi.org/10.3929/ethz-a-010025751

Kaw, A. K. 2006. Mechanics of Composite Materials, Broken, : CRC Press.

Kotsovos, M. D., Pavlovic, M. N. 1995. Structural Concrete Finite-element Analysis for Limit-state Design. , New York, : Thomas Telford Books: , 565.

Li, Z., Leung, C., Xi, Y. 2009. Structural Renovation In Concrete.

Masuelli, M. A. 2016. Introduction of Fiber-Reinforced Polymers- Polymers and Composites: Concepts, Properties and Processes. IntechOpen, 1:, 39. Retrieved from https://www.intechopen.com/books/advanced-biometric-technologies/liveness-detection-in-biometrics

Mbereyaho, L., Moyo, P. 2016. Finite Element Modeling of Reinforced Concrete Beam Patch Repaired and Strengthened with Fiber-Reinforced Polymers. International Journal of Engineering and Technical Research (IJETR), 0869(3):, 47–54.

Mohammed Ali Kadhim, M., Hadi Adheem, A. 2018. Numerical Modelling of Cfrp Strengthened Reinforced Concrete Beams Under Impact Loading. Journal of Engineering and Sustainable Development, 22(02):, 97–105. https://doi.org/10.31272/jeasd.2018.2.37

Mugahed Amran, Y. H., Alyousef, R., Rashid, R. S. M., Alabduljabbar, H., Hung, C. C. 2018. Properties and applications of FRP in strengthening RC structures: A review. Structures, 16(May 2019):, 208–238. https://doi.org/10.1016/j.istruc.2018.09.008

Mukhtar, Z. Z., Abwahid, A. H. H., Bakar, A. A., Fitriadhy, A., Majid, M. S. A., Saat, A. M. 2019. Ultimate strength analysis of CFRP confined concrete using finite element method (FEM). IOP Conference Series: Materials Science and Engineering, 670(1):. https://doi.org/10.1088/1757-899X/670/1/012005

Pravin, S., Waghmare, B. 2011. Materials And Jacketing Technique For Retrofotting of Structures. International Journal of Advanced Engineering Research and Studies, 11–16.

Raval, S. S., Dave, U. V. 2013. Effectiveness of various methods of jacketing for RC beams. Procedia Engineering, 51(NUiCONE 2012):, 230–239. https://doi.org/10.1016/j.proeng.2013.01.032

Report on Fiber-Reinforced Polymer (FRP) Reinforcement 2015.

Shidada, S. 2011. MATERIALS AND PROPERTIES. , 2:, 28–42.

Uzbaş, B. 2014. Beton İçin Geliştirilen Gerilme - Şekil Değiştirme Modellerinin Karşılaştırılması Comparison of Model Developed for Concrete Stress-. Journal of Polytechnic, 17(3):, 115–126.

V.Chaudhari, S., A. Chakrabarti, M. 2012. Modeling of Concrete for Nonlinear Analysis using Finite Element Code ABAQUS. International Journal of Computer Applications, 44(7):, 14–18. https://doi.org/10.5120/6274-8437

Wu, Y., Nan, B., Chen, L. 2014. Mechanical performance and parameter sensitivity analysis of 3D braided composites joints. Scientific World Journal, 2014:. https://doi.org/10.1155/2014/476262

RESUME

Name Surname	: Omar M M Murtaja
Place and Date of Birth	: Madinah / Kingdom of Saudi Arabia
Foreign Languages	: English, Turkish

Education Status

High School	: Khaled Bin El-Waleed
Bachelor's	: Islamic University of GAZA, Department of Civil Engineering.
Master's	: Bursa Uludag University, Faculty of Engineering, Civil Engineering.

Work Experience   : I've two years of experience as a planner and structural engineer in Saudi Arabia. Then, I worked as a site engineer on a hotel project. Now, I work as a freelance civil engineer for consultancy offices and construction companies.

Contact (e-mail)   : omarmortaja92@gmail.com